

G 8642

**Investigations of Nonlinear Optical Properties of  
Certain Organic Photonic Materials using Z-Scan  
and DFWM Techniques**

**Binoy Paul**

International School of Photonics  
Cochin University of Science & Technology  
Cochin – 682 022, India



Ph. D. Thesis submitted to  
Cochin University of Science & Technology  
In partial fulfillment of the requirements for the  
Degree of Doctor of Philosophy

February 2004

**Investigations of nonlinear optical properties of certain organic photonic materials using Z-Scan and DFWM techniques**

*Ph. D. Thesis in the field of Photonic Materials*

**Author**

Binoy Paul  
Research Fellow  
International School of Photonics  
Cochin University of Science & Technology  
Cochin – 682 022, India  
[binoypaul@cusat.ac.in](mailto:binoypaul@cusat.ac.in); [binoyajce@yahoo.com](mailto:binoyajce@yahoo.com)

K  
535.14  
170

**Present Address**

Binoy Paul  
Lecturer  
Amal Jyothi College of Engineering  
Koovapally, Kottayam – 686 518  
India

G 8642

**Research Supervisor**

Dr. C P Girijavallabhan  
Emeritus Professor, International School of Photonics  
Director, Centre of Excellence in Lasers & Optoelectronic Science  
Cochin University of Science & Technology  
Cochin – 682 022, India  
[vallabhan@cusat.ac.in](mailto:vallabhan@cusat.ac.in)

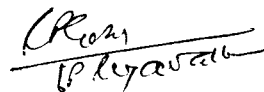
International School of Photonics, Cochin University of Science & Technology,  
Cochin 682 022, INDIA

February 2004

## CERTIFICATE

Certified that the work presented in the thesis entitled “**Investigations of nonlinear optical properties of certain organic photonic materials using Z-Scan and DFWM techniques**” is based on the original work done by **Mr. Binoy Paul**, under my guidance and supervision at the International School of Photonics, Cochin University of Science & Technology, Cochin 682 022, India and has not been included in any other thesis submitted previously for award of any degree.

Cochin 682 022  
February 05, 2004

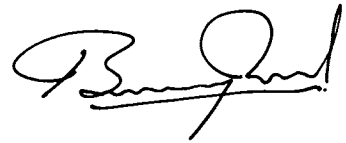


Prof. C P Girijavallabhan  
(Supervising Guide)

## DECLARATION

Certified that the work presented in the thesis entitled **“Investigations of nonlinear optical properties of certain organic photonic materials using Z-Scan and DFWM techniques”** is based on the original work done by me under the guidance and supervision of Dr. C P Girijavallabhan, Professor, International School of Photonics, Cochin University of Science & Technology, Cochin 682 022, India and has not been included in any other thesis submitted previously for award of any degree.

Cochin 682 022  
February 05, 2004

A handwritten signature in black ink, appearing to read 'Binoy Paul', with a stylized flourish at the end.

Binoy Paul

## ACKNOWLEDGEMENTS

I am grateful to my supervisor and guide **Dr. C. P. Girijavallabhan** for the support, encouragement and guidance given throughout my research work. The intellectual discussions with him on the various aspects encountered during my research was a great asset for me, both in professional as well as in personal front.

I also equally thankful to **Dr. V. P. N. Nampoori** for the keen interest that he has shown towards my research work. The personal relation that I have enjoyed with him helped me a lot in my research career, as he always been there for me with his innovative and interesting ideas.

I sincerely appreciate the help and support provided by **Dr. P. Radhakrishnan** and **Dr. V. M. Nandakumaran** during my research work. I also thank **Mr. Kailasnath** for his friendly attitude.

It is beyond words to express my gratitude of **Dr. Reji Philip**, RRI, Bangalore for his timely help, advice and support, which played an integral role in completing my thesis in the stipulated period.

At this moment, I remember with a great sense of gratitude about the help and encouragement given by **Dr. P. Basak**, Director, **Dr. (Fr.) James Thalachelloor**, Manager and **Dr. Komalavalli Amma**, Principal of Amal Jyothi College of engineering, Koovapally, especially at times when it really matters.

It is a great pleasure to convey my indebtedness and gratitude towards my colleagues **Dr. K. P. Unnikrishnan** and **Pramod Gopinath**, without their timely help and assistance I would not have been able to accomplish this task.

I always enjoyed the wonderful moments and intellectual discussions with my dear colleagues **Aneesh, Sajan, Jibu, Deepthy** and **Prasanth**. The help rendered by them is incomparable, especially for the literature collection. I, also very much enjoyed the motherly affection from **Dr. Achamma Kurian**, who showed a keen interest in my research and personal activities.

Timely advice and help given by my seniors **Dr. Riju. C. Issac, Dr. Shelly John, Dr. Jayan Thomas, Dr. Harilal, Dr. Bindhu. C. V, Dr. Geetha. K Varrier** was always been a guidance for my research work.

I am thankful to my dear friends **Thomas Lee, Suresh Kumar, Pravitha, Geetha, Bindhu, Santhi, Dilna, Sreeja, Rajesh. M. Rajesh. S, Manu, Vinu, Abraham, Rekha, Lekshmi, Sheeba** and **Lyjo**. I am so grateful to **Sr. Ritty Nedumpara** for the love and care that she has shown towards me. I am extremely thankful to **Mr. Jijo**, for the effort that he has taken in designing the cover page of my thesis. I am also grateful to various M. Phil and M. Tech batches, whom I have encountered during my research career, for all their love and support.

The essential part of the present thesis is provided by various collaborators of ISP in the form of samples. I thank **Prof. Prathapachandra Kurup, Dr. Mayadevi, Dr. Preetha** and **Sreekanth** of Chemistry Department, CUSAT for the various nonlinear materials used in this thesis.

I also thank my colleague **Dr. Soney C. George** for his constant support and encouragement, especially in the final phase of my thesis work.

I am thankful to Office Staff of ISP, Librarians of various departments and the people of USIC for their timely help.

The most important and integral part of this thesis is provided by **Council of Scientific and Industrial Research, India** in the form of Junior and Senior Research Fellowships. I also thank **NUFFIC** for the financial assistance through ISP-MHO program.

I am in loss of words to express my gratitude to **my loving parents, brother and sister** for the support, love and encouragement that they have given throughout my life. Their appreciation and wishes even in my small achievements, has always been a source of motivation for me. I am sure that I would not have been able to achieve anything without their support, help and prayers.

Above all, my gratitude towards the power that controls everything, without his blessings and mercy we cannot accomplish anything in this world. Thank **God**.

**Binoy Paul**

# CONTENTS

## **Chapter 1: Introduction to Nonlinear Optics and its Applications**

1.1 Introduction	3
1.2 Origin of Optical Nonlinearity	3
1.3 Mathematical Description of Optical Nonlinearities	5
1.3.1 Maxwell's Equations for nonlinear materials	5
1.3.2 Nonlinear Polarization	5
1.4 Specific nonlinear processes	9
1.4.1 Frequency Conversion Process	10
1.4.2 Self Action Effects	13
1.4.3 Coherent Optical Effects	17
1.4.4 Electro-optic and Magneto-optic effects	17
1.5 Susceptibility tensor and hyperpolarizability	17
1.6 NLO materials	18
1.6.1 Organic materials	20
1.6.2 NLO-Chromophore functionalised polymers	22
1.6.3 Organometallic Compounds	22
1.6.4 Liquid Crystals	24
1.6.5 Biomaterials	24
1.6.6 Nanoparticles	24
1.6.7 Semiconductors	24
1.7 Physics of NLO Behaviour in Organic Molecules	25
1.8 Applications	26
1.8.1 Nonlinear Spectroscopy	26
1.8.2 Harmonics Generation and frequency mixing	27
1.8.3 Frequency Up-Conversion	28



1.8.4 Optical short pulse generation and measurement	28
1.8.5 Optical Phase Conjugation	29
1.8.6 Nonlinear optical effects in optical communications	30
1.8.7 Optical switching	30
1.8.8 Optical limiting	31
1.9 Present work	32
1.10 References	34

## **Chapter 2: Experimental Techniques and Details: Z-Scan and Degenerate Four Wave Mixing**

2.1 Introduction	39
2.2 Z-Scan Technique	39
2.3 Open aperture Z-scan for absorptive nonlinearity	42
2.4 Theory of open aperture Z-scan technique	44
2.5 Closed aperture Z-scan	45
2.6 Theory of closed aperture Z-scan technique	48
2.7 Merits and demerits of z-scan techniques	52
2.8. Degenerate four-wave mixing (DFWM)	53
2.9 Theory of DFWM	58
2.10 Characteristic Properties of Phase Conjugate Waves	61
2.11 Applications of Phase-Conjugate Light	61
2.11.1 Optical Resonator	62
2.11.2 Laser Fusion	62
2.11.3 Optical image transmission	62
2.11.4 Interferometers	62
2.11.5 Optical frequency filters	63
2.11.6 Optical pulse compression	63
2.12 Instruments specifications	63

2.12.1 Pulsed Nd: YAG laser	63
2.12.2 MOPO	63
2.12.3 Photodiodes	64
2.12.4 Oscilloscope	64
2.12.5 Energy meter	64
2.12.6 Spectrophotometer	64
2.13 Reference	65

**Chapter 3: Nonlinear Optical Studies on Samarium Phthalocyanine in Methyl Methacrylate using Z-Scan and Optical Limiting Techniques**

3.1 Introduction	69
3.2 Experimental	71
3.3 Effective nonlinear absorption coefficient	71
3.4 Rate equations	72
3.5 Results and discussion	74
3.6 Concentration Dependence	83
3.7 Conclusion	86
3.8 References	88

**Chapter 4: Z-Scan and Degenerate Four Wave Mixing Studies in Metal Complexes of Quinoxaline-2-Carboxalidene-2-Aminophenol**

4.1 Introduction	93
4.2 Experimental	94
4.2.1 Sample Preparation	94
4.2.1.1 Preparation of Quinoxaline-2-Carboxaldehyde	94
4.2.1.2 Preparation of Quinoxaline-2-Carboxalidene -2-aminophenol (HQAP)	95
4.2.1.3 Preparation of metal complexes	96

4.2.2 Degenerate Four Wave Mixing	97
4.2.2.1 Calibration	98
4.2.3 Z-Scan	99
4.3 Results	100
4.3.1 Degenerate Four Wave Mixing	101
4.3.2 Z-Scan	106
4.4 Discussion	108
4.5 Optical Limiting	112
4.6 Conclusions	114
4.7 References	115

## **Chapter 5: Z-Scan and Degenerate Four Wave Mixing Studies on Certain Selected Tetra Phenyl Porphyrins**

5.1 Introduction	121
5.2 Experimental	125
5.2.1 Degenerate Four Wave Mixing	125
5.2.1.1 Calibration	127
5.2.2 Z-Scan	128
5.3 Results	129
5.4 Wavelength Dependence	134
5.5 Solvent Effect	135
5.6 Optical Limiting	139
5.7 Discussion	140
5.8 Conclusions	143
5.9 References	144

**Chapter 6: DFWM Studies on Cobalt Ternary Complexes of 2-Hydroxy  
Acetophenone N(4) Phenyl Semicarbazone Containing Heterocyclic Coligands**

6.1 Introduction	151
6.2 Experimental	153
6.2.1 Sample Preparation	153
6.2.1.1 Preparations of H <sub>2</sub> L	153
6.2.1.2 Synthesis of complexes	154
6.2.2 Degenerate Four Wave Mixing	154
6.2.2.1 Calibration	155
6.3 Results	156
6.4 Discussion	159
6.5 Conclusion	161
6.6 References	162

**Chapter 7: General Conclusion and Future Prospects**

7.1 General Conclusion	165
7.2 Future Prospects	168

## **Chapter 1**

# **Introduction to Nonlinear Optics and its Applications**

### **Abstract**

Basic concepts of nonlinear optics are introduced in this chapter. Physical origin of nonlinearity, specific nonlinear processes, important nonlinear optical materials and applications are explained in detail. Photo-physics of nonlinear optical behaviour of organic molecules are also presented. A brief account of the present work is given at the end.

### 1.1 Introduction

Optics is a subject that studies the properties and propagation of light and its interaction with matter. Because the light intensities that usually occur in nature are relatively low, the optical properties of materials can be considered independent of the light intensity to a very good approximation. Nonlinear optical phenomena do not show up in our daily life [1]. However, with the advent of the laser in 1960 [2], it became possible to create, in laboratories, conditions of illumination so intense that the optical properties were found to depend on the intensity. The medium then reacts to illumination and alters the optical field in a nonlinear way. Matter thus makes itself the vector of the interaction of light waves that would otherwise remain unaffected mutually. Nonlinear optics is thus the science that deals with the nonlinear action of light upon itself through its coupling to matter. Observation of the second harmonic generation (SHG), a process by which two photons of the same frequency are converted into a single photon with a doubled frequency, by P A Franken in 1961 marked the birth of nonlinear optics as a new discipline in the area of laser-matter interaction. Franken observed that light of 347.1 nm could be generated when a quartz crystal was irradiated with light of 694.2 nm, obtained from a ruby laser [3]. In the decade that followed, many other nonlinear optical effects were identified [4]. Even though some types of interaction are observable in certain types of materials and some materials are better suited to specific nonlinear interactions than others, nonlinear optical interactions of various kinds can occur in all types of materials. The discovery of different types of nonlinear optical materials and their applications in various fields of science and technology made the nonlinear optics a fascinating field of research and developments.

### 1.2 Origin of Optical Nonlinearity

When an electromagnetic wave propagates through a medium it induces electric polarization and magnetization in the medium. Motion of the electrons and nuclei in response to the field in the incident waves is responsible for the induced electric

## Investigations of nonlinear .....

polarization and magnetization in the medium. These induced polarizations and magnetizations oscillate at frequencies determined by a combination of the properties of the material and the frequencies contained in the incident light waves. This will result in the interference of the fields radiated by the induced polarizations or magnetizations and the incident fields. At low optical intensities, the induced polarization and magnetizations are proportional to the electric or magnetic fields in the incident wave and the response of the medium is termed linear. Various linear optical interactions can occur depending on the specific properties of the induced polarizations. Refraction, absorption, elastic and inelastic scattering etc are linear when the intensity of the interacting radiations is low. But when the intensity of the incident radiation is high enough the response of the medium changes qualitatively from its behaviour at low intensities and it produces nonlinear optical effects. Some nonlinear optical interactions arise from the large motion of the electrons and ions in response to the stronger optical fields. In most materials the electrons and ions are bound in potential wells. For small displacements from the equilibrium motion of the electrons and ions are harmonic but for larger displacements the motion is anharmonic [5]. As long as the optical intensity is low the electron or ion moves in the harmonic part of the well. In this regime the induced polarizations can oscillate only at frequencies that are contained in the incident waves and the response is linear. When the incident intensity is high enough the charges can be driven into the anharmonic portion of the potential well. The additional terms in the potential introduce terms in the induced polarization that depend on the second, third or higher powers of the incident fields, giving rise to nonlinear responses [6-8]. Parametric frequency mixing and various forms of harmonic generations are examples for this type nonlinear optical process.

A second type of nonlinear response results from a change in some property of the medium caused by the optical wave. When the optical field is strong enough it can change certain characteristics of the medium, which in turn changes the way the

medium affects the optical wave resulting in a nonlinear optical response. An example of such a response is a change in the refractive index of a medium induced by the optical wave. Many of the propagation characteristics of optical waves are determined by the refractive index of the medium [6].

### 1.3 Mathematical Description of Optical Nonlinearities

#### 1.3.1 Maxwell's Equations for nonlinear materials

The propagation of an optical wave in a medium is described by the Maxwell's equation for the optical fields and a specification of the dependence of the induced polarization and magnetizations on the optical fields. The Maxwell's equation for the electric field of an optical wave in a medium is [9]

$$\nabla^2 E(r,t) - \frac{1}{c^2} \frac{\partial^2 E(r,t)}{\partial t^2} = \mu_0 \frac{\partial^2 P(r,t)}{\partial t^2} - \frac{\partial [\nabla \cdot M(r,t)]}{\partial t} \quad (1.1)$$

where  $E(r,t)$  is the electric field of the optical wave and the terms in the right are the induced polarization ( $P$ ) and magnetization ( $M$ ). Maxwell's equations describe only half of the nonlinear problem. They only show how a nonlinear polarization generates another wave through an equation in which only derivatives of the electric field appear on the left hand side and only the induced nonlinear polarization appears as a driving term on the right hand side. Maxwell's equations do not address how a nonlinear polarization is generated by electric fields.

#### 1.3.2 Nonlinear Polarization

With the advent of lasers the electric field that can be generated with a medium is of the order of inter atomic fields within the medium itself. At such high fields the relationship between the electric polarization  $P$  and the field strength  $E$  ceases to be linear and some interesting nonlinear effects come to the fore. A dielectric medium



Investigations of nonlinear .....

when placed in an electric field is polarized, if the medium does not have a transition at the frequency of the field. Each constituent molecule act as a dipole with a dipole moment  $P_i$ . The dipole moment per unit volume  $P$  is given by

$$P = \sum_i P_i \quad (1.2)$$

where the summation is over the dipoles in the unit volume. The orienting effect of the external field on the molecular dipoles depend both on the properties of the medium and on the field strength. Therefore we can write [10]

$$P = \epsilon_0 \chi E \quad (1.3)$$

where  $\chi$  is called the polarizability or dielectric susceptibility of the medium. Eq. (1.3) is valid for the field strength of conventional sources. The quantity  $\chi$  is a constant only in the sense of being independent of  $E$ . The magnitude is a function of the frequency of the field used. With sufficiently intense laser radiation the relation does not hold good and has to be generalized to [10]

$$P = \epsilon_0 \left( \chi^{(1)} E + \chi^{(2)} E^2 + \chi^{(3)} E^3 + \dots \right) \quad (1.4)$$

where  $\chi^{(1)}$  is the same as  $\chi$  in Eq. (1.3). The coefficients  $\chi^{(2)}$ ,  $\chi^{(3)}$ , ..... define the degree of nonlinearity and are known as nonlinear susceptibilities. When the field strength of the radiation used is sufficiently low then only the first term of the Eq. (1.4) needs to be retained and the phenomenon that shows such behaviour belongs to the linear optics. As the strength of the field increases the higher order terms become more and more significant and this aspect forms the basis of nonlinear optics. Therefore, the medium of which the polarization is described by a nonlinear relation of the type Eq. (1.4) is called a "nonlinear medium"

In Eq. (1.4) the symbol  $E$  denotes the total field, which is often made up of a number of different waves at different frequencies, polarizations,  $k$  vectors etc. Thus, there are usually many terms in the expression for  $E$ . For this reason, each  $\chi$  in Eq. (1.4) has several components. Each nonlinear susceptibility is identified by the superscript  $n$  and each is written as a function of several frequencies, the first frequency being that of the induced nonlinear polarization and the remaining  $n$  frequencies being those of the  $n$  input light waves.

**(a) Linear Terms**

The  $\chi^{(1)}$  terms in Eq. (1.4) correspond to linear optical properties including index of refraction, absorption, gain and birefringence. These properties constitute the subject of classical optics. In a linear medium, waves pass through each other without influencing each other.

**(b) Second Order Terms**

The  $\chi^{(2)}$  term in Eq. (1.4) correspond to second order effects, which in general can be called three wave mixing. These effects are (a) Second Harmonic Generation [ $\chi^{(2)}(2\omega; \omega, \omega)$ ], Optical Rectification [ $\chi^{(2)}(0; \omega, -\omega)$ ], Parametric Mixing [ $\chi^{(2)}(\omega_1 \pm \omega_2; \omega_1, \pm \omega_2)$ ], Pockels effect [ $\chi^{(2)}(\omega; \omega, 0)$ ]. These effects occur only in materials that lack inversion symmetry. In second harmonic generation and parametric mixing the conversion efficiency is determined by phase matching conditions defined by relation [11]

$$\frac{\partial E}{\partial z} + \frac{n_0}{c} \frac{\partial E}{\partial t} = \pm i \frac{2\pi k}{n_0^2} P \tag{1.5}$$

The process will be efficient only when the newly created nonlinear polarization is modulated at the appropriate frequency and  $k$  vector. These conditions can be adjusted by changing propagation angles, light frequencies and material temperatures.

Investigations of nonlinear .....

### (c)Third Order Terms

The  $\chi^{(3)}$  terms in Eq. (1.4) corresponds to the third order effects and the third order effects occur independently of whether or not a material possesses inversion symmetry. The most common third order effects are Third Harmonic Generation [ $\chi^{(2)}(3\omega; \omega, \omega, \omega)$ ], Non-degenerate Four Wave Mixing [ $\chi^{(3)}(\omega_1 + \omega_2 \pm \omega_3; \omega_1, \omega_2, \pm \omega_3)$ ]; Raman Scattering [ $\chi^{(3)}(\omega \pm \Omega; \omega, -\omega, \omega \pm \Omega)$ ]; Instantaneous AC Kerr effect (Degenerate Four Wave Mixing) [ $\text{Re}(\chi^{(3)}(\omega; \omega, \omega, -\omega))$ ]; Brillouin Scattering [ $\chi^{(3)}(\omega \pm \Omega; \omega, -\omega, \omega \pm \Omega)$ ]; DC Kerr effect [ $\text{Re}(\chi^{(3)}(\omega; \omega, 0, 0))$ ]; Two Photon Absorption [ $\text{Im}(\chi^{(3)}(\omega; \omega, -\omega, \omega))$ ] and Electric Field Induced Second Harmonic Generation [ $\chi^{(3)}(2\omega; \omega, \omega, 0)$ ] [8]. Since the third order nonlinear effects is not affected by the symmetry of the crystal structure, all the materials in the universe exhibits third order nonlinearity. The real and imaginary part of the third order nonlinear susceptibility tensor are important in applications like optical switching, optical limiting etc [12, 13]. The general constitutive equation for the third order process can be written as [7]

$$\vec{P}_i^{(3)}(r, t) = \sum_{a,d,c} \chi_{ijkl}^{(3)}(\omega_a + \omega_b + \omega_c, \omega_a, \omega_b, \omega_c) E_j(\omega_a, \vec{r}) E_k(\omega_b, \vec{r}) E_l(\omega_c, \vec{r}) \quad (1.6)$$

in the above equation we have neglected the nonlocal terms.

Unlike in the case of linear optical interactions two light beams can interact and exchange energy through nonlinear interaction with the medium [7]. In the case of very intense laser beams, even air itself can act as nonlinear medium. It is well known that femtosecond laser pulses get self-focussed in air [14]. One of the best examples of nonlinear process is the generation of super continuum (white light), which occurs when some materials are irradiated with terra watts of power. Many of these nonlinear optical effects have important scientific and technological relevance. Therefore, study of nonlinear effects is very important. It helps us to understand the mechanism of nonlinearity as well as its spatial and temporal evolution. Besides,

detailed knowledge of NLO processes and their dynamics is also essential for the implementation of these techniques in appropriate areas of technology such as optical switching [15], optical communication [16], passive optical power limiting [17-19], data storage [20], design of logic gates [21-22].

Another important parameter in the nonlinear interaction is the wavelength of the radiation which is interacting with the medium. If the wavelength of excitation is close to one, two or three photon resonance, resonance enhancement will occur in the medium. Moreover at and near resonance frequencies, refractive index becomes a complex quantity. If wavelength of the light interacting with matter is at or near resonance, the power series expansion as in Eq.(1.4) is not relevant. In the case of resonant excitation [7] (one photon, two-photon or three-photon), the nonlinear susceptibility term corresponding to resonant absorption can have enormously large magnitude. Generally, resonant nonlinearity has large magnitude but slow response whereas, non-resonant nonlinearity is very fast in response but small in magnitude. Usually observed nonlinear susceptibility is due to the response of weakly bound outer most electrons of atoms or molecules. However, if the wavelength of excitation is very close to any of resonance frequency, magnitude of nonlinearity can be much higher. If the expansion of nonlinear polarization as power series in electric field is valid, the corresponding nonlinearity is called weak nonlinearity. On the other hand, if the frequency of excitation is very close to resonance, power series expansion as in Eq. (1.4) is not correct. Such nonlinearity is called strong nonlinearity [7].

### **1.4 Specific nonlinear processes**

Nonlinear optical processes can be classified into various categories. Generally they belong to the following categories (a) Frequency Conversion Process, (b) Self-action effects, (c) Coherent Optical Effects and (d) Electro Optic and Magneto Optic effects [9].

## Investigations of nonlinear .....

### 1.4.1 Frequency Conversion Process

Frequency conversion processes are those that involve the generation of radiation at wavelengths other than the ones that are contained in the incident radiation. Typical frequency conversion geometry is illustrated in Fig. 1.1

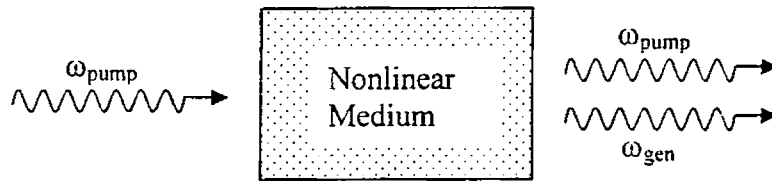


**Fig. 1.1** Schematic illustration of a typical geometry used in frequency conversion interactions. Input radiation is supplied at one or more incident frequencies ( $\omega_{\text{pump}}$ ). The wave at  $\omega_{\text{gen}}$  is generated through the nonlinear interaction

The major reason for the frequency conversion process is the second and third order effects explained earlier. The frequency conversion processes due to the second order effects are second harmonic generation, three wave sum-frequency mixing, three wave difference-frequency mixing and parametric down conversion. The frequency conversion processes like Stimulated Raman Scattering and Stimulated Brillouin Scattering are due to the third order nonlinear effects.

#### (a) Second Harmonic generation

In second harmonic generation, radiation at an incident frequency  $\omega_1$  is converted to radiation at twice the frequency of the incident radiation i.e.

$$\omega_2 = 2\omega_1 \quad (1.7)$$

It is observed only in non-centro symmetric crystals and the constitutive equation for typical second order process, under dipole approximation, is given by [5]

$$P_i^{(2\omega)} = \sum_{j,k=x,y,z} d_{ijk}^{2\omega} E_j^{(\omega)} E_k^{(\omega)} \quad (1.8)$$

Efficiency of SHG is proportional to phase mismatch  $\Delta k$  as given by the relation [5]

$$\eta_{SHG} \propto \frac{\sin^2(\Delta kl/2)}{(\Delta kl/2)^2} \quad (1.9)$$

It is obvious that as  $\Delta k$  deviate from zero, the conversion efficiency steadily decreases

### (b) Frequency mixing

The three wave sum frequency mixing is used to generate radiations at higher frequencies than those in the pump radiation. The laser beams at  $\omega_1$  and  $\omega_2$  interact in a nonlinear crystal and generate a nonlinear polarization  $P^{(2)}$  ( $\omega_3 = \omega_1 + \omega_2$ ). The generated radiation will have maximum intensity when the phase matching condition is satisfied. Just like the three wave sum frequency mixing is used for the generation of radiations with higher frequencies three-wave difference frequency mixing can be used for the generation of radiations with frequency less than the pump frequencies. Frequency of the generated radiation will be the difference in frequency between the two pump radiations interacting with the nonlinear medium i.e.  $\omega_3 = \omega_1 - \omega_2$  where  $\omega_1$  and  $\omega_2$  are the pump frequencies and  $\omega_3$  is the frequency of the generated radiation [7].

Investigations of nonlinear .....

**(c) Parametric down conversion**

Parametric down conversion is used to convert an optical radiation at frequency  $\omega_1$  into two optical waves at lower frequencies  $\omega_2$  and  $\omega_3$  according to the relation

$$\omega_1 = \omega_2 + \omega_3 \quad (1.10)$$

This process is illustrated schematically in Fig. 1.2

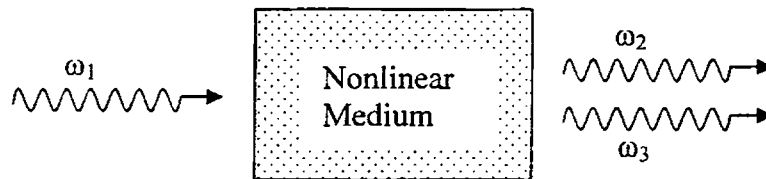


**Fig. 1.2** Schematic illustration of the waves used in parametric down conversion. Radiation at  $\omega_1$  is supplied and radiation at  $\omega_2$  and  $\omega_3$  are generated in the nonlinear interaction.

If there is no incident intensity supplied at  $\omega_2$  and  $\omega_3$  the process is termed parametric generation or parametric oscillation depending on the geometry. If the interaction involves a single pass through the nonlinear medium the process is termed parametric generation and this geometry is typically used with picoseconds pulses for generation of tunable infrared or visible radiation from pump radiation in the ultraviolet, visible or near infrared. Parametric down conversion can also be used with a resonant cavity that circulates the radiation at either or both of the generated frequencies. In this geometry the process is termed parametric oscillation. Optical parametric oscillators are typically used with pump radiation from Q-switched lasers with pulses lasting several tens of nanoseconds, allowing several passes of the generated radiation through the cavity while the pump light is present [23]. One of the

~~primary~~ uses of parametric down conversion is the generation of tunable radiation at ~~wavelengths~~ ranging from the visible to far infrared and the tuning is done by varying ~~one of the~~ phase matching parameters such as angle or temperature.

~~546:11~~

### **(d) Stimulated Raman scattering**

Stimulated Raman scattering can occur in solids, liquids, gases and plasma. It involves frequency shifts ranging from several tens of reciprocal centimeters for rotational scattering in molecules to tens of thousands of reciprocal centimeters for electronic scattering in gases. Forward stimulated Raman scattering is commonly used for generation of coherent radiation at the Stokes wavelength, amplification of an incident wave at the Stokes wavelength, reduction of beam aberrations, nonlinear spectroscopy, generation of tunable infrared radiation etc. Backward stimulated Raman scattering can be used for wave generation, amplification, pulse compression, phase conjugation etc [24].

### **(e) Stimulated Brillouin scattering**

Stimulated Brillouin scattering involves scattering from high frequency sound waves. This can be observed in almost all phases of matter in the universe. Generally, stimulated Brillouin scattering has a higher gain than stimulated Raman scattering in liquids and usually dominate the interaction for wave generation when the laser radiation consists of narrow band pulses that are longer than the response time of the acoustic phonon. In liquids and gases SBS is used most commonly for phase conjugation and for pulse compression. In solids, SBS is not commonly used for this purpose because the material can be easily damaged by the acoustic waves generated in the medium.

### **1.4.2 Self Action Effects**

Self-action effects are those that affect the propagation characteristics of the incident light beam. They are due to nonlinear polarizations that are at the same frequency as



## Investigations of nonlinear .....

that of the incident light wave. Depending on the particular effect they can change the direction of propagation the degree of focusing, the state of polarization or the bandwidth of the incident radiation. Self-action effects can also change the amount of absorption of the incident radiation. Sometimes one of these effects can occur alone but more commonly two or more of them occur simultaneously. The most common self-action effects arise from third order interactions. The various types of self-action effects depend on whether the susceptibility is real or imaginary and on the temporal and spatial distribution of the incident light. The real part of the nonlinear susceptibility gives rise to the spatial effects of self-focusing, self-defocusing, spectral broadening and changes in the polarization vector. The imaginary part of the susceptibility causes nonlinear absorption. The important self-action effects are self-focusing, self-defocusing, self-phase modulation, nonlinear absorption and saturable absorption.

### (a) Self-Focusing

The real part of the third order susceptibility causes a change in the index of refraction of the material according to the relation

$$n = n_1 - n_2 \langle E^2 \rangle \quad (1.11)$$

where

$$n_2 = \left( \frac{3}{4n_1} \right) \chi' \quad (1.12)$$

In Eq. 1.11 and 1.12  $\langle E^2 \rangle$  is the time average of the square of the total electric field which is proportional to the intensity,  $n_1$  and  $n_2$  are the linear and nonlinear refractive indices and  $\chi'$  is the real part of  $\chi$ . Self-focusing occurs as a result of a combination of a positive value of  $n_2$  and an incident beam that is more intense in the center than at the edge. In this situation the refractive index at the center of the beam is greater than

that at its edge and the optical path length for rays at the center is greater than that for rays at the edge. This is the same condition that occurs for propagation through a focusing lens and as a result the light beam creates its own positive lens in the nonlinear medium. As the beam focuses the strength of the nonlinear lens increases causing stronger focusing and increasing the strength of the lens still further. This behaviour results in catastrophic focusing in which the beam collapses to a very intense small spot in contrast to the relatively gentle focusing that occurs for normal lenses. Self-focusing can occur in any transparent material at sufficiently high intensities and has been observed in wide range of materials including glasses, crystals, liquids, gases and plasmas [24].

**(b) Self-defocusing**

Self defocusing results from a combination of a negative value of  $n_2$  and a beam profile that is more intense at the center than at the edge. In this situation the refractive index is smaller at the center of the beam than at the edge, resulting in a short optical path for rays at the center than for those at the edge. This is the same condition that exists for propagation through a negative focal length lens and the beam defocuses.

**(c) Self-Phase Modulation**

Self phase modulation results from a combination of a material with a nonlinear refractive index and incident field amplitude that varies in time. Because of the index of refraction depends on the optical intensity the optical phase which is given by

$$\phi = kz - \omega t = \frac{2\pi}{\lambda} \left[ n_0 - \frac{1}{2} n_1 |A(t)|^2 \right] z - \omega t \tag{1.13}$$

develops a time dependence that follows the temporal variation of the optical intensity. The phase shift incurred by an optical beam of power P and cross sectional area A traveling a distance in the medium is given by

Investigations of nonlinear .....

$$\Delta\phi = 2\pi n_1 \frac{l}{\lambda_0 A} P \quad (1.14)$$

which is proportional to the optical power P. Self phase modulation is useful in applications in which light controls light. For example it can be used for compression of optical pulses in a manner similar to pulse compression in chirped radar. Pulse compression of factors of 10 or more have been achieved with self phase modulation of pulses propagated freely in nonlinear media resulting in the generation of subpicosecond time range.

#### **(d) Nonlinear Absorption**

Self action effects can also change the transmission of light through a material. Nonlinear effects can cause materials that are strongly absorbing at low intensities to become transparent at high intensities in an effect termed ‘saturable absorption’ or they can cause materials that are transparent at low intensities to become absorbing at high intensities in an effect termed ‘multiphoton absorption’. The multiphoton absorption can occur through absorption of two, three or more photons. The photons can be of the same or different frequencies. When the frequencies are different the effect is termed sum frequency absorption.

#### **(e) Saturable absorption**

Saturable absorption involves a decrease in absorption at high optical intensities and it is usually observed in materials that are strongly absorbing at low light intensities. Saturable absorption occurs when the upper state of the absorbing transition gains enough population to become filled, preventing the transfer of any more population into it. Saturable absorption is used to mode lock solid state and pulsed dye lasers [25]. It can also be used with four wave-mixing interactions to produce optical phase conjugation [26].

### 1.4.3 Coherent Optical Effects

Coherent nonlinear effects involve interactions that occur before the wave functions that describe the excitations of the medium have time to relax or dephase. They occur primarily when the nonlinear interaction involve one or two photon resonances and the duration of the laser pulse is shorter than the dephasing time of the excited state wave function. Coherent nonlinear optical interactions generally involve significant population transfer between the states of the medium involved in the resonance [27]. As a result the nonlinear polarization cannot be described by the Eq. 1.4 which assumes that the population was in the ground state. It must be solved for as a dynamic variable along with the optical fields. Self induced transparency, Photon echoes etc. are examples for the effects produced due to the coherent interactions.

### 1.4.4 Electro-optic and Magneto-optic effects

Electro optic and magneto optic effects involve change in the refractive index of a medium caused by an external electric or magnetic field. These are not normally thought of as nonlinear optical effects but are technically nonlinear optical processes in which the frequency of one of the fields is equal to zero. Pockel's effect, quadratic Kerr effect, Farady effect, Cotton Mouton effect etc. are examples for various types of electro-optic and Magneto optic effects. Electro-optic and magneto-optic effects generally cause changes in the refractive indexes in different direction relative to the applied field or the crystal axes resulting in field induced birefringence. Electro optic and Magneto optic effects are commonly used in light modulators, shutters etc. [28]

### 1.5 Susceptibility tensor and hyperpolarizability

The constitutive equation between electric displacement  $D$  and electric field  $E$  can be written as

$$D = \epsilon E = \epsilon_0 E + P_l \quad (1.15)$$

## Investigations of nonlinear .....

where  $\epsilon$  and  $\epsilon_0$  are the permittivities of the medium and free space respectively related by the equation  $\epsilon = \epsilon_0 \epsilon_r$  and  $P_l$  is the linear polarization. In an isotropic media the induced polarization is along the direction of external electric field. But in anisotropic materials, electric induction vector is not oriented along the direction of inducing field alone, but it can have components in other directions as well. Magnitude of different components is usually different. Since refractive index (and hence velocity of light) is related to polarization, non-parallelism between the cause (excitation) and response (polarization) gives rise to optical anisotropy. Therefore, susceptibility is generally a tensor. Optical double refraction is the most familiar example of optical anisotropy. In the case of solids, the origin of non-parallelism between the response and excitation can be found in the crystalline nature of matter. In this type of materials, the vectorial nature of light is very important [29].

The  $n^{\text{th}}$  order susceptibility  $\chi_{i_1, \dots, i_n}^{(n)}$  is a tensor of rank  $(n+1)$  and the elements are subject to symmetry conditions relevant to geometry, dispersion properties and the class of materials. The susceptibilities are complex quantities having in phase as well as quadrature components. For example, in the case of linear susceptibility  $\chi^{(1)}$  the in-phase component describes the refractive index while the quadrature component gives absorption. Since  $(\chi^{(1)}E + \chi^{(3)}EEE)$  can be written as  $(\chi^{(1)} + \chi^{(3)}E^2)E$  we can infer that due to the third order term the refractive index governed by  $\chi^{(1)}$  gets modified by the term  $\chi^{(3)}E^2$  such that  $n$  becomes now dependent on the light intensity (proportional to  $E^2$ ). Similar effects on the refractive index are produced by  $\chi^{(5)}$  etc. so that nonlinearity leads to a functional dependence of refractive index on the light intensity [10].

### 1.6 NLO materials

The development of photonic technology during the past decade has intensified research activities on searching for new materials that display unusual and interesting

## Chapter 1. Introduction

**NLO properties.** New NLO materials are the key elements to future photonic technologies in which their functions can be integrated with other electrical, optical and magnetic components that have become important in the era of optical communication. Organic molecular and polymeric materials are relatively newcomers in the field of nonlinear optics compared with inorganic materials. The third order optical nonlinearities of inorganic materials are large but their response time is relatively slow [30- 33]. Large third order NLO susceptibilities have been measured in inorganic semiconductors using them as quantum wire and quantum dot materials

Recently, research activities have been directed towards developing new organic molecular and polymeric materials. The superiority of organic materials has been realized because of their versatility and possibility of tailoring material properties by applying the techniques of molecular engineering to them for particular end-uses. In addition organic materials also exhibit large nonlinear figure of merit, high damage thresholds, and ultrafast response time.

The applications of NLO materials are widespread in the field of solid state technology that includes harmonic generators, optical computing, telecommunications, laser lithography, image processing, sensors and over all optical systems. This shows that the study of NLO properties is truly an interdisciplinary area of research. The development of new materials can shed light on the theoretical understanding of the origin of NLO processes. Every year a wide variety of new NLO molecular and polymeric materials are discovered and the field continues to expand rapidly. Since the level of integration is also increasing rapidly in photonic technologies, organic polymers seem more promising compared with inorganic counterparts because of their compatibility with a variety of materials used in fabrication technology. Organic liquids, molecular solids, conjugated polymers and related model compounds, NLO chromophore functionalized polymers, organometallic compounds, organic composites, liquid crystals, semiconductors,

Investigations of nonlinear .....

nonparticles etc. are different types of nonlinear materials used for various applications in the photonic industry and a brief description of the important NLO materials is given below.

### **1.6.1 Organic materials**

As mentioned earlier the organic materials are the most promising candidates for the NLO applications because of their unique diversity and the ability to be tailored with variety of chromophores for the exogenous variables that stimulate photonic functions in a desirable manner. Moreover they also exhibit large nonlinear figure of merit, high damage thresholds, and ultrafast response time. Most of the compounds investigated in this thesis belong to this class.

#### **(a) Organic Liquids**

Studies on the third order nonlinear optical properties of wide variety of organic liquids and solvents have been made and these studies reveal that the third order nonlinear parameters are influenced by the number of carbon atoms, substituents, donor acceptor functionalities and  $\pi$  electron system present in the NLO materials. Benzene, Stilbene, nitrobenzene, nitrocyclohexane, carbon tetrachloride, chloroform, dichloromethane etc. are some of the organic liquids exhibiting NLO properties [34,35,36]. Some of these organic solvents are used for solubilizing organic solids and as a result, knowledge of their NLO parameters is necessary to apply suitable corrections to the measurement techniques.

#### **(b) Molecular Solids**

Various types of Dyes, charge transfer complexes and fullerenes are examples for this class of compounds showing nonlinear optical properties. The NLO properties of different types of dyes have been reported by several authors [37-41]

In charge transfer complexes the optical nonlinearity originates from the supermolecular electronic polarization along the charge transfer axis. Huggards et al. [75] measured the third order nonlinear susceptibility of one dimensional  $\alpha$ -(BEDT-TTF)<sub>2</sub>I<sub>3</sub> complex by DFWM technique and showed that the third order susceptibility strongly depends on the wavelength of excitation. Charge transfer complexes form an interesting class of NLO materials [42-44]

Carbon clusters have attracted attention for more than two decades. They are important and fascinating materials because of their chemistry and unique physics coupled with material science. C<sub>60</sub> has the symmetry of icosahedral group and consists of a large number of  $\pi$  electrons. The nonlinear optical properties of fullerenes in solution, thin film and solid medium like PMMA were most extensively investigated [45-48]. Third order optical nonlinearity measurements and theoretical calculations indicate that fullerenes are promising materials for third order nonlinear optics.

### (c) Conjugated Polymers

Conjugated organic polymers emerged as a new class of NLO materials. Organic polymers are expected to possess the following desirable properties to show their potential for NLO devices. They are (a) large third order NLO susceptibility, (b) fast response time (c) High resistance to laser radiation (d) low dielectric constant (e) wide bandwidth (f) Chemical tailoring of physical and optical properties (g) ease of processing into ultrathin films, fibers and liquid crystals (h) mechanical strength and flexibility (i) environmental stability and (j) nontoxicity. A combination of these physicochemical properties makes organic  $\pi$ -conjugated polymers ideal candidates for third order nonlinear optics applications. Unlimited opportunities for chemical modifications of the polymer properties keep them as fertile materials in NLO field. In particular, derivatives of polydiacetylenes, polyacetylenes, polythiophenes,



Investigations of nonlinear .....

polyaniline, Heteroaromatic ladder polymers etc. exhibit the largest third order NLO susceptibilities. [49-57]

### **1.6.2 NLO-Chromophore functionalised polymers**

Nonlinear optical chromophore functionalized polymers is a new class of NLO materials. The architectural flexibility of organic conjugated polymers provides easy modification of chemical structure according to the required functions of NLO prosperities and processibility into desired configurations. The  $\pi$ -electron conjugated system gives rise to the larger third order optical nonlinearity of these polymeric materials. Novel NLO polymers can be designed and synthesized by covalently attaching dye moiety to conventional polymers like PMMA, polystyrene etc. 3RDCVXY, 3RNO<sub>2</sub>, 2RNO<sub>2</sub>, 2A-PAA, AMPS-HC-1, AMPS-HC-2, DANS/MMA, PMMA-DR1 etc are examples for this class of NLO materials.[58-60]

### **1.6.3 Organometallic Compounds**

Like organic materials, organometallics also offer the advantages of architectural flexibility and ease of fabrication and tailoring. Organometallics have two types of charge transfer transitions, i.e. metal-to-ligand and ligand-to-metal. The metal ligand bonding displays large molecular hyperpolarizability caused by the transfer of electron density between the metal atom and the conjugated ligand systems. Furthermore, the overlapping of the electron orbitals of ligand with the metal ion orbital leads to larger intramolecular interactions in organometallic complexes. The diversity of central metal atoms, oxidation states, their size and nature of ligands help in tailoring materials to optimize the charge transfer interactions. Metallophthalocyanines, Naphthalocyanines, Metalloporphyrins, Polysilanes etc. belong to this class of NLO materials.

It is worth mentioning that metallophthalocyanines (MPcs) are not true organometallic compounds because there is no metal to carbon bonding in the

macrocycle. Still in some sense they may be regarded as organometallic materials. The MPcs possess exceptionally high thermal stability, ease of fabrication and processing, architectural flexibility and environmental stability which make them multipurpose material for solid state technology.

Each Phthalocyanine (Pc) unit contains 18  $\pi$  electrons [61-65]. The center hydrogen atom of free base Pcs has a lone-pair electrons, which make these compounds weakly acidic. The hole in the center of these macromolecules can accommodate hydrogen or metals ions. Accordingly, they are called metal free Pc ( $H_2Pc$ ) or metal Pc (MPc) [67]. Nearly 60 metal ions have been incorporated at the center of Pc ring [62, 64]. Idealized molecular structures, as are found in solution, are used to classify the molecular structures. These structures show the highest symmetry ( $D_{4h}$  and  $C_{4v}$ )[66]. The versatility of the macrocycle offers tremendous opportunities for tailoring of electronic and photonic functions through chemical modifications. Lanthanide and actinide metal ions can form homo or dimers of phthalocyanines  $M(Pc)_2$  [69-70]. Such compounds are called bis-phthalocyanines.

Metalloporphyrins are another class of two dimensional  $\pi$ -electron conjugated systems. Like metallophthalocyanines, they have a cyclic conjugated structure, a variety of central metal atoms can be incorporated into the ring structures and many modifications can be made at the peripheral sites of the ring. The structure of porphyrin in its free base form has  $D_{2h}$  symmetry. When a metal is substituted at the center of the porphyrin the  $D_{2h}$  symmetry changes to  $D_{4h}$  symmetry. [71-72]. Quinoxaline-2-Carboxalidene-2-Aminophenol (QAP) is another material belong to this class of compounds. The characterization of the nonlinear optical properties of Bis-Phthalocyanines, Tetra Phenyl Porphyrins and QAP's is the most important part of the present thesis and it will be discussed in detail in the succeeding chapters.

Investigations of nonlinear .....

#### **1.6.4 Liquid Crystals**

Liquid crystals are an interesting class of NLO materials because their physical properties can be controlled by achieving orientation from a modest field. The optical nonlinearities in liquids can arise from several mechanisms, from collective reorientations to electronic. An excellent review on the NLO response of liquid crystal has been published by Palffy-Muhoray [73]. Temperature as well as donor acceptor side chain substitutions can greatly influence the NLO properties of liquid crystals and they found important applications in electronic displays [74-75].

#### **1.6.5 Biomaterials**

Third order NLO properties of naturally occurring chemical species in Chinese tea, herbal medicine, black tea, chlorophyll and their solutions in chloroform have been the subject of interesting studies and they form another class of nonlinear optical materials.[76-77]

#### **1.6.6 Nanoparticles**

Nanomaterials, which include metal and semiconductor nanoparticles , carbon nanotubes, nanowires etc. are a new class of technologically important nonlinear optical (NLO) materials [78-81]. Nanophotonics and nanotechnology are relatively new and rapidly developing areas of science and technology, wherein the unique properties of confined electron in nanostructures are exploited. Metal nanoparticles may be considered as typical examples of nanomaterials, which form an intermediate region between the domain of atomic and molecular physics and that of condensed matter

#### **1.6.7 Semiconductors**

Semiconductors exhibit a broad range of diverse nonlinearities. Two photon absorption, free carrier absorption, the electronic Kerr effect and nonlinear refraction

associated with free carrier generation etc. can be observed in several semiconductors [82-83].

### 1.7 Physics of NLO Behaviour in Organic Molecules

The absorption electromagnetic radiation in molecules results in the excitation of electrons from their lower occupied states to higher molecular states. There are number of different possible path ways for de-excitation from these higher energy states to the lower states. The most favourable de-excitation path way depends on the type of the molecules and nature of electronic states involved in the process [84]. One of the interesting properties of electronically excited molecules is their tendency to re-emit radiation on returning to the ground state. By the light absorption two excited electronic states can be derived from electronic orbital configuration. In one state, the electron spins are paired and in the other the electron spins are unpaired. A state with paired spins remains as a single state in the presence of a magnetic field and is termed as singlet states. But a state with paired spins can interact with magnetic fields and splits into three quantized states and is termed as triplet states. An energy state is a display of the relative energies of these energy states of a molecule for a given fixed nuclear geometry [85].

The electronic ground state of a molecule is a singlet state and is denoted as  $S_0$ . The higher singlet states are denoted as  $S_1, S_2, S_3, \dots, S_n$ . Similarly the higher triplet states are denoted as  $T_1, T_2, T_3, \dots, T_n$ . Each electronic state has a broad continuum of levels and the optical transitions between these continua leads to broad absorption and emission spectra. Transition between singlet states are spin allowed and gives rise to strong absorption bands. Transitions between the ground level of one energy state and the higher vibrational states of the same level is also possible and these transitions occur within a few pico second time duration. Decay process included in this type of transitions are non-radiative in nature. From the first excited singlet state  $S_1$ , the molecule can relax back radiatively or non-radiatively to the

ground state  $S_0$  or cross over to the triplet state. The spontaneous radiative decay from  $S_1$  to  $S_0$  is known as Fluorescence and is governed by the life time of  $S_1$  state. The non-radiative transition from  $S_1$  to  $S_0$  state is known as Internal Conversion and the transition from  $S_1$  to  $T_1$  state is known as intersystem crossing. Similarly the decay from  $T_1$  to  $S_0$  can also be radiative or non-radiative. If this transition is radiative it is termed as Phosphorescence. Typical phosphorescence life times are in the range of milliseconds to microseconds and the life time of triplet state is generally large since the triplet-singlet transition is dipole forbidden. Under special experimental conditions the molecules in the ground state  $S_0$  can be excited to higher energy states  $S_n$ . These higher states relax back to the  $S_1$  state on a very fast time scale and generally this is of the order of few femto seconds. In certain cases, the  $T_1$  state can be populated by the intersystem crossing. Similarly the higher triplet states can also be populated under suitable conditions through the intersystem crossing in the upper states. Therefore, even though the direct absorption from singlet state to triplet state is forbidden by selection rule it can be populated indirectly and these type of transitions between the energy levels are responsible for most of the nonlinear phenomena observed in organic molecules.

## **1.8 Applications**

Nonlinear optics has found large number of applications in various fields of science and technology. Their contribution to the field of basic research also has special importance and it has helped us in understanding the mechanism of laser matter interaction in detail [20-25, 86-90]. Therefore the study of nonlinear optics is highly relevant and desirable. In this section, some of the applications of nonlinear optics are discussed.

### **1.8.1 Nonlinear Spectroscopy**

Nonlinear spectroscopy involves the use of a nonlinear optical interaction for spectroscopic studies. It makes use of the frequency variation of the nonlinear

ability to obtain information about a material in much the same way that variation of the linear susceptibility with frequency provides information in linear spectroscopy. In nonlinear spectroscopy the spectroscopic information is obtained directly from the nonlinear interaction as the frequency of the pump radiation is varied. Many different types of nonlinear effects can be used for nonlinear spectroscopy, including various forms of parametric frequency conversion, harmonic generation, four wave sum and difference frequency mixing, degenerate four wave mixing, multi photon absorption, multi photon ionization and stimulated scattering [7]. Nonlinear spectroscopy can provide information different from that available in linear spectroscopy. For example Doppler free spectroscopy makes use of nonlinear properties of materials for improving the spectral resolution obtainable in linear spectroscopy. Similarly nonlinear spectroscopy can be used for the measurement of the frequency of states that have the same parity as the ground state which is not accessible through linear spectroscopy, study of energy levels that are in the regions of the spectrum in which radiation for linear spectroscopy either gets absorbed or is not available, study of excited levels in materials providing information on their coupling strength to other excited states or to the continuum, study the kinetics of excited states such as life times, dephasing times, energy decay paths etc. Therefore the nonlinear spectroscopy is a wonderful tool in the hands of scientists for probing the mysteries of laser matter interaction.

### **1.8.2 Harmonics Generation and frequency mixing**

The mixing of optical frequencies in crystals provides a source of narrow band coherent radiation in various regions including those in which there are no primary lasers available. Primary laser radiation is available from the IR through the visible and UV. Optical frequency mixing has enabled researchers to extend the range of wavelength to the XUV reaching almost to the soft x-ray range. Currently it is the only source of coherent radiation in the XUV region. Frequency doubled YAG laser is the most popular source of green light. Frequency tripled YAG laser is used for

Investigations of nonlinear .....

fusion applications. Optical parametric oscillators, which work on the principle of parametric wave mixing, are now used to get continuously tunable laser output from 400nm to 2000nm [23].

### 1.8.3 Frequency Up-Conversion

A frequency up converter converts a wave of frequency  $\omega_1$  into a wave of higher frequency  $\omega_3$  by use of an auxiliary wave at frequency  $\omega_2$  called the pump. A photon  $\hbar\omega_2$  from the pump is added to a photon  $\hbar\omega_1$  from the input signal to form a photon  $\hbar\omega_3$  of the output signal at an up converted frequency  $\omega_3 = \omega_1 + \omega_2$

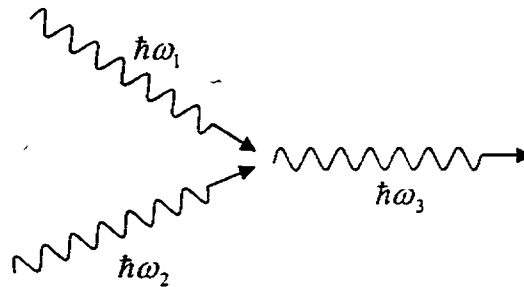


Fig. 1.3 Photon interaction in a frequency up converter

Materials in which this can be realized is useful for the detection of infrared radiations and many useful devices making use of this property is now available in market. [25]

### 1.8.4 Optical short pulse generation and measurement

Optical pulses having pulse width less than nanosecond can be obtained only by using nonlinear techniques. Mode locking is one of the promising techniques for the generation of short optical pulses [91]. Stankov et.al. proposed that intercavity harmonic generation could be used for pulse narrowing in lasers [92]. Parametric

mode locking demonstrated by Zhao and McGraw is another technique by which pulse compression can be realized [93]. Pulses as short as 65 fs over a broad tuning range were obtained by synchronously pumping an OPO resonator with Nd: Glass laser with negative feedback [94]. Laser pulses with enhanced chirp can be compressed in a grating pair compressor. Pulses of 50 fs at 920 nm were obtained by this technique with the natural chirp of frequency doubled pulses from Nd: Glass laser [95]. Additive mode locking, Self starting mode locking, Kerr lens mode locking etc. are various other techniques by which pulse compression is demonstrated [96]. Thus, appropriate nonlinear processes can realize generation and characterization of ultra short pulses.

### 1.8.5 Optical Phase Conjugation

Optical phase conjugation, also referred as time reversal or wavefront reversal, is a technique involving the creation of an optical beam that has the variations in its wavefront or phase reversed relative to a reference beam. If the optical field is represented as the product of an amplitude and complex exponential phase

$$E = Ae^{i\phi}$$

then the process of reversing the sign of the phase is equivalent to forming the complex conjugate of the original field, an identification that gives rise to the name phase conjugation. When the optical phase conjugation is combined with a reversal of the propagation direction it allows for compensation of distortions on an optical beam which develops as a result of propagation through distorting media. Therefore, optical phase conjugation finds large number of application like Optical resonators, Laser fusion, Optical image transmission, Interferometers, Optical frequency filters, Optical pulse compression etc [26, 97-98].



## Investigations of nonlinear .....

### **1.8.6 Nonlinear optical effects in optical communications**

One of the most important boosts of research in nonlinear optics came in the late 1970s with the advent of optical telecommunications systems using optical fibers and semiconductor lasers [99]. Current communication networks with fiber transmission lines have a much greater information-carrying capacity than conventional coaxial cable-based systems. Also, optical signals can be transmitted in fibers over tens of kilometers before requiring amplification. In these optical communication schemes, modulated semiconductor lasers are used for the generation of information-carrying light waves, and can also be used in repeaters, for the amplification of attenuated signals. Other important applications of semiconductor lasers include optical disks for information storage, barcode readers, and printers. Unfortunately, semiconductor lasers tend to react strongly to perturbations from the outside world. This leads to dynamical instabilities that can hamper technological progress. Therefore, it is not surprising that much research effort is devoted to the understanding and control of these instabilities. Sometimes, however, a highly pulsating laser response can be desirable for practical applications. Nowadays, the use of chaotic information carriers is contemplated for secure communication schemes [91].

### **1.8.7 Optical switching**

Nonlinear optical effects may be used to make all optical switches. In an all optical switch light controls light with the help of a nonlinear optical material. Nonlinear optical effects can be either direct or indirect. Direct effects occur at the atomic or molecular level when the presence of light alters the atomic susceptibility or the photon absorption rates of the medium. Optical Kerr effect and saturable absorption are examples for direct nonlinear optical effects. Indirect nonlinear effects involve an intermediate process in which electric charges and or electric fields play an important role in the nonlinear behaviour of the material. Indirect nonlinear effects can occur in Photorefractive materials, liquid crystal etc. The optical phase modulation in the Kerr medium may be converted into intensity modulation by placing the medium in one

leg of an interferometer so that as the control light is turned on and off the transmittance of the interferometer is switched between 1 and 0 as in Fig. 1.4

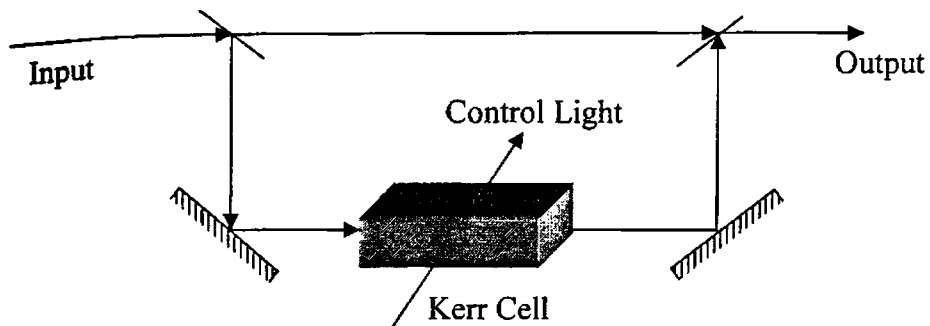


**Fig 1.4** An all optical on off switch using a Mach- Zehnder interferometer and a material exhibiting the optical Kerr effect

The retardation between two polarizations in an anisotropic nonlinear medium may also be used for switching by placing the material between two crossed polarizers. All optical switching can also be realized using an optically addressed liquid crystal spatial modulator. In this case the control light alters the electric field applied to the liquid crystal layer and therefore alters its reflectance. Organic materials with large and fast nonlinearity are promising candidates for optical switching [15]. The response time of the nonlinearity determines the operating speed of the devices. Optical switching by third order effects has advantages over linear electro-optic effect. The former has instantaneous response (of the order of picoseconds) while the latter's response time can be higher [6]. This is because of the fact that electro-optic effects involve charge separation and hence the speed of switching is determined by the mobility of the carries [100].

### 1.8.8 Optical limiting

Optical limiters are devices that strongly attenuate intense optical beams while exhibiting high transmittance for low intensity ambient light levels. These nonlinear

optical devices are currently of significant interest for the protection of human eye and optical sensors from intense laser pulses [17-19]. The optical response of an ideal optical limiter is presented in Fig 1.5

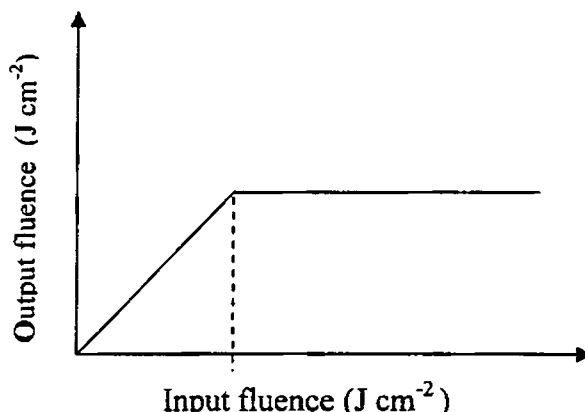


**Fig. 1.5** Ideal optical limiting graph

An ideal optical limiter will have a linear transmission upto a threshold input fluence  $I_{th}$  value, which can vary for different materials. If incident fluence is increased beyond  $I_{th}$ , transmittance remains constant. The occurrence of optical limiting is generally achieved within a limited range of radiation frequencies by a single optical limiter depending on its specific features. Optical limiting behaviour has been reported in various types of materials like carbon black suspension, organometallics, fullerenes, semiconductors, liquid crystals etc. The important fundamental physical processes responsible for the optical limiting effect are (a) reverse saturable absorption, (b) two photon absorption, (c) free carrier absorption, (d) nonlinear refraction, (e) photorefractive, and (f) induced scattering. [101-103]

### **1.9 Present work**

The result of experimental studies carried out on third order NLO properties in certain organic materials is the focus of the present thesis. The materials studied are Samarium Phthalocyanine, Tetra Phenyl Porphyrins, Quinoxaline-2-Carboxalidene-2-

## Chapter 1. Introduction

**Aminophenol (QAP) and Cobalt (III) Ternary Complexes of 2-Hydroxy Acetophenone N(4) Phenyl Semicarbazone Containing Heterocyclic Coligands.** Degenerate four wave mixing (DFWM) and Z-scan were used as experimental techniques. Nonlinear absorption coefficient and imaginary part of the nonlinear susceptibility of Samarium Phthalocyanine in MMA as well as PMMA medium were calculated and the results were compared. Figure of merit (F), Second hyperpolarizability  $\langle\gamma\rangle$  and Extinction coefficient ( $\epsilon$ ) of various TPP's, QAP's and metal complex of phenyl semicarbazone were measured and their corresponding optical limiting behaviour is analyzed. Attempts are made to explain the experimental results in terms of the structure and electronic configuration of the molecules. The following chapters contain the details of the above work.

## investigations of nonlinear .....

### 1.10 References:

1. P. N. Butcher and D. Cotter, *The elements of nonlinear optics*, Cambridge Studies in Modern Optics 9, Cambridge University Press, (1990) Cambridge
2. T. H. Maiman, *Nature* **187** (1960) p. 493.
3. P. A. Franken, A. E. Hill, C. W. Peters, and G. Weinreich, *Phys. Rev. Lett.* **7** (1961) p. 118
4. N Bloembergen, *Nonlinear Optics*, World Scientific, (1996), Singapore
5. P N Butcher and D Cotter, *Elements of nonlinear optics*, Cambridge University Press, (1991) Cambridge
6. E G Sauter, *Nonlinear optics*. John Wiley & Sons Inc (1996) New York
7. Y R Shen, *Principles of nonlinear optics*, John Wiley and Sons (1991) New York
8. G L Wood and E J Sharp, *Nonlinear Optics. Electro-Optic hand Book*. (Eds) R E Fischer and W J Smith, McGraw Hill Inc. (1994) New York
9. *Encyclopedia of lasers and optical technology*, Elsevier, London (1997) UK
10. V V Rampal, *Photonics Elements and devices*, Wheeler publishing, Allahabad
11. R A Fisher (Ed.), *Optical Phase Conjugation*, Academic press (1983) New York
12. B L Davies and M Samoc, *Current Opinion in Solid State and Material Science*, (1997) p. 213
13. J W Perry, K Mansour, I Y S Lee, X L Wu, P V Bedworth, C T Chen, N Ng, S R Marder, P Miles, T Wada, M Tian and H Sasabe, *Science*, **273** (1996) p.1533
14. T W Yau, C H Lee and J Wang. *J. Opt. Soc. Am. B* **17** (2000) p. 1626
15. B L Davies and M Samoc, *Current Opinion in Solid State and Material Science* (1997) p. 213
16. O Aso, M Tadakuma, S Namiki, *Furukawa Review*, **19** (2000) p.63
17. J S Shirk, R G S Pong, F J Bartoli and A W Snow, *Appl. Phys. Lett.* **63** (1993) p. 1880
18. D Dini, M Barthel and M Hanack, *Eur. J. Org. Chem.* (2001) p. 3759
19. G H He, C Weder, P Smith and P N Prasad., *IEEE J. OE* **34** (1998) p.2279
20. H Ditlbacher, J R Krenn, B Lamprecht, A Leitner and F R Aussenegg, *Opt. Lett* **25** (2000) p. 563
21. A Bhardwaj, P O Hedekvist and K Vahala., *J. Opt. Soc. Am. B* **18** (2001) p.657
22. P O Hedekvist, A Bhardwaj, K Vahala and H anderson., *Appl. Opt.* **40** (2001) p.1761
23. *Instruction Manual MOPO 700 Series. Spectra Physics Lasers Inc.* CA (1997) USA
24. Reintjes J F, *Nonlinear Optical Parametric Process in Liquids and Gases*, Academic Press, (1984) New York
25. B A Saleh and M C Teich., *Fundamentals of photonics*, John Wiley and Sons, Inc. (1991) New York
26. Jun-ichi Sakai, *Phase conjugate optics*, McGraw-Hill, Inc, New York
27. K P Unnikrishnan, V P N Nampoore, V Ramakrishnan, M Umadevi and C P G Vallabhan, *J. Phys. D: Appl. Phys.* **36** (2003) p.1
28. G L Wood and E J Sharp (Eds.), *Electro-optic hand book*, McGraw Hill Inc. (1994) New York
29. S Huard, *Polarization of Light*. John Wiley & Sons. (1997) Chichester
30. T. Kobayashi, *Introduction to nonlinear optical materials*, *Nonlin. opt.*, **1**, (1991) p.91
31. Miyata S, *Proceedings of 5<sup>th</sup> Toyota conference on nonlinear optics*, North Holland (1992) Amsterdam
32. Takagahara T, *Enhanced excitonic optical nonlinearity of quantum dot lattice*, in *Nonlinear optics*, Miyata S, (1992)Amsterdam

33. Nasu H, Uchigaki T, Kamiya K, Kanbara H and Kubodera K, *Jpn. J Appl. Phys.* **31** (1992) p. 3899
34. Kajzar F and Messier J, *Phys. Rev. A* **32**, (1985) p. 2352
35. Oudar J L and Person H L, *Opt. Commun.* **15**, (1975) p.258
36. Levine B F and Bethea C G, *J. Chem. Phys.* **63**, (1975) p. 1975
37. Sakai T, Kawabe Y, Ikeda H and Kawasaki K, *Appl. Phys. Lett.* **56**, (1990) p. 411
38. Ikeda H, Sakai T and Kawasaki K, *Chem. Lett.* (1991) p.1075
39. Morita K, Suehiro T, Yokoh Y and Ashitaka H, *J Photopolym. Sci. Tech.* **6**, (1993) p. 229
40. Ashitaka H, Yokoh Y, Shimizu R, Yokozawa T, Morita K, and Suehiro T, *Nonlinear Opt.* **4**, (1993) p.281
41. Ashitaka H and Sasabe H, *Nonlinear Opt.* **14**, (1995) p. 81
42. Huggards P G, Blau W and Schweitzer D, *Appl. Phys. Lett.* **51** (1987) p.2183
43. Truong K D, Genier P, Houde D and Bandrauk A D, *Chem. Phys. Lett.* **196** (1992) p. 280
44. Gotoh T, Kondoh T, Egawa K and Kubodera K, *J. Opt. Soc. Am. B* **6**, (1989) p. 703
45. Blau W J, Byrne H J, Crdin D J, Dennis T J, Hare J P, Kroto H W, Taylor R and Walton D R M., *Phys. Rev. Lett.* **67** (1991) p. 1423
46. Zhang S, Wang D, Ye P, Li Y, Wu P and Zhu D, *Opt. Lett.* **17** (1992) p. 973
47. Wang Y and Cheng L T, *J Phys. Chem.* **96** (1992) p. 1530
48. Lindle J R, Pong G S, Bartoli F J and Kafafi Z H, *Phys. Rev. B* **48** (1993), p. 9447
49. Sauteret C, Hermann J P, Frey R, Pradere F, Ducuing J, Baugman R H, and Chance R, *Phys. Rev. Lett* **36** (1976) p. 956
50. Kajzar F and Messier J, *Polym. J.* **19**, (1987) p. 275
51. Le Moigne, Kajzar F and Messier J, *Macromolecules* **24**, (1991) p. 2622
52. Molyneux S, Kar A K, Wherrett B S, Axon T L and Bloor D, *Opt. Lett.* **18**, (1993) p.2093
53. Kondo K, Okuda M and Fujitani T, *Macromolecules* **26**, (1993) p. 7382
54. Fleitz P A, McLean D G and Sutherland R L, *SPIE Proc.* **2229**, (1994) p. 33
55. Kim S H, Choi S K, Baek S H, Kim S C, Park S H, and Kim H K, *Polym. Preprints*, **35**, (1994) p. 224
56. Nalwa H S, *Thin Solid Films* **225**, (1993) p.175
57. Nalwa H S, Hamad T, Kakuta A and Mukoh A, *Synth. Met.* **57**, (1993) p.3091
58. Hari Singh Nalwa, *Nonlinear optics of organic molecules and polymers*, CRC Press, New York
59. Amano M, Kaino T and Matsumoto S, *Chem. Phys. Lett.* **170**, (1990) p. 515
60. Kajzar F and Zagorska M, *Nonlinear Opt.* **6**, (1993) p. 181
61. J H Chou, M E Kosal, H S Nalwa, N A Rakow and K S Suslick. *Applications of Porphyrins and Metalloporphyrins to Materials Chemistry from Porphyrin Handbook* K Kadish, K Smith, K Guillard (Eds). Academic Press, Vol. 7. Ch.41 (2000) New York
62. G de la Torre, P Vazquez, F A Lopez and T Torres. *J Mater. Chem.* **8** (1998) p. 1671
63. J E Riggs and Y P Sun, *J Phys. Chem. A* **103** (1999) p. 485
64. M K Engel, *Report Kawamura Inst Chem. Res.* **1996** (1997) p. 11
65. F H Moser and A L Thomas, *Phthalocyanine Compounds*, Reinhold Publishing Corporation (1963) New York
66. C Li, L Zhang, M Yang, H Wang, Y Wang., *Phys. Rev A* **49** (1994) p. 1149
67. R Kubiak, J Janczak. *Cryst. Res. Technol.* **36**(2001) p. 1095
68. G R J Williams, *J. Molecular Structure (Theochem)* **332** (1995) p. 137

69. N Ishikawa, Y Kaizu, *Coord. Chem. Revs.* **226** (2002) p. 93
70. A Yamashita, S Matsumoto, S Sakata and T Hayashi., H Kanbara, *J. Phys. Chem. B* **102** (1998) p. 5165
71. K Kandasamy, P N Puntambekar, B P Singh, S J Shetty, T S Srivastava, *J. Nonlinear Opt. Phys. Mater.* **6** (1997) 361
72. K Kandasamy, Sankar J Shetty, p N Puntambekar, T S Srivastava, T Kundu and Bhanu P Sing, *J. Porphy. and Phthalo.* **3**, (1999) p. 81
73. Palffy-Muhoray, *The nonlinear optical response of liquid crystals, in Liquid Crystals: Applications and uses*, World Scientific, Vol. 1, (1991) Singapore
74. Li L, Yuan H J, Hu G and Palffy-Muhoray, *Liq. Crystl.* **16** (1994) p.703
75. Smith D A and Coles H J, *Liq. Crystl.* **14** (1993) p.937
76. Zhang H J, Dai J H, Wang P Y and Wu L A, *Opt. Lett.* **14**, (1989) p. 695
77. Cheung Y M and Gayen S K, *J. Opt. Soc. Am B* **11**, (1994) p. 636
78. Wen Chu Huang and Juh Tzeng Lue, *Phys. Rev. B* **49** (1994) p. 17279
79. E C Dawnay, M Fardad, M Green and E M Yeatman, *J. Mater. Res.* **12** (1997) p. 3115
80. P Chen, X Wu, X Sun, J. Lin, W Ji and K L Tan, *Phys. Rev. Lett.* **82** 12 (1999) p. 2548
81. C N R Rao and A Govindaraj. *Proc. Indian Acad. Sci. (Chem. Sci.)* **113** (5 & 6) (2001) p. 375
82. E W Van Stryland, H Vanherzeele, M A Woodall, M J Soileau, A L Smirl, S Guha and T F boggess, *Opt. Eng.* **24** (1985) p.613
83. D C Hutchings and E W Van Stryland, *J Opt. Soc. Am. B* **9**, (1992) p. 2065
84. K.K. Rohatgi-Mukherjee, *Fundamentals of Photo- Chemistry*, Wiley Eastern Ltd., (1992) New Delhi
85. S Venugopal Rao, *Ph.D. Thesis*, School of physics, University of Hyderabad, India
86. B L Davies and M Samoc. *Current Opinion in Solid State and Material Science* (1997) p. 213
87. Osamu Aso, M tadakuma, S Namiki., *Furukawa Review No.* **19** (2000) p.63
88. J S Shirk, R G S Pong, F J Bartoli and A W Snow, *Appl. Phys. Lett.* **63** (1993) p. 1880
89. D Dini, M Barthel and M Hanack, *Eur. J. Org. Chem.* (2001) p. 3759
90. G H He, C Weder, P Smith and P N Prasad, *IEEE J. OE* **34** (1998) p.2279
91. A Yariv, *Optical Electronics In Modern Communications*, Oxford University Press (1997) New York
92. K A Stankov, *Appl. Phys. B* **45** (1998) p.191
93. X M Zhao and D McGraw, *IEEE J of Quan. Elec.* **QE-28** (1992) p. 930
94. R Laenen, H Graener and A Laubereau. *Opt. lett.* **15** (1990) p.971
95. R. Danielius, A Piskarskas, V Sirutkitis, A Stabinis and A Yankauskas, *JETP Lett.* **42** (1985) p.122
96. Michael Bass (editor in chief), *Hand book of Optics*, Volume 1, McGraw Hill Inc. New York (1995)
97. A Yariv *Appl. Phys. Lett.* **28** (1976) p. 88
98. D M Pepper and R L Abrams, *Opt. Lett.* **3** (1978) p.212
99. K. Iga, *Fundamentals of Laser Optics*, Plenum, (1994) New York
100. Th. Schneider, D Wolfframm, R Mitzner and J Reif, *Appl. Phys. B* **69** ( 1999) p. 749
101. L W Tutt, T F Boggess, *Progress in Quantum Electronics*, **17** (1993) p. 299
102. R W Boyd, *Nonlinear Optics*, Academic Press, (1991) New York
103. C R Guiliano and L D Hess, *IEEE J. Quantum Electron.* **3** (1967) p. 358

## **Chapter 2**

### **Experimental Techniques and Details: Z-Scan and Degenerate Four Wave Mixing**

#### **Abstract**

Z-scan and Degenerate Four Wave Mixing are the two techniques used for the nonlinear optical measurements in presented in this thesis. The experimental details of these techniques along with the relevant theory are explained in this chapter. Moreover the specifications of the laser source and those of the other instruments utilized for the measurements are also presented.



### Introduction

The characterization of the nonlinear optical properties of various NLO materials for various applications like frequency mixing, optical short pulse generation and measurement, optical communication, optical switching, optical limiting etc. is a fascinating field in modern optics[1-6]. The magnitude and response of third order nonlinear susceptibility is one of the important parameters of this class of materials and several techniques are available for the measurement of such parameters. Z-scan, Degenerate Four Wave Mixing (DFWM), Third Harmonic Generation (THG), Time resolved optical Kerr effect, Electro Absorption etc. are some of the techniques used for this purpose. Using z-scan, the sign and magnitude of the third order susceptibility tensor can be calculated. Degenerate Four Wave Mixing can give both the magnitude and response of the third order nonlinearity. Similarly THG is another technique used for the measurement of the magnitude of the third order susceptibility tensor. Electro absorption is used for the dispersion studies of third order nonlinearity and the time resolved optical Kerr effect is used for the photo physical processes determining the nonlinearity.

#### 2.2 Z-Scan Technique:

The Z-scan technique is a simple and popular experimental technique to measure intensity dependent nonlinear susceptibilities of materials and it was originally introduced by Sheik Bahae *et.al* [7-8]. In this method, the sample is translated in the Z-direction along the axis of a focussed Gaussian beam, and the far field intensity is measured as function of sample position. Consequently increases and decreases in the maximum intensity incident on the sample produce wavefront distortions created by nonlinear optical effects in the sample being observed. This is a simple and sensitive single beam technique to measure the sign and magnitude of both real and imaginary part of the third order nonlinear susceptibility  $\chi^{(3)}$  of materials. The z-scan is obtained by moving the sample along a well-defined, focused laser beam, and thereby varying the light intensity in the sample. In the original single beam configuration, the

## Investigations of nonlinear .....

transmittance of the sample is measured, as the sample is moved, along the propagation direction of a focussed gaussian laser beam. A laser beam propagating through a nonlinear medium will experience both amplitude and phase variations. If transmitted light is measured through an aperture, placed in the far field with respect to focal region, the technique is called closed aperture Z-scan experiment [7-8]. By varying the aperture in front of the detector, one makes the z-scan transmittance more or less sensitive to either the real or imaginary parts of the nonlinear response of the material, i. e., nonlinear refractive index and nonlinear absorption, respectively.

In the closed aperture z-scan the transmitted light is sensitive to both nonlinear absorption and nonlinear refraction. In this case, phase distortion suffered by the beam while propagating through the nonlinear medium is converted into corresponding amplitude variations and the real part of the susceptibility tensor can be calculated. On the other hand, if transmitted light is measured without an aperture the z-scan obtained is known as open aperture z-scan and in this case entire light from the sample is collected [8]. In the open aperture z-scan the output intensity is sensitive only to the nonlinear absorption of the sample and the imaginary part of the susceptibility tensor can be calculated from the data obtained. The graph obtained by dividing the closed aperture z-scan data by the open aperture z-scan data measured simultaneously is known as “divided z-scan graph”[8]. In the “divided z-scan” the effect of nonlinear absorption is cancelled out and the measured nonlinear effect is due to the nonlinear refraction alone.

In a z-scan measurement, it is assumed that the sample thickness is always less than the Rayleigh's range  $z_0$  defined by the expression [9]

$$z_0 = \frac{k\omega_0^2}{2} \quad (2.1)$$

where  $k$  is the wave vector and  $\omega_0$  is the beam waist and is given by

$$\omega_0 = \frac{f\lambda}{D} \quad (2.2)$$

in this expression 'f' is the focal length of the lens used, 'λ' is the wavelength of the radiation used and 'D' is the beam diameter. The sample thickness is always kept less than the Rayleigh range for ensuring that the beam profile does not vary appreciably inside the sample. The experimental setup for single beam z-scan technique is given in Fig. 2.1

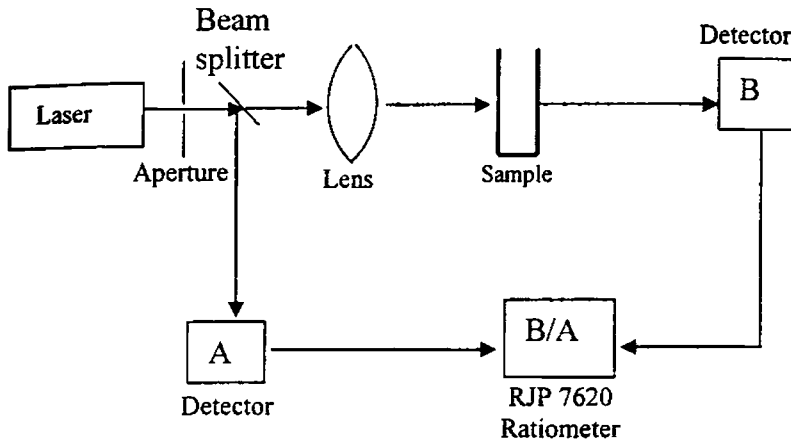


Fig. 2.1 Experimental setup

Z-scan technique is highly sensitive to the profile of the beam and also to the thickness of the samples [7, 8,10 ]. Any deviation from the gaussian profile of the beam and also from thin sample approximation will give rise to erroneous results. To enhance it's sensitivity and applicability new extensions have been added. A two color Z-scan is used to perform the studies of non-degenerate optical nonlinearities [11-12]. A much more sensitive technique, EZ-scan (eclipsed Z-scan), has been developed which utilizes the fact that the wings of a circular Gaussian beam are much more sensitive to the far-field beam distortion [13]. A reflection Z-scan technique was introduced to study the optical nonlinearities of surfaces [14]. Z-scan with top-hat

## Investigations of nonlinear .....

beams and elliptical Gaussian beams have been performed resulting in better sensitivity [15]. The dual wavelength (two-color) extension of the standard Z-scan technique has been used to measure the non-degenerate nonlinearities [11]. This has been further used to time resolve the dynamics of the nonlinear process by introducing a delay between the pump and probe beams [11]. Z-scan measurements can also be done with astigmatic gaussian beams [16]. In the case of astigmatic gaussian beam, a slit is used instead of a (circular) aperture. Z-scan measurement for non gaussian beams with arbitrary sample thickness [17] and arbitrary aperture [18] have also been suggested. In the case of the former, nonlinear parameters are measured in comparison with a standard sample, mostly carbon disulphide ( $\text{CS}_2$ ) [15]. A comprehensive review of different techniques of z-scan could be found in any of the following references [19-24]. The Z-scan technique has been used extensively to study different materials like semiconductors, nano-crystals, semiconductor-doped glasses, liquid crystals, organic materials, biomaterials etc.

### 2.3 Open aperture Z-scan for absorptive nonlinearity

Nonlinear absorption of the sample is manifested in the open aperture Z-scan measurements. For example, if nonlinear absorption like two-photon absorption (TPA) is present, it is manifested in the measurements as a transmission minimum at the focal point [8]. On the other hand, if the sample is a saturable absorber, transmission increases with increase in incident intensity and results in a transmission maximum at the focal region [25]. A straight-line z-scan graph is obtained in the case of samples with linear absorption.

In the case of excited state absorption (ESA), the sample experiences the strongest intensity and fluence at focus; therefore it absorbs the most energy and allows least transmittance. Away from the focus in the direction of both increasing and decreasing z transmittance increases evenly because the irradiance decreases symmetrically about the focus.

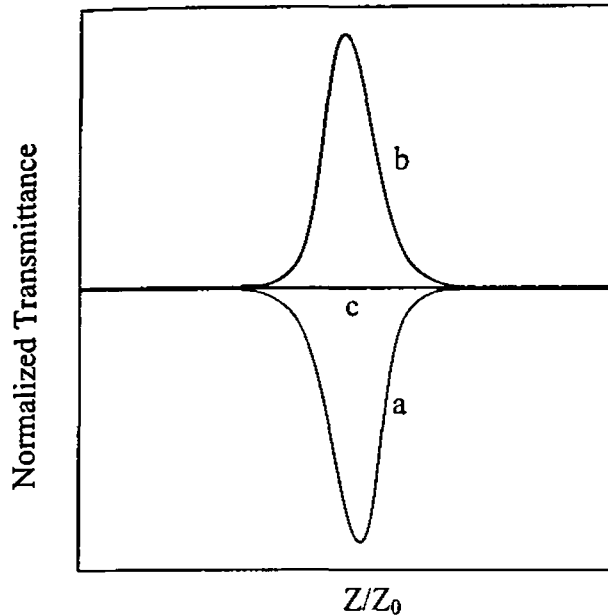


**Fig. 2.2** Open aperture z-scan curves for a) ESA, b) SA and c) linear absorption.

This feature has been observed experimentally and is shown by curve (a) of the above figure (Fig. 2.2). Accompanying curve (a) we also show curve (b) simulated for the situation of saturable absorption (SA) i.e. absorption coefficient  $\alpha$  decrease with intensity or fluence and curve (c) for linear absorption i.e.  $\alpha$  remains constant irrespective of intensity or fluence. All three curves are normalized to give a transmittance of one in the linear region (i.e. regions of large  $|z|$ ). Sample positions are presented in units of  $z/z_0$  where  $z_0$  is the diffraction length. It has been shown that the model originally developed by Bahae et. al [8] for pure TPA can also be applied to excited state absorption (ESA) [26]. ESA is a sequential TPA process, where two photons are successively absorbed [27]. However, in this case nonlinear absorption coefficient  $\beta$  is renamed as  $\beta_{\text{eff}}$ , the details of which are discussed in later chapters.

Investigations of nonlinear .....

## 2.4 Theory of open aperture Z-scan technique

In the case of an open aperture z-scan the transmitted light measured by the detector is sensitive only to the intensity variation. Therefore the phase variations of the beam can be neglected safely. The theory of Z-scan experiment given here is same as that given by M Sheik Bahae et. al. in reference [8].

The intensity dependent nonlinear absorption coefficient  $\alpha(I)$  can be written in terms of linear absorption coefficient  $\alpha$  and TPA coefficient  $\beta$  as [8]

$$\alpha(I) = \alpha + \beta I \quad (2.3)$$

The irradiance distribution at the exit surface of the sample can be written as

$$I_r(z, r, t) = \frac{I(z, r, t)e^{-\alpha l}}{1 + q(z, r, t)} \quad (2.4)$$

where

$$q(z, r, t) = \beta I(z, r, t)L_{eff} \quad (2.5)$$

$L_{eff}$  is the effective length and is given, in terms of sample length  $l$  and  $\alpha$  by the relation

$$L_{eff} = \frac{(1 - e^{-\alpha l})}{\alpha} \quad (2.6)$$

The total transmitted power  $P(z, t)$  is obtained by integrating Eq. (2.4) over  $z$  and  $r$  and is given by

$$P(z, t) = P_i(t)e^{-\alpha l} \frac{\ln[1 + q_0(z, t)]}{q_0(z, t)} \quad (2.7)$$

$P_i(t)$  and  $q_0(z, t)$  are given by the equations (2.8) and (2.9) respectively.

$$P_i(t) = \frac{\pi \omega_0^2 I_0(t)}{2} \quad (2.8)$$

$$q_0(z, t) = \frac{\beta I_0(t) L_{eff} z_0^2}{z^2 + z_0^2} \quad (2.9)$$

For a pulse of Gaussian temporal profile, eq.(2.7) can be integrated to give the transmission as

$$T(z) = \frac{C}{q_0 \sqrt{\pi}} \int_{-\infty}^{\infty} \ln(1 + q_0 e^{-t^2}) dt \quad (2.10)$$

Nonlinear absorption coefficient is obtained from fitting the experimental results to the Eq. (2.10).

If  $|q_0| < 1$ , the Eq. (2.8) can be simplified as

$$T(z, S = 1) = \sum_{m=0}^{\infty} \frac{[-q_0(z, 0)]^m}{(m+1)^{\frac{1}{2}}} \quad (2.11)$$

Once an open aperture z-scan is performed, nonlinear coefficient  $\beta$  can be unambiguously deduced.

### 2.5 Closed aperture Z-scan

The transmittance characteristics of the sample with a finite aperture depend on the nonlinear refractive index of the sample. Consider, for instance, a material with a negative nonlinear refraction and of thickness smaller than the diffraction length ( $k\omega_0^2/2$ ) of the focused beam being positioned at various points along the Z-axis.

This situation can be regarded as treating the sample as a thin lens of variable focal length due to the change in the refractive index at each position ( $n = n_0 + n_2 I$ ).

When the sample is far from the focus and closer to the lens, the irradiance is low and the transmittance characteristics are linear. Hence the transmittance through the aperture is fairly constant in this region. As the sample is moved closer to the focus,

the irradiance increases inducing a negative lensing effect. A negative lens before the focus tends to collimate the beam. This causes the beam narrowing leading to an increase in the measured transmittance at the aperture. A negative lens after the focus tends to diverge the beam resulting in the decrease of transmittance. As the sample is moved far away from the focus, the transmittance becomes linear in  $Z$  as the irradiance becomes low again. Thus the curve for  $Z$  versus transmittance has a peak followed by a valley for a negative refractive nonlinearity. The curve for a positive refractive nonlinearity will give rise to the opposite effect, i.e. a valley followed by a peak [7,8].

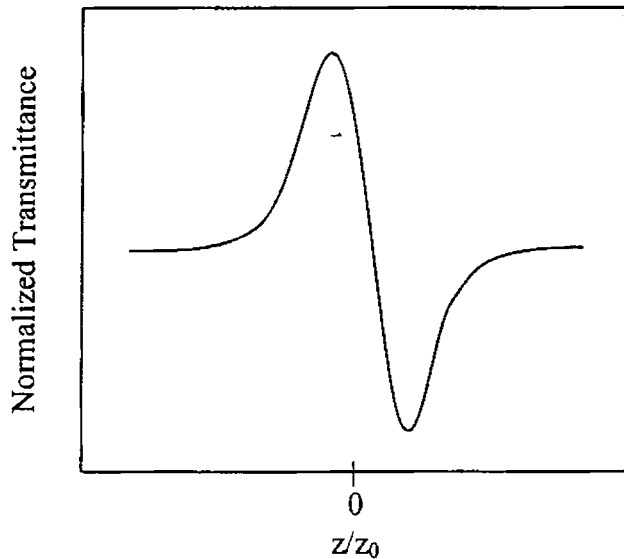


**Fig. 2.3** Typical closed aperture z-scan curve of samples having negative nonlinearity

The former is called self-defocusing and the later is called self-focussing. Fig. 2.3 and 2.4 shows a typical closed aperture z-scan curve of samples having negative and positive nonlinearities respectively



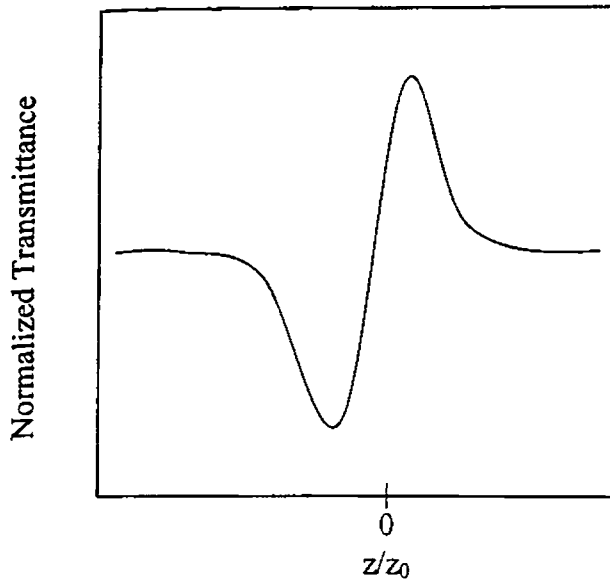


**Fig. 2.4** Typical closed aperture z-scan curve of samples having positive nonlinearity

One of the mechanisms of self-focussing is optical Kerr effect [28] which has instantaneous response. In this case the electric field of a light beam exerts a torque on anisotropic molecules by coupling to oscillating dipole induced in the molecule by the field itself. Resulting light induced molecular reorientation is the main mechanism for optical nonlinearity in transparent liquids. Nonlinear refractive index depends linearly on light intensity. Other mechanism of optical Kerr effect includes off resonant excitation of narrow band absorbers and consequent distortion of electronic distribution among energy levels in the materials. The resultant intensity dependant refractive index is responsible for self-focussing or self-defocusing. In self-focussing beam collapses upon itself spatially. Kerr like nonlinearity has very fast response time, of the order of picoseconds.

Investigations of nonlinear .....

## 2.6 Theory of closed aperture Z-scan technique

In a cubic nonlinear medium the index of refraction  $n$  is expressed in terms of nonlinear indices  $n_2$  (esu) or  $\gamma$  ( $\text{m}^2/\text{W}$ ) through

$$n = n_0 + \frac{n_2}{2} |E|^2 = n_0 + \gamma I \quad (2.12)$$

where  $n_0$  is the linear index of refraction,  $E$  is the peak electric field;  $n_2$  the intensity dependent refractive index and  $I$  denote the irradiance of the laser beam within the sample.

Assume a  $\text{TEM}_{00}$  beam of waist radius  $w_0$  travelling in the  $+z$  direction.  $E$  can be written as [8]

$$E(z, r, t) = E_0(t) \frac{w_0}{w(z)} \exp \left[ -\frac{r^2}{w^2(z)} - \frac{ikr^2}{2R(z)} e^{-i\phi(z,t)} \right] \quad (2.13)$$

Where  $w^2(z) = w_0^2 (1 + z^2 / z_0^2)$  is the beam radius,  $R(z) = z(1 + z^2 / z_0^2)$  is the radius of curvature of the wave front at  $z$ ,  $z_0 = \frac{k\omega_0^2}{2}$  is the diffraction length of the beam and  $k$  is the wave vector.  $E_0(t)$  denotes the radiation electric field at the focus and contains the temporal envelope of the laser pulse. The  $e^{-i\phi(z)}$  term contains all the radially uniform phase variations. For calculating the radial phase variations  $\Delta\phi(r)$ , the slowly varying envelope approximation (SVEA) was used and all other phase changes that are uniform in  $r$  are ignored.  $L \ll z_0 / \Delta\phi(0)$ , where  $L$  is the sample length, the amplitude and the phase  $\phi$  of the electric field as a function of  $z'$  are now governed in the SVEA by a pair of simple equations  $\sqrt{I}$

$$\frac{d\Delta\phi}{dz} = \Delta n(I)k \quad (2.14)$$

and

$$\frac{dI}{dz} = -\alpha(I)I \quad (2.15)$$

where  $z'$  is the propagation depth in the sample and  $\alpha(I)$  in general includes linear and nonlinear absorption terms.

In the case of cubic nonlinearity and negligible nonlinear absorption Eq. 2.14 and Eq 2.15 are solved to give the phase shift  $\Delta\phi$  at the exit of the sample is given by

$$\Delta\phi(z, r, t) = \Delta\phi(z, t) \exp\left[-\frac{2r^2}{w^2(z)}\right] \quad (2.16)$$

with

$$\Delta\phi(z, t) = \frac{\Delta\phi_0(t)}{\left[1 + \frac{z^2}{z_0^2}\right]} \quad (2.17)$$

$\Delta\phi_0(t)$  the on axis phase shift at the focus is defined as

$$\Delta\phi_0(t) = k\Delta n_0(t)L_{eff} \quad (2.18)$$

where  $L_{eff} = \frac{(1 - e^{-\alpha l})}{\alpha}$  with  $\alpha$  the linear absorption coefficient. Here  $\Delta n_0 = \gamma I_0(t)$  with  $I_0(t)$  being the  $z$  axis irradiance at the focus (i.e. at  $z=0$ ).

The complex electric field exiting the sample  $E_e$  now contains the nonlinear phase distribution

$$E_e(z, r, t) = E(z, r, t) e^{\frac{\alpha l}{2}} e^{i\Delta\phi(z, r, t)} \quad (2.19)$$

By virtue of Huygen's principle and making use of Gaussian decomposition method [ ] one can show that

$$e^{i\Delta\phi(z, r, t)} = \sum_{m=0}^{\infty} \frac{[i\Delta\phi_0(z, r, t)]^m}{m!} e^{-2mr^2/w^2(z)} \quad (2.20)$$

After including the initial beam curvature for the focused beam the resultant electric field pattern at the aperture is

$$E_a(r, t) = E(z, r = 0, t) e^{-\alpha t/2} \sum_{m=0}^{\infty} \frac{[i\Delta\phi_0(z, t)]^m}{m!} \frac{w_{m0}}{w_m} \exp\left[-\frac{r^2}{w_m^2} - \frac{ikr^2}{2R_m} + i\theta_m\right] \quad (2.21)$$

Defining  $d$  as the propagation distance in free space from the sample to the aperture plane and  $g=1+d/R(z)$  the remaining parameters in Eq. 2.21 are expressed as

$$w_{m0}^2 = \frac{w^2(z)}{(2m+1)} \quad (2.22)$$

$$d_m = \frac{kw_{m0}^2}{2} \quad (2.23)$$

$$w_m^2 = w_{m0}^2 \left[ g^2 + \frac{d^2}{d_{m0}^2} \right] \quad (2.24)$$

$$R_m = d \left[ 1 - \frac{g}{g^2 + d^2/d_m^2} \right]^{-1} \quad (2.25)$$

and

$$\theta_m = \tan^{-1} \left[ \frac{d/d_m}{g} \right] \quad (2.26)$$

Where  $d$  is the propagation distance in free space for the sample to the aperture plane and  $g$  is defined as  $g=1+d/R(z)$ . The expression given in Eq. 2.21 is a general case of that derived by Weaire et. al [29]. Gaussian decomposition method is useful for the small phase distortions detected with z-scan method since only a few terms of the sum in Eq. 2.21 are needed.

The on-axis z-scan transmittance for cubic nonlinearity and a small phase change can then be derived as follows. The on-axis electric field at the aperture plane can be obtained by letting  $r=0$  in Eq. 2.21 In the limit of small nonlinear phase

For  $(\Delta\phi_0 \ll 1)$  only two terms in the sum in Eq. 2.21 needed to be retained. The normalized z-scan transmittance can be written as

$$T(z, \Delta\phi_0) = \frac{|E_a(z, r=0, \Delta\phi_0)|^2}{|E_a(z, r=0, \Delta\phi_0=0)|^2} = \frac{|(g + id/d_0)^{-1} + i\Delta\phi_0(g + id/d_1)^{-1}|^2}{|(g + id/d_0)^{-1}|^2} \quad (2.27)$$

The far field condition  $d \gg z_0$  can be give a geometry independent normalized transmittance as

$$T(z, \Delta\phi_0) = 1 - \frac{4\Delta\phi_0 x}{(x^2 + 9)(x^2 + 1)} \quad (2.28)$$

where  $x = z/z_0$

The peak and valley of the z-scan transmittance can be calculated by solving the equation

$$\frac{dT(z, \Delta\phi_0)}{dz} = 0 \quad (2.29)$$

Solution to this equation yield  $x_{p,v} \approx 0.858$  therefore we can write the peak valley separation as

$$\Delta Z_{p,v} = 1.7z_0 \quad (2.30)$$

Also inserting the z value from Eq. 2.27 and Eq. 2.28 the peak valley transmittance change is

$$\Delta T_{p,v} = 0.406\Delta\phi_0 \quad (2.31)$$

This relation is accurate to 0.5% for  $|\Delta\phi_0| \leq \pi$ . For large aperture this equation is modified and is

$$\Delta T_{p,v} \approx 0.406(1 - S)^{0.25} |\Delta\phi_0|, \text{ for } |\Delta\phi_0| \leq \pi \quad (2.32)$$

Thus by measuring the transmitted power in a closed aperture z-scan one can obtain the nonlinear refractive index by knowing the value of  $\Delta\phi_0$  from Eq. 2.29

All the measurements mentioned in this thesis have been carried out using a nano second laser and since the closed aperture measurements, in the present experimental conditions, can give only thermal response [30], which is not of interest with respect to the scope of the present work. Therefore closed aperture Z-scan measurements were not attempted in detail.

## 2.7 Merits and demerits of z-scan techniques

This technique has several *advantages*, some of which are

Simplicity: No complicated alignment is needed except for keeping the beam centered on aperture.

- Simultaneous measurement of both sign and magnitude of nonlinearity.
- Data analysis is quick and simple except for some particular conditions.
- Possible to isolate the refractive and absorptive parts of nonlinearity unlike in DFWM.
- High sensitivity, capable of resolving a phase distortion of  $\lambda/300$  provided the sample is of high optical quality
- Close similarity between the Z-scan the Optical Power Limiting geometry.

Some of the *disadvantages* include

- Stringent requirement of high quality Gaussian TEM00 beam for absolute measurements
- For non-Gaussian beams the analysis is completely different. Relative measurements against a standard samples allows relaxation on requirements of beam shape

- Beam walk-off due to sample imperfections, tilt or distortions
- Not suitable for measurement of off-diagonal elements of the susceptibility tensor except when a second nondegenerate frequency beam is employed

### 2.8. Degenerate four-wave mixing (DFWM)

Four wave mixing is a technique to study the third order optical nonlinearity of the medium. In this method three coherent beams interact in a nonlinear medium to generate a fourth wave. If the frequencies of all the waves are the same (their wave vectors can be different) then it is called Degenerate Four Wave Mixing (DFWM). DFWM is one of the most important and versatile techniques, which provides information about the magnitude and response of the third-order nonlinearity. The strength of this fourth beam is dependent on a coupling constant that is proportional to effective  $\chi^3$  and hence measurements on phase conjugate signal will yield information about the  $\chi^3$  tensor components of the medium [31-40]. DFWM can be employed in backward (or generally called the Phase Conjugate), forward or boxcar configurations, with the choice on the experimental conditions and the requirements. Using different polarizations of the three beams it is possible to measure all the independent  $\chi^3$  tensor components of an isotropic material. Schematic diagram of DFWM is shown in fig.5

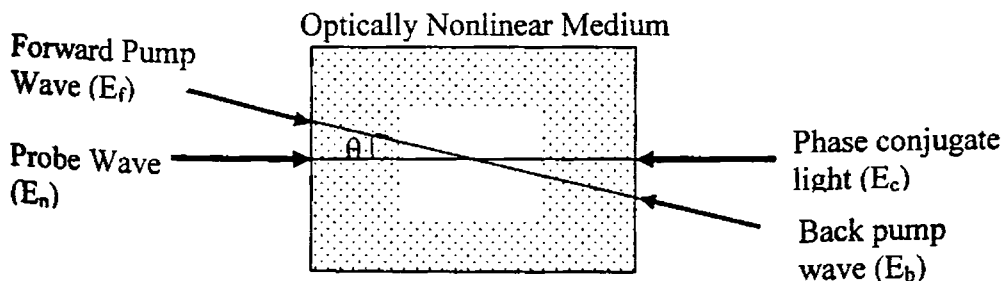
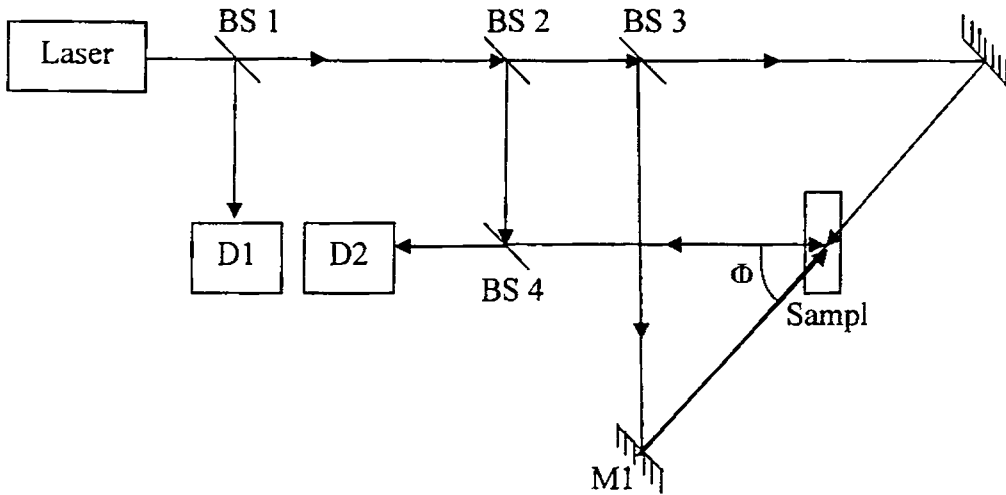


Fig. 2.5 Schematic diagram of Degenerate Four Wave Mixing

Investigations of nonlinear .....



**Fig. 2.6** Experimental setup of Degenerate Four Wave Mixing BS: Beam splitters; PD: Photo-detectors; M: Mirrors;  $\Phi$ : Pump-probe beam angle

The presence of a third-order optical nonlinear susceptibility  $\chi^3$  leads to the creation of various components of material polarisation, giving rise to new optical fields. If the phase-matching condition is fulfilled (i.e. the phase relation between the waves emitted by different parts of the nonlinear medium leads to constructive build up of the resulting wave), new beams of light are created. If the fields are of identical frequencies, the process is termed as Degenerate Four Wave Mixing and the output beam will have the same frequency. The time resolution of the FWM measurements depends on two parameters. The first is related to the time duration of the laser pulses and the second is related to the coherence time of the laser pulses.

In the experimental setup, two beams of equal intensity generally called forward and backward pump beams, are made exactly counter propagating. Therefore sum of their wave vector is zero ( $\mathbf{k}_f + \mathbf{k}_b = 0$ ). The actual experimental setup for DFWM is given in Fig. 2.6. A third beam (called probe beam), which has an intensity



less than those of the pump beams, make a small angle with respect to one of the pump beams (in the present case  $\approx 8^\circ$ ) as shown in the Fig. 2.6. Pump-probe intensity ratio is kept about five. The generated fourth wave is called phase conjugated beam, because its amplitude remains everywhere the complex conjugate of the probe beam. From phase matching condition ( $\Delta k = 0$ ) it can be seen that wave vector of the phase conjugate beam  $k_c = -k_p$ , i.e. phase conjugate light retraces the path of the probe beam.

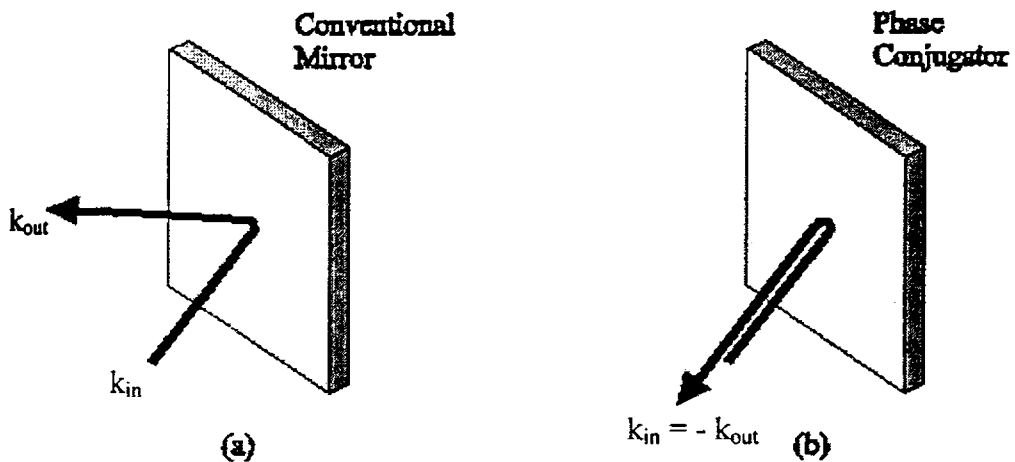


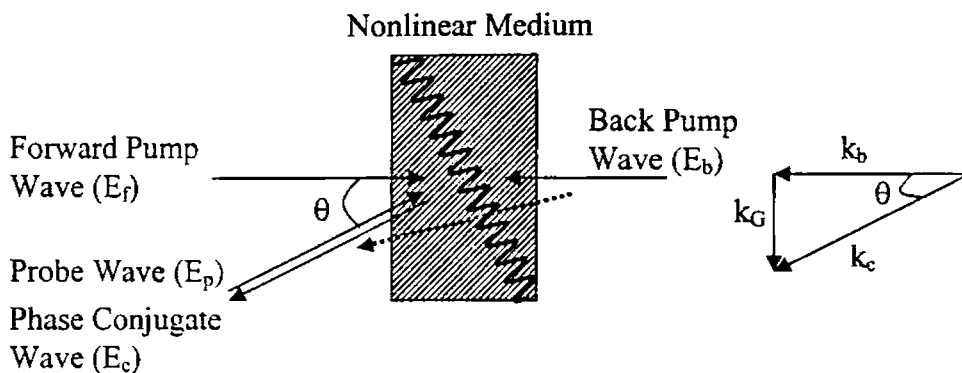
**Fig. 2.7** Comparison of the reflection properties of (a) conventional and (b) phase conjugate mirrors. The PCM reverses the total propagation direction of the incoming ray while the conventional mirror only changes the sign of the wave vector component normal to the mirror surface.

It is to be noted that in a phase conjugate reflection, the wave vector of the incident beam is totally reversed, whereas in an ordinary reflection, only normal component of the wave vector component is reversed. Thus phase conjugate reflection does not obey the Snell's law. Reflection from a phase conjugate mirror and that from an ordinary mirror is illustrated in the Fig. 2.7 [41].

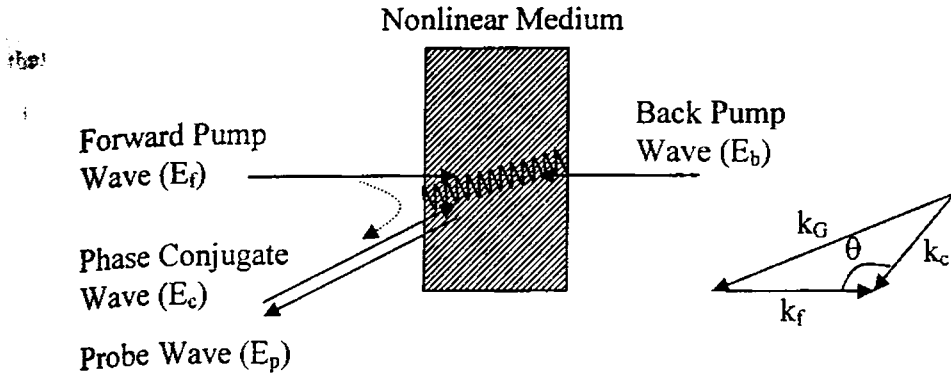
Generation of phase conjugate light can be understood as diffraction of one of the input beams from a grating formed by interference of the other two input beams [42-45]. Grating essentially means spatial (or temporal) modulation of certain properties of the medium. Therefore DFWM is also called real time holography (simultaneous writing and reading of the hologram). For an isotropic medium the nonlinear polarization of the three superposed light waves can be represented in terms of the respective complex amplitude vectors  $A_j$  as follows

$$P_c^{(3)} = A(A_f \cdot A_p^*)A_b + A(A_b \cdot A_p^*)A_f + 2C(A_f \cdot A_b)A_p^* \quad (2.33)$$

As Fig. 2.8 (a) shows the first term in Eq. 2.33 describes a generation process giving rise to conjugate wave  $E_c$ . A stationary three dimensional diffraction grating is formed by the forward pump  $E_f$  and the probe  $E_p$  and the back pump wave  $E_b$  experiences Bragg diffraction on this grating. Since  $E_b$  is transmitted through the medium the process is said to involve a transmission grating. The transformation to  $E_c$  can be described in terms of a grating vector  $k_G = k_f - k_p$ . The second term in Eq. 2.33 describes diffraction of the pump  $E_f$  on the grating formed by interference between the pump  $E_b$  and the probe as shown in Fig. 2.8 (b). Since  $E_f$  appears to be reflected from the medium to form  $E_c$  the process is said to involve a reflection grating with grating vector  $k_G = k_b - k_p$ . Since the grating vectors  $(k_f - k_p)$  and  $(k_b - k_p)$  are almost orthogonal one is dominant while the other is relatively weak



a) Transmissive diffraction grating



(b) Reflective diffraction grating

**Fig. 2.8** Two types of spatial diffraction lattices in four wave mixing. (a) Phase conjugate light diffracted in the  $k_c = k_b + k_G$  direction (b) phase conjugate light diffracted in the  $k_c = k_f + k_G$  direction.  $k_G$  : diffraction lattice vector.

The third term in Eq. 2.33 represents a temporally modulated grating (at a frequency  $2\omega$ ) which is stationary in space. The probe beam is diffracted from this grating. This grating is free from wash out effects.

The spacing of the diffraction grating described above is given by

$$\Lambda = \frac{2\pi}{k_G} = \frac{\lambda}{2n \sin(\theta/2)} \tag{2.34}$$

where  $\theta$  is the angle between the pump and probe waves in the medium and  $n$  is the refractive index in the nonlinear medium.

Periodic modulation of any material property can be considered as a grating. Nature of the grating formed depends on the characteristics of medium as well as those of interacting fields. The gratings formed as a result of the interference of the

beams may be classified into a number of categories like population grating [46], orientational grating [47], thermal grating, polarization grating [44,45] etc. Population grating is formed in an absorptive medium due to electronic excitation of the molecules. Orientational gratings are formed by induced reorientation of anisotropic molecules in presence of electromagnetic fields. Absorption of light and subsequent nonradiative de-excitation usually results in temperature rise, which results in the formation of thermal grating [44,45].

Some of the several advantages of the degenerate four wave mixing technique are

- The Phase Conjugate signal is distinguishable from others by simple spatial separation.
- The detected signal has a characteristic dependence on the input intensities, which can be used for verification of the experiment.
- The sample could be in any form (isotropic) and all the independent tensor components of  $\chi^{(3)}$  can be measured in a single experiment
- Beams other than true Gaussian modes can be employed

The time dependence of the probe beam gives information about the response time of the nonlinearity

## 2.9 Theory of DFWM

The theory of degenerate four wave mixing is based on coupled mode equations, which govern the spatial and temporal evolution of the signal under slowly varying amplitude approximation (SVAP) [43,48,49]. Using SVAP second order Maxwell's equations are reduced to first order differential equation. Practically, this approximations implies that growth of the signal wave modulated at a particular frequency and wave vector is determined only by the nonlinear polarization having the same modulation frequency and wave vector. This follows from the fact that power transferred to electric field is given by the volume integral of  $\mathbf{E} \cdot \mathbf{P}$ . If  $\mathbf{E} \cdot \mathbf{P}$

not have the same frequency and wave vector, their volume integral will vanish as they are orthogonal functions. Mathematically SVAP is given by the inequality

$$|k^2 E| \gg \left| k \frac{\partial E}{\partial z} \right| \gg \left| \frac{\partial^2 E}{\partial z^2} \right| \quad (2.35)$$

It is assumed that two pump beams are of equal intensity and there is no pump depletion: i.e.  $|E_1| = |E_2| =$  a constant. Therefore probe beam and phase conjugate beam are only considered. Nondestructive buildup of the signal occurs when nonlinear polarization (the source term in Maxwell's equation) is given by the relation

$$P_i(\omega = \omega + \omega - \omega) = 6 \chi_{ijkl}(-\omega, \omega, \omega, -\omega) E_{1j}(\omega) E_{2k}(\omega) E_{pl}(\omega) \exp[-i(K_1 + K_2 - K_p) \cdot R] \dots\dots\dots (2.36)$$

The interaction between probe beam and phase conjugate beam is given by

$$\frac{dE_p}{dz} = -i\kappa^* E_c^* \qquad \frac{dE_c}{dz} = i\kappa^* E_p^* \quad (2.37)$$

where  $\kappa$  is the coupling constant, given by Eq. (2.38)

$$\kappa^* = (2\pi\omega / cn) \chi^{(3)} E_1 E_2 \quad (2.38)$$

The solution to above equations are given by

$$E_c(0) = -i \left[ \frac{\kappa^*}{|\kappa|} \right] \tan(|\kappa|L) E_p^* \quad (2.39)$$

Eq. (2.38) shows that the phase conjugate signal is the complex conjugate of  $E_p$ . [Here we have used the boundary condition that  $E_p(0)$  is finite and  $E_c(L)=0$ ]. If the ratio of the intensities of the pump and probe beams are always constant (ie. if all the

three beams are taken from a parent source) intensity of the phase conjugate signal is given by the relation

$$I(\omega) \propto \left( \frac{\omega}{2\varepsilon_0 c n^2} \right)^2 |\chi^{(3)}|^2 I_0^3(\omega) \quad (2.40)$$

In absence of linear absorption third order susceptibility is given by

$$\chi^{(3)} = \chi_{ref}^{(3)} \left[ \frac{\left( \frac{l}{l_0} \right)}{\left( \frac{l}{l_0} \right)_{ref}} \right]^{1/2} \left[ \frac{n}{n_{ref}} \right]^2 \frac{l_{ref}}{l} \quad (2.41)$$

Third order susceptibility  $\chi^3$  is usually measured with respect to a standard sample  $CS_2$ .

If sample has linear absorption, Eq. (2.41) has to be modified by considering the effect of linear absorption. It assumed that optical density of the sample (ie.  $\alpha l$ , where  $\alpha$  is the linear absorption coefficient and  $l$  is the sample length) is much less than one. In presence of linear absorption, susceptibility is given by the following equation

$$\chi^{(3)} = \chi_{ref}^{(3)} \left[ \frac{\left( \frac{l}{l_0} \right)}{\left( \frac{l}{l_0} \right)_{ref}} \right]^{1/2} \left[ \frac{n}{n_{ref}} \right]^2 \frac{l_{ref}}{l} \frac{\alpha l}{(1 - e^{-\alpha l}) e^{-\alpha/2}} \quad (2.42)$$

The reflectivity of the phase conjugate mirror  $R$ , is defined as the ratio of phase conjugate intensity to probe beam intensity.

$$R = \frac{I_c}{I_p} \quad (2.43)$$

Eq. (2.43) can be written in terms of the coupling coefficient  $\kappa$  as in Eq. (2.44).

$$R = \tan^2(\kappa |L|) \quad (2.44)$$

## **2.10 Characteristic Properties of Phase Conjugate Waves**

The phase conjugate light has a variety of characteristics and properties not associated with normal light and they can be enumerated as follows

- **Phase compensation effect**  
Waves that pass through an aberrating medium are injected into a phase conjugate mirror. If the outgoing wave is repropagated through the medium the waves phase distortion is compensated.
- **Space domain multiplicative interaction**  
Since phase conjugate waves are produced by interaction in a nonlinear medium the spatial multiplicative effect among the light waves appears in the phase conjugate waves.
- **Intensity dependant phase shift**  
Due to the optical Kerr effect in a nonlinear medium the phase shift of the electric field depends on the wave intensity.
- **Detuning dependence**  
The reflectance of a phase conjugate mirror strongly depends on the detuning between the pump and probe wave frequencies.
- **Time inversion**  
A phase conjugate wave can be regarded as a time inverted wave since its direction of propagation is exactly opposite that of the probe wave and the wave front is identical to that of the probe wave.
- **Time domain multiplicative interaction**  
When pulsed waves are used in the production of phase conjugate light the resulting polarization, that is, the generalized phase conjugate wave intensity depends on the product of the interacting waves in the waves' temporal domains.
- **Quantum correlation**  
When the waves are treated quantum theoretically, the probe and phase conjugate waves correspond the photon annihilation and creation operators respectively

## **2.11 Applications of Phase-Conjugate Light**

Phase conjugate light has found large number of applications in various fields of science and technology. The following are some of them

### **2.11.1 Optical Resonator**

Conventional resonators suffers from large number of problems like change in length due to thermal effects, mode hopping, frequency drift etc. Utilizing a phase conjugate mirror as one of the wave resonator's mirror can solve this type of problems. This type of resonator is called a phase conjugate optical resonator. The phase distortion correction is automatically performed during round trips of a light beam even if there are aberrating substances within the optical resonator.

### **2.11.2 Laser Fusion**

A light beam is concentrated into a small surface area in laser fusion for increasing the optical energy concentration and approximating the conditions that occur in fusion. In order for increasing the energy concentration it is necessary that the amplifying medium is adjusted in several stages and hence beams from several directions are to be focused on to the fuel pellet. Use of phase conjugate mirrors for directing the beams on to the fuel pellet can free the beam from several types of distortions.

### **2.11.3 Optical image transmission**

While transmitting images through multimode optical fiber the phase of different modes present in the fiber experiences different phase shifts and this will distort the optical image. If this image is injected into a phase conjugate mirror made from a nonlinear medium the resulting waves will be free from distortions. Therefore the quality of the image transmission can be increased considerably[50].

### **2.11.4 Interferometers**

If phase conjugate light is applied to an interferometer the phase change doubles and the sensitivity increases and the interference fringes are visible independent of changes in the intensity of the incident light.



### **2.11.5 Optical frequency filters**

When the frequency of the probe wave is different from that of the pump wave in four wave mixing, the reflectance shows a strong dependence on detuning [51]. This feature is being actively used in optical frequency filters.

### **2.11.6 Optical pulse compression**

By injecting two optically intense pulsed pump waves into a nonlinear medium at a small angle, radiations with pulse width narrower than that of the input pulses can be produced by wave mixing. This technique is used for the optical pulse compression.

## **2.12 Instruments specifications:**

Specifications of the laser sources, photo diodes and laser energy meters used for making measurements are given below:

### **2.12.1 Pulsed Nd: YAG laser [52]**

A Q-switched Nd:YAG laser (Spectra Physics Quanta Ray GCR: 170) which has a fundamental wavelength at 1.06  $\mu\text{m}$  is used in the experiments described in this thesis. The high peak power of the Q-switched pulses permit second harmonic generation at 532 nm by introducing KDP crystal in the beam path. This wavelength is used for the z-scan and four wave mixing studies included in this thesis. The pulse width is 6 – 7 ns and maximum energy per pulse available at this wavelength is 450 mJ. The pulse repetition frequency is 10 Hz and the beam has a Gaussian output (70%).

### **2.12.2 MOPO [53]**

For the wavelength dependent studies using the z-scan and DFWM techniques, a MOPO laser (Quanta Ray MOPO – 170) that can be tuned from 410 nm (signal) to 2000 nm (idler) is used. The Gaussian (70%) output from this laser has a pulse width of 4-5 ns and the beam shape was approximately circular ( $\pm 20\%$ ).

## Investigations of nonlinear .....

### 2.12.3 Photodiodes [54,55]

Photodiodes from Newport and Melles Griot were used for the energy measurements. The Newport 818 UV has a spectral range of 190nm – 1100nm and 1cm<sup>2</sup> active area. The Melles Griot, 13DAS 007 has a spectral range of 350nm – 1100nm and 0.1cm<sup>2</sup> active area.

### 2.12.4 Oscilloscope [56]

Degenerate four wave mixing signals were monitored using photodiodes and Tektronix TDS 360 oscilloscope. The oscilloscope had a rise time of 1.75 ns and an input impedance of 1 M $\Omega$  . The sensitivity range of the oscilloscope was 2mV/division to 10V/division.

### 2.12.5 Energy meter [57, 58]

For the energy measurements in z-scan and DFWM experiments Rj – 7620 dual channel energy Ratio meter is with two Rjp – 735 pyroelectric detector heads were used. The details of the detector head is as follows

Spectral response	0.18 - 20 $\mu$ m
Maximum total energy	1.0 J
Maximum energy density	1.0 J/cm <sup>2</sup>
Minimum detectable energy	100 nJ
Maximum pulse rep rate	40 Hz
Detector active area	1.0 cm

### 2.12.6 Spectrophotometer [59]

The absorption spectra of the samples used in the present study were taken using Jasco 570 spectrophotometer. The wavelength range of the same was 190 nm to 2500 nm and the is 0.1 nm in the UV/Visible region and 0.5nm (NIR region).

**2.13 Reference:**

1. J O Gorman, A F J Levi, T T Ek and R A Logan, *Appl. Phys. Lett.* **59** (1991) p. 16
2. A Yariv, *Optical Electronics In Modern Communications*, Oxford University Press (1997) New York
3. J G Fujimoto and E P Ippen, *Opt. Lett.* **8**, (1983) p.446
4. G J Dunning and R C Lind, *Opt. Lett.* **7** (1982) p.558
5. M Samoc, A samoc, B L Davies, Z Bao, L Yu, B Hsieh and U Scherf, *J. Opt. Soc. Am. B* **15** (1998) p. 817
6. J S Shirk, R G S Pong, F J Bartoli and A W Snow, *Appl. Phys. Lett.* **63** (1993) p. 1880
7. M S Bahae, A A Said and E W Van Stryland, optics, *Opt. Lett.* **14** (1989) p.955
8. M S Bahae, A A Said, T H Wei, D J Hagan, E W V Stryland, *IEEE J. Quantum Electronics* **26** (1990) p. 760
9. B L Justus, A L Huston and A J Campillo, *Appl. Phys. Lett.* **63**(11), (1993) p.1483
10. F E Hernandez, A Marcano O, H Maillotte, *Optics. Commun.* **134** (1997) p.529
11. J M S Bahae, J. Wang, R De Salvo, D J Hagan and E W Van Stryland, *Opt. Lett.* **17** (1992) p.258
12. H Ma and C B de Araujo, *Appl. Phys. Lett.* **66** (1995) p. 1581
13. T Xia, D J Hagan, M S Bahae and E W Van Stryland, *Opt. Lett.* **19** (1994) p. 317
14. P.B. Chapple, J.M. Staromlynska, J.A. Hermann, and T.J. McKay, *J. Nonlinear Opt. Phys. and Mat.* **3**, (1997) p. 251
15. Robert E Bridges, George L Fischer and Robert W Boyd *Opt. Lett.* **20** (17), (1995) p. 1821
16. Yong-Liang Huang and Chi-Kuang Sun, *J. Opt. Soc. Am. B* **17** (1) (2000) p.43
17. P B Chapple, J Staromlynska and R G McDuff, *J. Opt. Soc. Am. B* **11** (1994) p. 975
18. J A Herman, T McKay and R G McDuff, *Opt. Commun.* **154** (1998) p. 225
19. T. Xin, D.J. Hagan, M. Sheik-Bahae, and E.W. Van Stryland, *Opt. Lett.* **19**, (1994) p.317
20. D.V. Petrov, *J. Opt. Soc. Am.* **B13**, (1996) p.1491
21. J. -G. Tian, W. -P. Zang, and G. Zhang, *Opt. Commun.* **107**, (1994) p.415
22. S.M. Mian, B. Taheri, and J.P. Wicksted, *J. Opt. Soc. Am.* **B13**, (1996) p.856
23. M. Sheik-Bahae, A.A. Said, D.J. Hagan, M.J. Soileau, and E.W. Van Stryland, *Opt. Engg.* **30**, (1991) p.1228
24. S.V.Kershaw, *J. Mod. Opt.* **42**, (1995) p.1361
25. T H Wei, T H Huang, H D Lin and S H Lin, *Appl. Phys. Lett.* **67**(16), (1995) p.2266
26. S Couris, E Koudoumas, A A Ruth and S Leach, *Phys. B At. Mol. Opt. Phys.* **28**, (1995) p. 4537
27. T Xia, D J Hagan, A Dogariu, A A said and E W V Stryland, *Appl. Opt.* **36**, (1997) p. 4110
28. T Hattori and T Kobayashi, *J. Chem. Phys.* **94** (1991) p. 3332
29. D. Wearie, B S Wherrett, D A B Miller and S D Smith, *Opt. Lett.* **4**, (1974) p.331
30. S J Bentley, R W Boyd, W E Butler and A C Melissions, *Opt. Lett.* **25** (2000) p. 1192
31. A.D. Walser, G. Coskun, and R. Dorsinville, *Electrical and Optical Polymer Systems*, ed.'s D.L. Wise, G.E. Wnek, D.J. Trantolo, T.M. Cooper, and J.D. Gresser, Marcel Deccer Inc., New York, 423
32. M. Zhao, Y. Cui, M. Samoc, P.N. Prasad, M.R. Unroe, and B.A. Reinhardt, *J. Chem.*

33. S.K. Ghoshal, P. Chopra, B.P. Singh, J. Swiatkiewicz, and P.N. Prasad, *J. Chem. Phys.* **90**, (1989) p.5078
34. M. -T. Zhao, B.P. Singh, and P.N. Prasad, *J. Chem. Phys.* **89**, (1988) p.5535
35. B.P. Singh, M. Samoc, H.S. Nalwa, and P.N. Prasad, *J. Chem. Phys.* **92**, (1990) p.2756
36. Y. Pang, M. Samoc, and P.N. Prasad, *J. Chem. Phys.* **94**, (1991) p.5282
37. B.P. Singh, P.N. Prasad, and F.E. Karasz, *Polymer* **29**, (1988) p.1940
38. M. Samoc and P.N. Prasad, *J. Chem. Phys.* **91**, (1989) p.6643
39. Y. Cui, M. Zhao, G.S. He and P.N. Prasad, *J. Phys. Chem.* **95**, (1991) p.6842
40. M.K. Casstevens, M. Samoc, J. Pflieger, and P.N. Prasad, *J. Chem. Phys.* **92**, (1990) p.2019
41. Y R Shen, *Principles of Nonlinear Optics*. John Wiley & Sons (SEA) Pvt. Ltd, Singapore
42. Jun Ichi Sakai. *Phase Conjugate Optics*. Mc. Grow Hills New York
43. R A Fischer (Ed.) *Optical Phase Conjugation*. Academic Press (1983) New York
44. J A Nunes, W G Tong, D W Chandler, and L A Rahn. *J. Phys. Chem. A* **101** (1997) p. 3279
45. D W Neyer, L A Rahn, D W Chandler, J A Nunes and W G Tong. *J. Am. Chem. Soc.* **119** (1997) p. 8293
46. P C de Souza, G Nader, T catunda, M Muramatsu and R J Horowicz. *Opt. Commun.* **163** (1999) p. 44
47. M F Yung and X Y Wong. *Appl. Phys. B* **66** (1998) p. 585
48. A Yariv. *Optical Electronic in Modern Communications*, Oxford University Press (1997) New York
49. A Yariv and D M Pepper, *Opt. Lett.* **1** (1997) p. 16
50. A Yariv, *Appl. Phys. Lett.* **28** (1976) p. 88
51. D M Pepper and R L Abrams, *Opt. Lett.* **3** (1978) p.212
52. *User Manual*, GCR Series, Spectra Physics Lasers Inc. (1997) CA, USA
53. *Instruction Manual*, MOPO 700 Series. Spectra Physics Lasers Inc. (1993) CA, USA
54. *818-UV Detector Calibration Report*, Newport Corporation, CA, USA
55. *Melles Griot Catalogue 1997-98*, Melles Griot Inc, USA
56. *User Manual TDS 360*, Tektronix Inc. (1995) Wilsonville
57. *User Manual*. Rj-7620 series Energy Ratio Meter, Laser Probe Inc., USA
58. *Users Manual*, Rjp-700 series Energy Probes, Laser Probe Inc., USA
59. *Hardware Manual*,. Jasco 570, Jasco Corporation, Tokyo, Japan

## Chapter 3

### Nonlinear Optical Studies on Samarium Phthalocyanine in Methyl Methacrylate using Z-Scan and Optical Limiting Techniques

#### Abstract

The effective nonlinear absorption coefficient  $\beta_{\text{eff}}$  and the imaginary part of the nonlinear susceptibility  $\text{Im}(\chi_{\text{eff}}^3)$  of Samarium Phthalocyanine are calculated from open aperture z-scan measurements. The sample is taken in Methyl Methacrylate, both in liquid (Methyl Methacrylate Monomer - MMA) and solid (Poly Methyl Methacrylate - PMMA) matrices. For sample excitation, nanosecond laser pulses at 532 nm have been employed. Nonlinear absorption is explained in terms of a five level model. Compared to the sample in solid matrix, sample in liquid medium is found to show better nonlinear behaviour and this is explained using bimolecular process taking place in these samples. Optical limiting efficiency of the samples is studied in both phases and the results are compared. The concentration dependence on the optical limiting nature is studied both in liquid as well as in solid medium and the role of RSA in the limiting behaviour is verified.

## 3.1 Introduction

In most of the materials the amount of light transmitted is a linear function of the intensity of light incident on these materials. In such cases, the absorption in these samples can be fully described by Beers-Lambert law [1].

$$\frac{dI}{dz} = -\alpha I \quad (3.1)$$

where  $\alpha$  is the absorption coefficient,  $I$  is the intensity of radiation and  $z'$  denotes the propagation depth inside the material. Obviously  $\alpha$  is independent of intensity and depends only on the wavelength of excitation. But there are some materials which show marked difference from this behaviour and they are called nonlinear absorbers. In recent year, the z-scan technique has been widely used to study the reverse saturable absorption (RSA) of various materials [1-2]. By RSA we mean the absorption coefficient  $\alpha$  in the Beer's equation increases with irradiance  $I$  (energy per area per time) or fluence  $F$  (energy per area). The z-scan technique involves measurements of the transmittance (transmitted energy/input energy) of tight focused laser beams ( $TEM_{00}$  mode, pulsed) of equal energy through the sample at various  $z$  positions relative to the focus. In the case of reverse saturable absorption (RSA), the sample experiences the strongest intensity and fluence at focus; therefore it absorbs the most energy and allows least transmittance. Away from the focus in the direction of both increasing and decreasing  $z$ , transmittance increases evenly because the irradiance decreases symmetrically about the focus. RSA is the main topic of discussion in this chapter. In the case of saturable absorption (SA) the absorption coefficient  $\alpha$  decrease with intensity or fluence. But in the case of linear absorption  $\alpha$  remains constant irrespective of intensity or fluence of the incident radiation. Thus, it is evident that in the presence of nonlinear absorption,  $\alpha$  becomes a function of intensity also and hence it is usually written as  $\alpha(I, \lambda)$ .

Materials showing saturable absorption become more transparent when the incident intensity is increased and this phenomenon is exploited for applications like passive mode locking in lasers [3]. Reverse saturable absorbers become more opaque on increasing the incident intensity and found applications in the design of passive optical power limiters to protect optical sensors, including human eye, from intense laser pulses [4-9]. Design and fabrication of devices based on the nonlinear optical (NLO) properties of materials is an exciting area of research in the field of optoelectronics and photonics. The measurement of nonlinear optical parameters of various materials has acquired great importance in this context. Useful data is now available in the literature on the NLO properties of materials like fullerenes, semiconductors, liquid crystals, conjugated polymers, dyes, organo- metalics [10-19] etc. Large non-resonant optical susceptibility, ultrafast response, thermal and chemical stability, ease of molecular structural engineering etc. are the most desired properties of a good NLO material. In general, it is not possible to simultaneously satisfy all these criteria in a single material. However, organic macromolecules with extensive  $\pi$  electron conjugation like porphyrins, phthalocyanines, naphthalocyanines and their different derivatives form a class of compounds which satisfy many of such requirements [20]. The relatively low linear absorption and high ratios of excited state to ground state absorption cross section in the 400 – 600 nm region make the metallo-phthalocyanines ideal for the realization of design and fabrication of good quality optical limiters in the visible region. There are various reports in literature on the nonlinear optical properties of these materials in different solvents [21-22]. But when device applications are considered, the incorporation of these materials into solid matrices and the study of their behaviour in different host materials become important. Therefore we studied the NLO properties of Samarium Phthalocyanine in solid (PMMA) as well as in liquid (MMA) matrices.

## **Experimental**

In a typical open aperture z-scan experiment the transmittance of the sample is measured as the sample is moved along the propagation direction ( $z$ ) of a focused Gaussian laser beam. In the present experiment the beam is focused with a lens of focal length 30 cm producing a spot size  $\omega_0$  of  $2 \times 10^{-5}$  m and Rayleigh range  $z_0$  of  $2.3 \times 10^3$  m. The z-scan measurements in liquid phase are done by dissolving the samples directly in Methyl methacrylate monomer and the samples are taken in a 1.5 mm cuvette. Doped PMMA samples are prepared by directly dissolving the sample in MMA containing suitable initiators and keeping the solution at a constant temperature ( $50^\circ\text{C}$ ) waterbath for a period of 48 hours. Fine polished solid samples of suitable dimensions (1.5 mm) are prepared from the polymer thus obtained. The damage thresholds of the samples thus obtained were measured and it is found to be  $1.9 \text{ J/cm}^2$  for the doped PMMA samples and  $2.2 \text{ J/cm}^2$  for the undoped PMMA. The damage threshold of the undoped PMMA is in agreement with the value already reported in the literature [23]. The decrease of the laser damage threshold in the doped polymer samples is due to the defects in the microstructure of the polymer as well as the presence of foreign bodies within the polymer. Incident energy as well as the transmitted energy from the sample is measured using a dual channel energy ratio meter (Rj-7620, Laser probe inc.) and averaged over hundred pulses.

### **3.3 Effective nonlinear absorption coefficient**

Though the original theory of Z-scan was derived for pure TPA, it has been shown that the same theory can also be used for ESA. However, in this case we have to properly redefine the nonlinear absorption coefficient  $\beta$  as  $\beta_{\text{eff}}$ . The present measurements have been taken using nanoseconds pulses and therefore, two assumptions can be made: (1) intersystem crossing [from  $S_1(v=0)$  to  $T_1(v=0)$ ] is fast compared to the laser pulse width and (2) intersystem crossing yield  $\Phi_{\text{isc}}$  is nearly one i.e. virtually all the atoms excited from  $S_0$  reach the first excited triplet state  $T_1$ .



As mentioned previously, atoms then get excited from  $T_1$  to  $T_2$  as a result of ESA. Under these assumptions, intensity variation through the sample and population in the first excited triplet state  $T_1$  are respectively given by following equations [24]

$$\frac{dI}{dz} = -\sigma_0 n_0 I - \sigma_t n_t I \quad (3.2)$$

$$n_t = \sigma_0 n_0 I \Phi_{isc} \quad (\Phi_{isc}=1) \quad (3.3)$$

Here  $\sigma_0$ ,  $\sigma_t$ ,  $n_0$  and  $n_t$  are ground state absorption cross-section, first excited triplet state absorption cross-section, number of molecules in the ground state per ml, and number of molecules in the first excited triplet state per ml respectively. ( $z$  corresponds to sample length). From equations (3.2) and (3.3), the intensity dependent absorption coefficient  $\alpha(I)$  and  $\beta_{eff}$  are given respectively by

$$\alpha(I) = \sigma_0 n_0 + \sigma_t \sigma_0 n_0 I \quad (3.4)$$

$$\beta_{eff} = n_0 \sigma_0 \sigma_t \quad (3.5)$$

It is clear that  $\beta_{eff}$  is intensity dependant for STPA through the factor  $n_0$ , whereas  $\beta$  is independent of intensity for pure TPA.  $\beta_{eff}$  is a measure of the over all absorptive nonlinearity present in the sample [24].

### 3.4 Rate equations

Dynamics of ESA can be described using rate equations. Under nanosecond excitation, amongst singlet states, populations at  $S_1$  alone is important. This is because of the fact that higher excited singlet states have a lifetime of the order of picosecond, which is much less than the laser pulse width. Therefore, only the ground state ( $S_0$ ), first excited singlet state ( $S_1$ ) and first excited triplet state ( $T_1$ ) are considered. If  $\sigma_g$ ,

and  $\sigma_i$  represent the absorption cross sections of  $S_0$ ,  $S_1$  and  $T_1$  respectively, the rate equations for the population in these energy levels may be written as [4]

$$\frac{dn_0}{dt} = -\frac{\sigma_0 I}{h\nu} n_0 + \frac{1}{\tau_{10}} n_1 + \frac{1}{\tau_{20}} n_2 \quad (3.6)$$

$$\frac{dn_1}{dt} = \frac{\sigma_0 I}{h\nu} n_0 - \left( \frac{1}{\tau_{10}} + \frac{1}{\tau_{12}} \right) n_1 \quad (3.7)$$

$$\frac{dn_2}{dt} = \frac{1}{\tau_{12}} n_1 - \frac{1}{\tau_{20}} n_2 \quad (3.8)$$

Here  $n_0$ ,  $n_1$  and  $n_2$  are the populations in  $S_0$ ,  $S_1$  and  $S_2$  levels respectively.  $\tau_{10}$ ,  $\tau_{12}$  and  $\tau_{20}$  are the life times of  $S_0 \leftarrow S_1$ ,  $T_1 \leftarrow S_1$  and  $S_0 \leftarrow T_1$  transitions respectively. Transmitted light intensity may be written in terms of total absorption coefficient, which is also a function of time. The equations (3.9) and (3.10) give total absorption coefficient and transmitted intensity respectively.

$$\alpha(t) = \sigma_0 n_0(t) + \sigma_1 n_1(t) + \sigma_2 n_2(t) \quad (3.9)$$

$$\frac{dI}{dz} = -(\sigma_0 n_0 + \sigma_1 n_1 + \sigma_2 n_2) I \quad (3.10)$$

The equations (3.9) and (3.10) can be numerically solved using the initial conditions,  $n_0(t = -\infty, z) = N = n_0 + n_1 + n_2$ ,  $n_1(t = -\infty, z) = n_2(t = -\infty, z) = 0$ .  $\sigma_1$  and  $\sigma_2$  are kept as adjustable parameters. In macromolecules the vibrational levels of excited singlet states ( $S_1$  &  $S_2$ ) and triplet states ( $T_1$  &  $T_2$ ) overlap in most cases. Intersystem crossing occurs in nanosecond time scales. Hence under picosecond excitation,  $S_2$  level is considered instead of  $T_1$ . In the steady state conditions, the nonlinear absorption coefficient is written as [4]

$$\alpha = \alpha_0 \left[ \frac{1 + KI'}{1 + I'} \right] \quad (3.11)$$

## Investigations of nonlinear .....

Here  $I' = I/I_s$ , where  $I_s$  is the saturation intensity and  $K = \sigma_T/\sigma_0$ . If  $K$  is greater than one, we get RSA and a value of  $K$  less than one, yields SA. In this chapter,  $\beta_{\text{eff}}$  is measured using two-photon absorption theory introduced by Sheik Bahae et. al [1].

### 3.5 Results and discussion

The structure of the sample used in the present study, Samarium Phthalocyanine [ $\text{Sm}(\text{Pc})_2$ , Bis-Phthalocyanine], and a typical absorption spectrum in MMA and PMMA are given in figures 3.1 and 3.2 respectively. Bis-Pc's have a sandwich structure in which the metal ion lies in between the two Pc planes [25]. Phthalocyanine has a characteristic low energy absorption band in the 600-800 nm region and it is generally called the Q-band. They also have a high energy absorption band in the 300-400 nm region called Soret or B band and an absorption valley around 532 nm in the visible region. In the valley of the linear absorption spectrum, reverse saturable absorption could occur because in this wavelength region the absorption cross section of the excited state is larger than that of the ground state [4].

The advantages of polymer matrices over solution phase such as their compactness, ease of handling etc. are obvious in a wide range of applications. However, the extent to which the optical properties of the sample may differ in different matrices is an important aspect to be considered. We did not observe any marked differences between the absorption spectra obtained for the sample, Samarium Phthalocyanine, in methyl methacrylate monomer (MMA) and poly methyl methacrylate (PMMA) matrices. The spectra obtained are also identical with those reported in literature [26]. This clearly shows that the solid matrix (PMMA) does not modify the sample properties appreciably.

Investigations of nonlinear .....

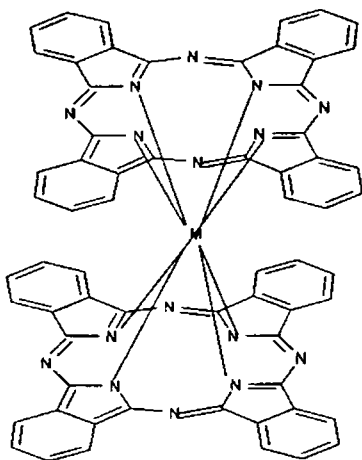


**Fig 3.1** Structure of Sm(Pc)<sub>2</sub>

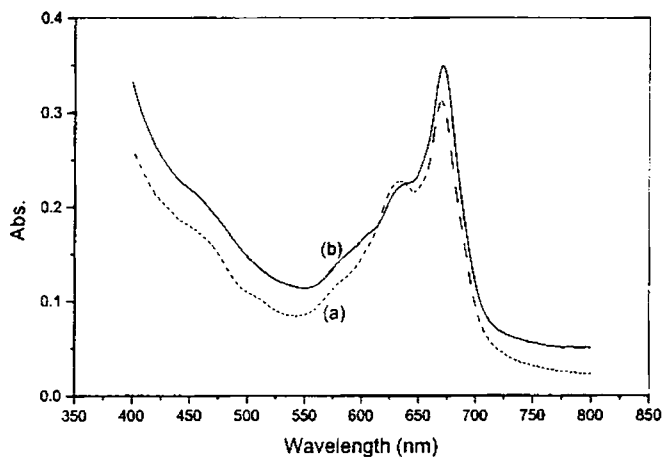


**Fig 3.2** Typical absorption spectrum of 0.23 mM Samarium phthalocyanine in (a) Methyl Methacrylate Monomer (b) Poly Methyl Methacrylate

From the open aperture z-scan experimental data, nonlinear absorption coefficient  $\beta$  is calculated using the model suggested by Sheik Bhahe et.al. [1]. Nonlinear absorption coefficient  $\beta$  is calculated by fitting the experimental data to the normalized transmittance given by the equation

$$T(z) = \frac{C}{q_0 \sqrt{\pi}} \int_{-\infty}^{\infty} \ln(1 + q_0 e^{-t^2}) dt \quad (3.12)$$

In equation 3.12, C is the normalization constant,  $q_0 = (\beta I_0 l_{eff}) / (1 + x^2)$  where  $I_0$  is the irradiance at focus,  $x = z/z_0$  and  $l_{eff} = (1 - e^{-\alpha l}) / \alpha$  is the effective length of the sample,  $\alpha$  is the linear absorption coefficient and  $l$  is the sample length. It is well known that in Porphyrins like Pc's, nonlinear absorption at 532nm is not due to pure two photon absorption but due to sequential two photon absorption, also known as excited state absorption or reverse saturable absorption (RSA) [27-28]. Therefore to distinguish this from the essentially non-resonant two-photon absorption, the nonlinear absorption coefficient in RSA media is usually referred to as  $\beta_{eff}$  [29]. The imaginary part of the nonlinear susceptibility ( $\text{Im}\chi_{eff}^3$ ) can be calculated from  $\beta_{eff}$  using the expression

$$\text{Im}(\chi_{eff}^3) = \frac{\lambda \epsilon_0 n^2 c \beta_{eff}}{4\pi} \quad (3.13)$$

To explain nonlinear absorption under nanosecond excitation, a five level model involving the states  $S_0, S_1, S_2, T_1$  and  $T_2$  as shown in figure 3.3 [30] can be used. Here  $S_n$  and  $T_n$  are the singlet and triplet states respectively where  $n = 0, 1$  or  $2$  and every electronic energy level involves many vibronic sublevels. Also  $\sigma$ 's represent absorption cross sections and  $\tau$ 's represent relaxation times of atoms in different energy levels. When interacting with a laser pulse at 532 nm, atoms get excited from the  $S_0 (v=0)$  to the upper vibrational level of  $S_1$ . Here  $v$  corresponds to the vibrational quantum number. Through the nonradiative decay within picoseconds they can relax to the lowest vibrational level of  $S_1 (v=0)$ . Since Pc's have very low fluorescence [4] the transition from  $S_1 (v=0)$  to  $S_0$  can be neglected. The occurrence of the  $S_2 \leftarrow S_1$  transition does not appreciably deplete the  $S_1$  state, as the  $S_1 \leftarrow S_2$  decay also takes place within picoseconds. However the  $T_1(v=0) \leftarrow S_1(v=0)$  intersystem crossing

cross section is large, leading to a strong triplet – triplet absorption  $T_2 \leftarrow T_1$ . Here we assume that the intersystem crossing [31] is fast compared with the laser pulse width (9 ns) and virtually all the atoms excited from  $S_0$  reach first excited triplet state  $T_1$ . In fact the intersystem crossing is higher for heavy atom substituted Pc's due to large spin orbit coupling of the metal orbital and their mixing with the orbitals of the conjugated ring [26]. Therefore under nanosecond pulse excitation, the nonlinear absorption observed here is a consequence of  $T_2 \leftarrow T_1$  absorption [ $T_2 \leftarrow T_1(v=0)$ ]

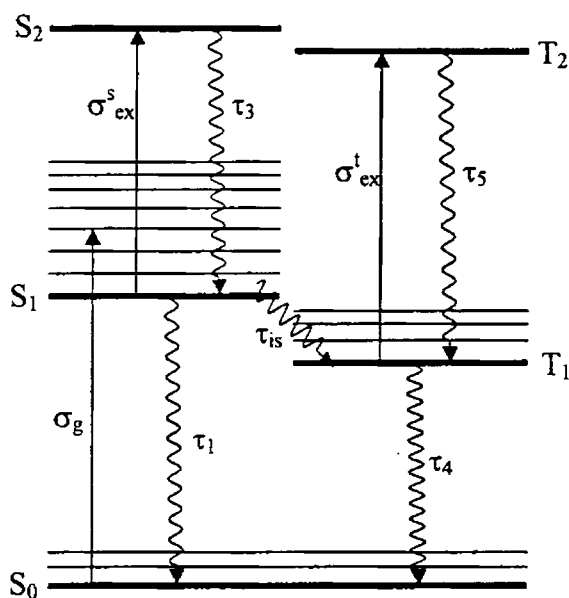


**Fig 3. 3** Five level energy diagram for Phthalocyanine.  $S_n$  ( $n = 0,1,2$ ): Singlet levels;  $T_n$  ( $n = 1, 2$ ): Triplet levels  $\sigma$ : Absorption cross section  $\tau$ : Relaxation times. Solid lines are radiative and curved lines are non-radiative

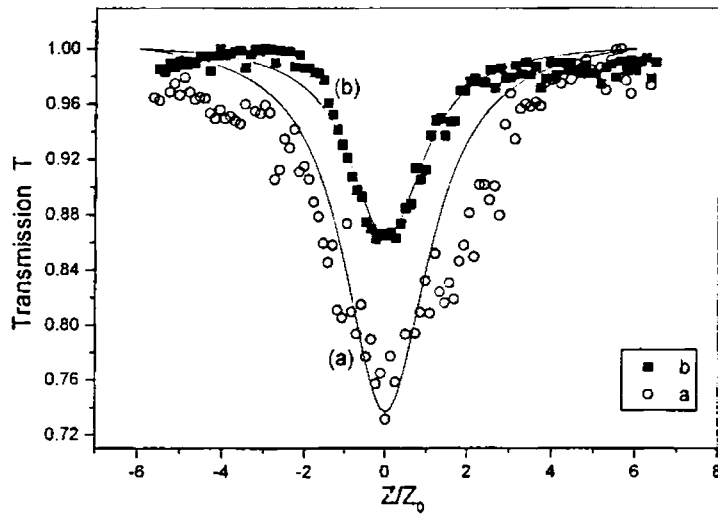


**Fig 3. 4** Z-Scan of Samarium Phthalocyanine in (a) Methyl Methacrylate monomer (MMA) [LT 39%] (b) Poly methyl methacrylate (PMMA) [46 %]

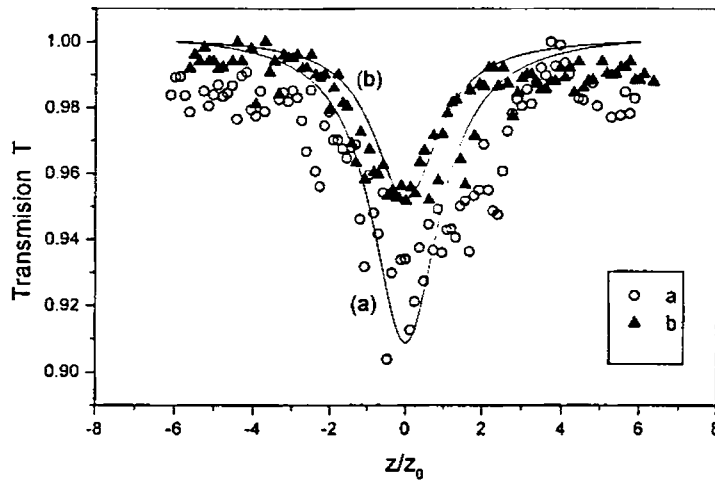


**Fig 3. 5** Z-Scan of Samarium Phthalocyanine in (a) Methyl Methacrylate monomer (MMA) [LT 74%] (b) Poly methyl methacrylate (PMMA) [74 %]

Figs. 3.4 and 3.5 show the open aperture z-scan curves obtained for the samples investigated. Solid curves are numerical fits to the experimental data. The nonlinear absorption seen in both solid (PMMA) and liquid (MMA) matrices is found to be similar. Sample thickness is 1.5 mm in both cases and the reduction in transmittance around the focal region reveals the nonlinearity. The experiments have been repeated in the pure host materials MMA and PMMA in identical conditions but no measurable nonlinearity could be observed. The calculated values of  $\beta_{\text{eff}}$  and  $\text{Im}(\chi_{\text{eff}}^3)$  along with the linear absorption coefficient are given in table 1.

Sample	Host Matrix	Absorption Coefficient $\alpha$ (cm <sup>-1</sup> )	Linear Transmittance (LT)%	$\beta_{\text{eff}}$ cm/GW	$\text{Im}(\chi_{\text{eff}}^3) \times 10^{-17}$ m <sup>2</sup> V <sup>-2</sup>
SmPc	MMA	0.086	74	47.83	1.075
		0.475	39	198.45	4.460
	PMMA	0.119	74	20.49	0.511
		0.328	46	69.66	1.74

**Table 1:** Measured values of nonlinear absorption coefficient and imaginary part of susceptibility tensor of Samarium Phthalocyanine in PMMA and MMA

The nonlinear absorption seen in these samples reveal that they can be used as potential optical limiters. For being used as a good optical limiter, a number of important requirements should be met by the nonlinear material. Fast response, high damage threshold and an excited state absorption cross-section larger than the ground state absorption cross-section are the most important among them [32]. At 532nm the excited state absorption cross section of phthalocyanine is higher than the ground



state absorption cross section [26]. Moreover, this class of materials responds to both fast and slow laser pulses via the ( $S_2 \leftarrow S_1$ ) and ( $T_2 \leftarrow T_1$ ) transitions respectively. Consequently, these molecules can be used for passive optical power limiting. Figures 3.6 and 3.7 show the normalized transmittance of the present samples as a function of the input fluence, plotted using data extracted from the z-scan curves. From the curves and the  $\beta_{\text{eff}}$  values we can conclude that limiting in the liquid samples is somewhat better as compared to that in the solid matrix.

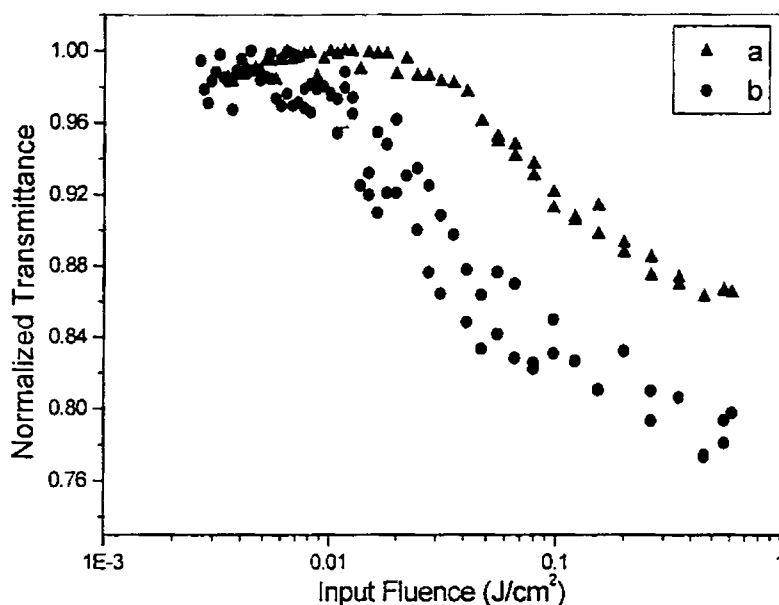


**Fig 3. 6** Optical limiting response of Samarium Phthalocyanine in  
 (a) Methyl Methacrylate monomer (MMA) [LT 46%]  
 (b) Poly methyl methacrylate (PMMA) [39%]

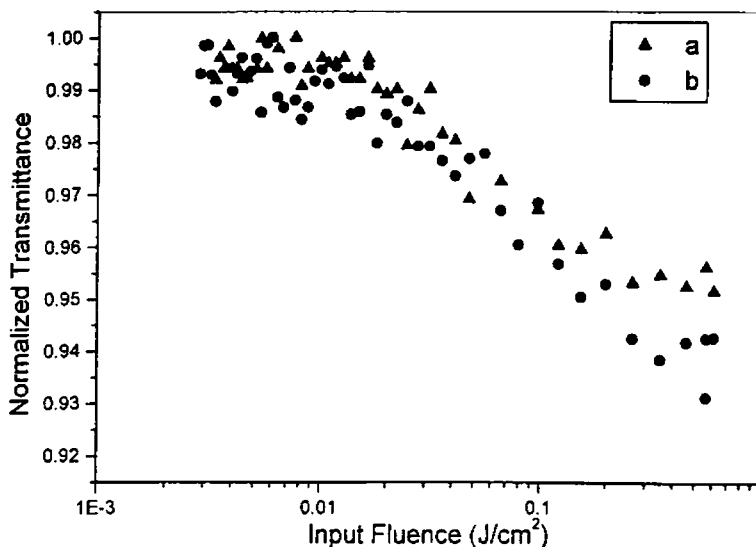


**Fig 3. 7** Optical limiting response of Samarium Phthalocyanine in  
 (a) Methyl Methacrylate monomer (MMA) [LT 74%]  
 (b) Poly methyl methacrylate (PMMA) [74%]

The observed better optical limiting behaviour of the sample in liquid phase as compared to the same in solid can be explained on the basis of the bimolecular process suggested by Jason et. al. [33]. Diffusion of molecules in solutions will provide an extra contribution towards the optical limiting property through bimolecular process of excitation and de-excitation mechanism. The energy level diagram corresponding to bimolecular process is given below (Fig. 3.8). Where S's and T's represent singlet and triplet transitions and  $\sigma$ 's represent relation time. The excited state energy of one molecule will be transferred to another one and this will result in the enhancement in optical limiting property of the sample. However in the case of solids such diffusion process is not possible in the time scale (ns) of the laser pulse used in the present experiment. Hence the optical limiting in solids can arise from excited state absorption process through the phenomenon of reverse saturable absorption. This argument supports the present observation that at low concentration

Investigations of nonlinear .....

(as indicated by high linear transmittance) the optical limiting efficiency (as indicated by  $\beta_{\text{eff}}$ ) does not differ much as in the case of higher concentration for both liquid and solid matrices[Fig.3.7]. At this level of concentration there may not be sufficient amount of diffusion so as to support bimolecular processes.

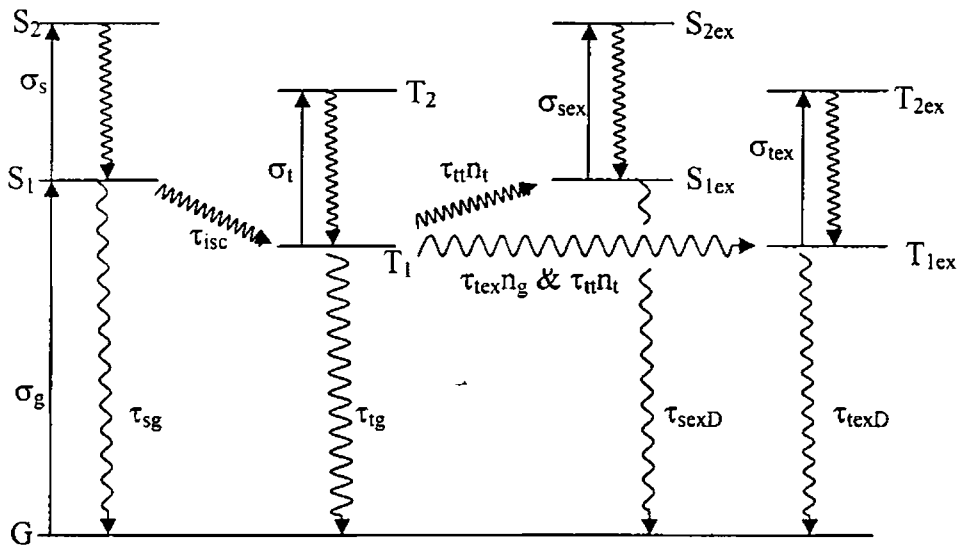
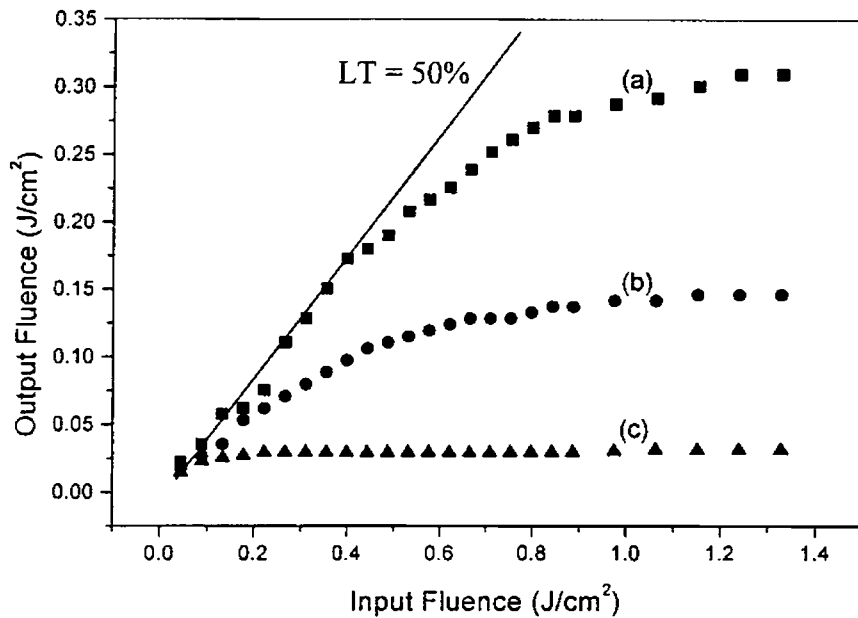


Fig 3. 8 Reverse saturable absorption mechanism for phthalocyanine that includes both unimolecular and bimolecular excited state processes

As concentration is increased, the additional contribution through bimolecular process results in the higher optical limiting efficiency in liquids as compared to solids. Enhancements in the  $\beta_{\text{eff}}$  at higher concentration in both solid and liquid media are due to the availability of more number of molecules to take part in the light-matter interaction. In liquids, over and above this, extra contributions to the optical limiting efficiency come from diffusion processes.

### 3.6 Concentration Dependence

In order to understand the effect of thickness and concentration of the material on the RSA the optical limiting responses were measured in a series of doped PMMA and MMA samples. To keep the linear transmittance constant same sample with different path length were used [4]. Figure 3.9 and 3.10 shows the optical limiting graphs thus obtained with Samarium Phthalocyanine in PMMA and MMA medium.



**Fig 3. 9** Variation of transmitted fluence with respect to incident fluence for Samarium Phthalocyanine doped PMMA of 50% linear transmittance (a) Path length 1.5 mm (b) Path length 3.0 mm (c) Path length 5.0 mm

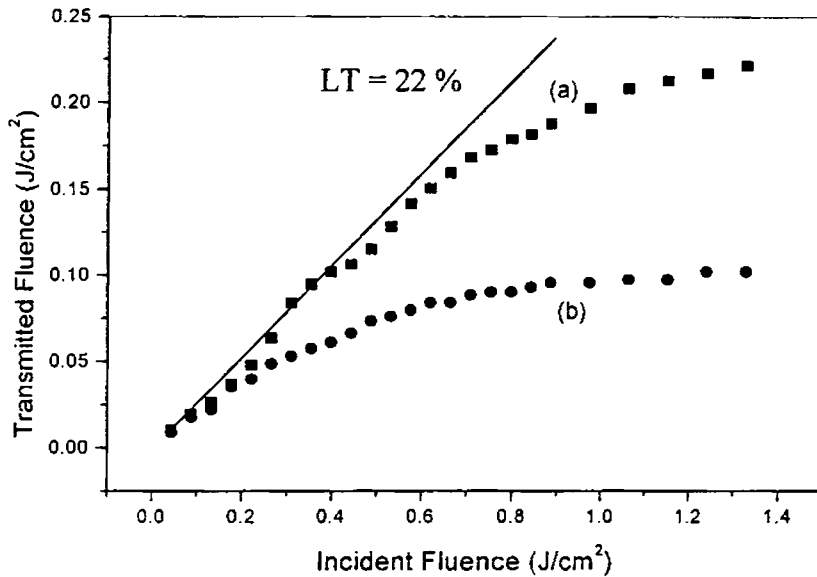


**Fig 3. 10** Variation of transmitted fluence with respect to incident fluence for Samarium Phthalocyanine doped MMA of 22% linear transmittance (a) Path length 1.5 mm (b) Path length 3.0 mm

From the results shown in Fig.3.9 and 3.10 it is obvious that the limiting shows clear concentration dependence. This result is in good agreement with the report on copper phthalocyanine by Li et.al. [4]. The sample with larger path length (lower concentration) shows a better optical limiting property, and its saturation threshold is rather low. It may be noted here that the ratio of the effective excited state to ground state absorption cross section  $\sigma_{exc}/\sigma_g$  can be used as a figure of merit for RSA based optical limiters. This can be defined as  $\sigma_{exc}/\sigma_g = \ln(T_{sat})/\ln(T_{lin})$  where  $T_{lin}$  is the linear transmittance at very low excitation energy and  $T_{sat}$  is the saturated transmittance at high excitation energies [26]. The saturation thresholds of output fluence are 0.18, 0.06 and 0.026 J/cm<sup>2</sup> corresponding to sample lengths of 1.5 mm, 3.0 mm and 5.0 mm respectively. The figure of merit calculated is 1.86. While the reported values of figure of merit are about 3 for C<sub>60</sub> and more than 10 for Phthalocyanine complexes, that of the rare-earth metallo-phthalocyanine doped

PMMA samples have been found to be lower [34], and this agrees with the present measurements. The linear transmittance of the sample in liquid medium used for the present study is very low (LT = 22%). Therefore the saturation threshold is further smaller in this case. The measured values are  $0.10 \text{ J/cm}^2$  and  $0.035 \text{ J/cm}^2$  corresponding to sample length 1.5 mm and 3.0 mm respectively.

Kojima et. al. [35] while explaining the optical limiting property of a polyacene based oligomer using a five level energy diagram, have shown that, in the case of reverse saturable absorption due to excited state absorption the incident laser intensity  $I_0$  and the transmitted laser intensity  $I$  obey the relation

$$\ln(I_0/I) = k(I_0 - I) + A_g \quad (3.14)$$

where  $k$  is a constant that depends on the absorption cross sections and lifetimes of the ground, excited singlet and excited triplet states and  $A_g$  is the ground state absorbance. Equation (3.14) says that the plot of  $\ln(I_0/I)$  versus  $(I_0 - I)$  should be a straight line with slope  $k$  and intercept  $A_g$ .

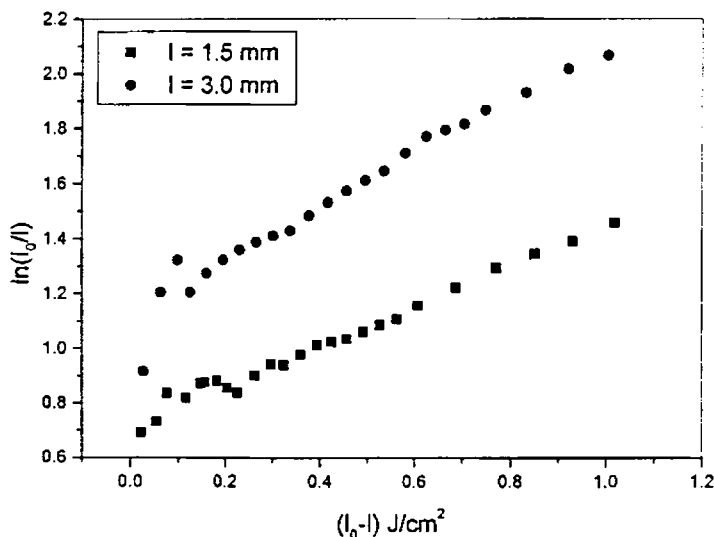
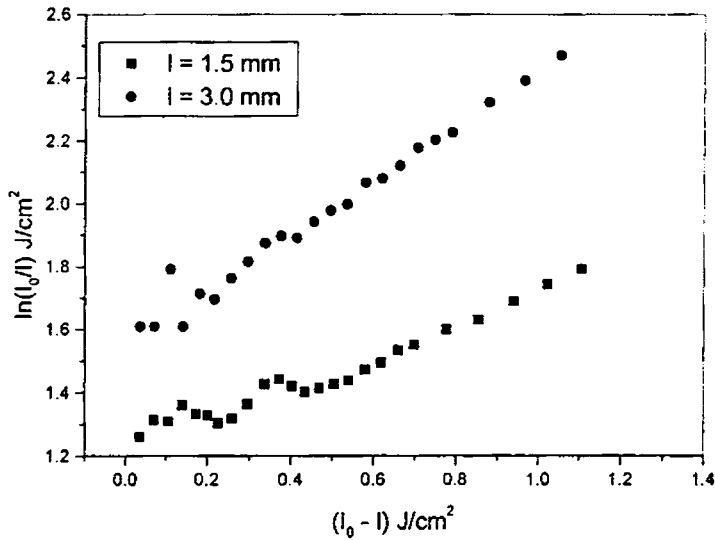


Fig 3. 11 Plot of  $\ln(I_0/I)$  versus  $(I_0 - I)$  of  $\text{Sm}(\text{Pc})_2$  doped in PMMA



**Fig 3. 12** Plot of  $\ln(I_0/I)$  verses  $(I_0 - I)$  of  $\text{Sm}(\text{Pc})_2$  in MMA

Figure 3.11 and 3.12 shows the plot of  $\ln(I_0/I)$  verses  $(I_0 - I)$  for samarium Phthalocyanine doped PMMA and MMA respectively. The straight-line nature of the graph is a clear indication that RSA is the main mechanism causing optical limiting in these samples.

### 3.7 Conclusion

Using the open aperture z-scan technique, the effective nonlinear absorption coefficient  $\beta_{\text{eff}}$  and imaginary part of the nonlinear susceptibility ( $\text{Im}\chi_{\text{eff}}^3$ ) of Samarium Phthalocyanine in Methyl Methacrylate at 532 nm has been calculated, in both liquid and solid media. The optical limiting behaviour of the samples is also studied. The nonlinearity originates from the large excited state absorption cross section, the characteristic property of Phthalocyanines. Enhancement in optical

limiting property of samples in liquid phase over the solid phase is attributed to the bimolecular processes taking place in liquid media. The measured  $\beta_{\text{eff}}$  values as well as the optical limiting curves show that samples in liquid phase are moderately better in their optical limiting efficiency. However, the solid matrix gives rigidity to the nonlinear medium and the handling is more convenient. Therefore for a device application the polymeric solid matrix may be preferred over the monomeric solution phase. The concentration dependence on the optical limiting nature is studied both in liquid as well as in solid medium and the role of RSA in the limiting behaviour is verified.



### 3.8 References

1. Mansoor Sheik Bahae, Ali A Said, Tai -Huei Wei, David J Hagan and E W Van Stryland, *IEEE J. Quant. Electron.* **26** (4), (1990) p. 760
2. A A Said, M Sheik Bahae, D J Hagan, T H Wei, J Wang, J Young and E.W Van Stryland, *J. Opt. Soc.Am. B* **9**, (1992) p.405
3. M Wittmann, A Penkofer, *Appl. Phys. B.* **65** (1997) p. 761
4. Chunfei Li, Lei Zhang, Miao Yang, Hui Wang and Yuxiao Wang, *Phys. Rev. A* **49**(2), (1994) p. 1149
5. Yinglin song, Guangyu Fang, Yuxiao Wang, Shutian Liu, Chunfei Li, Licheng Song, Yinghuai Shu and Qingmei Hu, *Appl. Phys. Lett.* **74**(3), (1999) p. 332
6. T C Wen and I D Lian, *Synthetic Metals* **83**, (1996) p. 111
7. S Venugopal Rao, N K M Naga Srinivas, D Narayana Rao, L Giribabu, Bhaskar G Maiya, Reji Philip and G Ravindra Kumar, *Optics Communication* **182**, (2000) p.255
8. N Ono, S. Ito, C H Wu, C H Chen and T C Wen, *Chem. Phys.* **262**, (2000) p.467
9. W Ji, H Du, S H Tang, S Shi, *J. Opt. Soc. Am. B* **12**(5), (1995) p.876
10. C. Taliani, G Ruani and R. Zamboni (eds): *Fullerenes: Status and Perspectives*, World Scientific, Singapore (1972)
11. H. Haug (ed.): *Optical nonlinearities and instabilities in semiconductors*, Academic, New York (1998)
12. P Palffy-Muhoray: *Liquid crystals: Applications and uses*, Vol.1 World Scientific, Singapore, (1991) p.493
13. H S Nalwa: *Nonlinear optics of organic molecules and polymers*, C R C Press, Boca Raton, FL, (1997) p. 611
14. M A Kramer, W R Tompkin and R W Boyd, *Phys. Rev. A* **34**, (1986) p.2026
15. H S Nalwa: *Appl. Organomet. Chem.* **5**, (1991) p.349
16. E W Van Stryland, Y Y Wu, D J Hagan, M J Solileau and Kamjou Mansour, *J. Opt. Soc. Am. B* **5**(9), (1998) p.1980
17. Kamjou Mansour, M J Soileau and E W Van Stryland, *J. Opt. Soc. Am. B* **9**(7), (1992) p.1100
18. X Sun, R Q Yu, G Q Xu, T S A Hor and W Ji, *Appl. Phys. Lett.* **73**(25), (1998) p.3632
19. L Vivien, E Anglaret, D Riehl, F Hache, F Bacou, M Andrieux, F Lafonta, C Journet, g Goze, M Brunet and P Bernier, *Optics Communication* **174**, (2000) p.271
20. K Kadish, K Smith, R giulard (Eds.) *The Phorphyrin Hand Bood*, 6, Academic Press, New York 2000
21. Masahide Terazima, Hitoshi Shimizu and Atsuhiko Osuka, *J. Appi. Phys.* **81**(7), (1997) p.2946
22. K P Unnikrishnan, Jayan Thomas, V P N Nampoori and C P G Vallabhan, *Chem. Phys.* **279**, (2002) p.209
23. Olga V Przhonska, Jin Hong Lim, David J Hagan and E W Van Stryland, *J. Opt. Soc. Am. B* **15**(2), (1998) p.802
24. K P Unnikrishnan, Jayan Thomas, Binoy Paul, Achama Kurian, Pramod Gopinath, V P N Nampoori and C P Girijavallabhan, *J. Nonlin. Opt. Phys. & Mat.* **10**(1), (2001) p.113
25. J S Shirk, J R Lindle, F J Bartoli, M E Boyle, *J. Phys. Chem.* **96**, (1992) p.5847

26. Joseph W Perry, Kamjou Mansour, Seth R Marder and Kelly J Perry, *Opt. Lett.* **19** (9), (1994) p.625
27. T H Wei, D J Hagan, M J Sence, E W V Strynland, J W Perry and D R Coutler, *Appl. Phys. B* **54**, (1992) p.46
28. M A Diaz-Garcia, A Dogariu, D J Hagan and E W V Strynland, *Chem. Phys. Lett.* **266**, (1997) p.86
29. S.Couris, E Koudoumas, A A Ruth, S Leach, *Phys. B. At. Mol. Opt. Phys.* **28**, (1995) p.4537
30. T H Wei, T Hsiang, H Der Lin, S Hsein Lin, *Appl. Phys. Lett.* **67**, (1995) p. 2266
31. Tiejun Xia, D J Hagan, A Dogariu, A A Said and E W Van Stryland *Appl. Opti.* **36**, (1997) p.4110
32. H steil, A Volkmer, I Ruckmann, A Zeug, B Ehrengerg and B Roder, *Opt. Commun.* **155**, (1998) p.135
33. Jason E Riggs and Ya-Ping Sun, *J. Phys. Chem. A* **103**, (1999) p.485
34. B Aneeshkumar, Pramod Gopinath, C P G Vallabhan, V P N Nampoori and P Radhakrishna, *J. Opt. Soc. Am. B* **20**(7), (2003) p.1486
35. K Kojima, T Matsuoka, N Sato, H Takahashi, *Macromolecules* **28**, (1995) p.2893

## Chapter 4

### Z-Scan and Degenerate Four Wave Mixing Studies in Metal Complexes of Quinoxaline-2-Carboxalidene-2-Aminophenol

#### Abstract

Degenerate four wave mixing experiments were carried out in solutions of various metal complexes of Quinoxaline-2-Carboxalidene-2-Aminophenol (QAP). 532 nm radiation from a Q-switched Nd:YAG laser operating in the nanosecond region is used for the sample excitation. Figure of merit of third order nonlinearity ( $F$ ), Third order susceptibility ( $\chi^3$ ) and Second hyper polarizability  $\langle\gamma\rangle$  of these samples were measured in different solvents using DFWM technique. The nonlinear absorption coefficient ( $\beta_{eff}$ ) and imaginary part of susceptibility tensor [ $\text{Im}(\chi_{eff}^3)$ ] of these samples were measured using z-scan technique. The measured nonlinear parameters are explained as due to the combined effect of nonlinear absorption, oscillator strength and resonance effects at the wavelength of excitation. The optical limiting nature of these samples were also studied and it is observed that Ni and Co QAP's are very good candidates for device applications.

## 1.1 Introduction

Nonlinear optical processes in  $\pi$ -electron organic systems have attracted considerable interest because their understanding has led not only to compelling technological promise but also to new phenomena, new theoretical insights and new materials and devices [1]. The  $\pi$ -electron excitation occurring on the individual molecular units is the basic origin of the observed non-resonant nonlinear optical coefficients, which are often unusually large in magnitude. As shown by theory and experiments, 'many body correlation effects' determine the sign, magnitude and frequency dependence of these nonlinear optical parameters and this level of understanding helps us for the development of new NLO materials with many useful properties.

In recent years the research in this field is focused on high performance NLO materials with technological applications and considerable progress has been achieved towards the realization of the same. Many challenges in material synthesis have been met so far and this has resulted in various methods for ultra-structure synthesis and the discovery of entirely new materials exhibiting high thermal, mechanical and chemical stability. Semiconductors, conjugated polymers, liquid crystals, dyes, fullerenes, charge transfer complexes, organometallics, biomaterials, nanocomposites etc. are different class of materials with varying degree of NLO behaviour and several new compounds are being studied for their applications in various fields [2-15]. Out of the large number of compounds with varying degree of NLO behaviour, as mentioned earlier organic compounds like Porphyrins, Phthalocyanines etc. with large number of delocalized  $\pi$ -electrons have got a great deal of attention because of their architectural flexibilities, large nonlinear optical susceptibilities and ease of fabrication [16-17]. Different types of structural modifications can considerably modify the nonlinear optical properties of various organic compounds and the structural modifications include peripheral and axial substitutions to the molecules, complex formation with different metal atoms etc. [18-20]. The metal substitution can be effective in improving the nonlinear optical

Investigations of nonlinear .....

response through the polarisable valance electrons. With the motivation to develop an understanding of the effect of metal ion substitution on the nonlinear behaviour of organic compounds, we have studied the effect of different metal ions on the second hyperpolarizability of the compound, Quinoxaline-2-Carboxalidene-2-Aminophenol (QAP).

Quinoxaline-2-Carboxalidene-2-Aminophenol (QAP) is an organic compound derived from the well known class of compounds named Schiff bases. Schiff's bases are organic compound containing the azomethine group (-RC=N-) and are usually formed by the condensation of a primary amine with an active carbonyl compound. Metal complexes of schiff bases represent an important and interesting class of nonlinear optical material and there are reports on the NLO properties of various Schiff base compounds in different forms [20-22]. There are various methods by which we can synthesis the Schiff's base. The preparation and isolation of the free base ligand followed by coplexation with a metal ion has traditionally been the usual method for the preparation of metal ion complexes of Schiff' bases.

## **4.2 Experimental**

The experimental part of the present study is divided into two sections viz. sample preparation and Degenerate Four Wave Mixing

### **4.2.1 Sample Preparation**

The samples used for the present study were prepared by the method explained below

#### **4.2.1.1 Preparation of Quinoxaline-2-Carboxaldehyde**

For the synthesis of the base compound Quinoxaline-2-Carboxaldehyde we have used the reported procedure in the literature [23-24]. Treatment of D-glucose with O-phenylenediamine in the presence of hydrazine hydrate and acetic acid on a boiling water bath under carbon dioxide atmosphere gave the compound 2-(D-arabinotetrahydroxybutyl) quinoxaline. Oxidation of this

compound with sodium metaperiodate in water in the presence of acetic acid at laboratory temperature gives the compound Quinoxaline-2-Carboxaldehyde. The product thus obtained is isolated by extraction with ether and purified by re-crystallization from petroleum ether. The structure of Quinoxaline-2-Carboxaldehyde is as shown below [25].

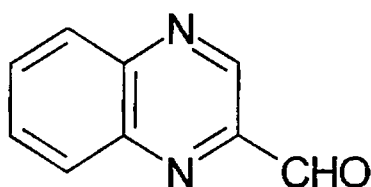


Fig 4.1 Structure of quinoxaline-2-carboxaldehyde

#### 4.2.1.2 Preparation of Quinoxaline-2-Carboxalidene-2-aminophenol (HQAP)

The ligand Quinoxaline-2-Carboxalidene-2-aminophenol (HQAP) was prepared by mixing an ethanolic solution of Quinoxaline-2-Carboxaldehyde and 2-aminophenol. The solution was refluxed for one hour. The ligand separated out was filtered and dried in vacuum over anhydrous calcium chloride. The structure of HQAP thus obtained is as shown below [25].

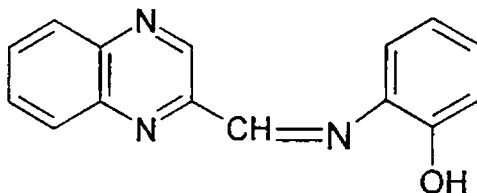


Fig. 4.2 Structure of HQAP

Investigations of nonlinear .....

#### 4.2.1.3 Preparation of metal complexes

The metal complexes of Quinoxaline-2-Carboxaldene-2-aminophenol were prepared by the following procedure. An ethanolic solution of the Schiff base (HQAP) was mixed with the corresponding metal salt solution. The solution was refluxed for two hours. The volume of the resulting solution was then reduced by evaporation and the solution was cooled in a freezer for about one hour. The crystalline complexes separated out was filtered, washed with ether and dried in vacuum over anhydrous calcium chloride. Fig. 4.3 shows the structure of the metal complexes thus obtained [25]

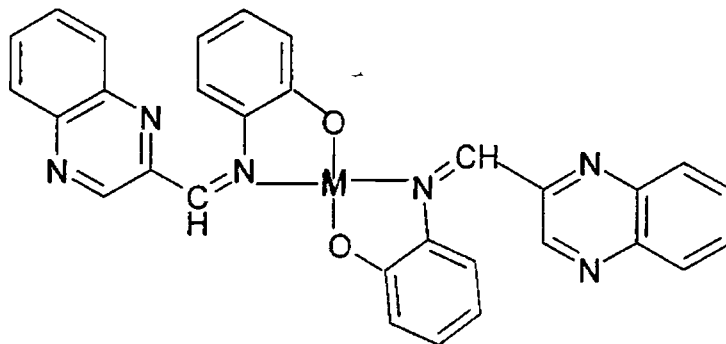


Fig. 4.3 Schematic structure of QAP Complexes

The samples thus obtained are dissolved in highly purified, spectroscopic grade solvents and the absorption spectra are recorded using a UV/VIS/NIR spectrophotometer (Jasco V-570). In all experiments, sample solutions are taken in 1-mm quartz cuvettes. Fresh solutions are prepared for each measurement to avoid any complications arising from photodegradation.

### 4.2.2 Degenerate Four Wave Mixing

Detailed theory and experimental setup of degenerate four wave mixing were discussed in chapter 2. We employ the standard back scattering geometry for making the measurements. Radiation at 532 nm from a Q-switched Nd:YAG laser is used as the source of excitation. One of the advantages of DFWM experiment is that by suitably choosing the polarizations of interacting beams we can select different components of third order susceptibility tensor [26-27].

This property is exploited to avoid thermal contribution occurring in experiments with nanosecond pulses. In the present experiment, polarizations of the interacting beams were so chosen that measurements gave only electronic response. The two pump beams were vertically polarized and the probe beam was horizontally polarized. The polarization of the phase conjugate beam is same as that of pump beam. The angle between the pump and probe beams is  $\sim 8^\circ$  and the phase conjugate signal counter propagating to the probe is separated by using a beam splitter. The energy of the phase conjugate signal as well as the pump beams were measured by using a dual channel energy ratio meter Rj-7620 and Rjp-735 pyroelectric probes (Laser Probe International, USA).

The values of the second hyperpolarizability  $\langle \gamma \rangle$  were calculated using the following equations

$$\chi_s^{(3)} = \chi_{ref}^{(3)} \left[ \frac{(I/I_0^3)}{(I/I_0^3)_{ref}} \right]^{\frac{1}{2}} \left( \frac{n_0}{n_{ref}} \right)^2 \left( \frac{l_{ref}}{l} \right) \left( \frac{\alpha l \exp(\alpha l/2)}{1 - \exp(-\alpha l)} \right) \quad (4.1)$$

and

$$\langle \gamma \rangle = \frac{\chi^{(3)}}{L^4 N} \quad ; \quad L = \frac{n^2 + 2}{3} \quad (4.2)$$



## Investigations of nonlinear .....

where 'n' is the refractive index 'l' is the length of the sample, 'α' is the linear absorption coefficient and 'P' is the intensity. For a solution of non-interacting particles, the effective  $\chi^{(3)}$  assuming a pairwise additive model [28] is given by

$$\chi_{solution}^{(3)} = L^4 [N_{solvent} \gamma_{solvent} + N_{solute} \gamma_{solute}] \quad (4.3)$$

where  $N_{solute}$ ,  $N_{solvent}$  are the number densities of molecules of the solute and the solvent respectively. For dilute solutions with  $N_{solute} = (A \times C)/M$ , we may write

$$\chi_{solution}^{(3)} = \chi_{solvent}^{(3)} + \frac{L^4 \gamma_{solute} AxC}{M} \quad (4.4)$$

where 'A' being the Avagadro's number, 'M' being the molecular weight and 'C' the concentration of the solute in g/ml. For lower concentrations the  $\chi^{(3)}$  of the solution follows a linear relationship with respect to the concentration of the solute.  $\chi^{(3)}$  may have both real and imaginary components originating from the solute as well as solvent. The real part is responsible for the nonlinear refraction whereas the imaginary part is responsible for nonlinear absorption, SA, TPA or ESA. The real part can be positive or negative. The figure of merit, independent of concentration, F is defined as  $\chi^{(3)}/\alpha$ . We have taken the value of  $\chi^{(3)}$ , for the reference sample CS<sub>2</sub> as  $2.73 \times 10^{-13}$  esu [29]. L is the local field correction factor and N is the number density of the solute molecules in solution. The  $\chi^{(3)}$  contribution from solvent is taken to be zero, as it is negligibly small in comparison to the solute.

### 4.2.2.1 Calibration

For the measurements of the nonlinear parameters using degenerate four wave mixing technique the experimental setup has to be standardized using a nonlinear optical material. Carbon disulphide (CS<sub>2</sub>) is used as the standard material because of its completely non-resonant Kerr nonlinearity due to orientational response. Fig. 4.3 shows the log-log plot of optical phase conjugate signal intensity against pump beam

intensity for CS<sub>2</sub> when polarization of the probe beam was orthogonal to the pump beam. The graph obtained is a straight line with slope 2.98 which is very close to the theoretical value 3 showing the cubical dependence of phase conjugate signal against the pump beam intensity.

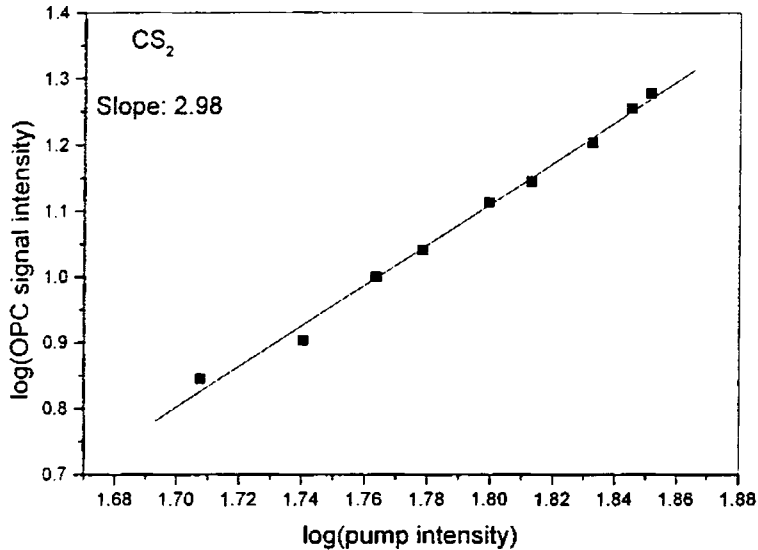


Fig. 4.4 log-log plot of OPC signal against pump beam intensity

### 4.2.3 Z-Scan

The detailed theory of the z-scan measurements was explained earlier in this thesis. Here also we have used the standard open aperture z-scan technique developed by Sheik Bahae *et. al.* [30]. for evaluating the nonlinear optical parameters of the samples. Radiation at 532 nm from a Q-switched Nd:YAG laser were used for the excitation. The samples were taken in 1 mm quartz cuvette and scanned across the focus a lens of 20 cm focal length by using a micrometer translation stage. This configuration gives a Raleigh range of 1.36 mm so that the thin sample approximation condition is satisfied for the measurements carried out here. The input and output energies were measured by using a duel channel energy ratio meter (Rj-7620, Laser Probe International, USA) with pyroelectric detector heads (Rjp-735)

### 4.3 Results

Fig. 4.5 and 4.6 show the absorption spectra of the samples used for the present study. Fig. 4.5 shows the absorption spectrum of 0.1 mM solution of the samples in Dimethyl Formamide (DMF) and Fig. 4.6 represent the same in chloroform (0.25 mM). From the absorption spectra it is clear that in DMF, Nickel Quinoxaline-2-Carboxalidene-2-aminophenol [Ni(QAP)<sub>2</sub>], Cobalt Quinoxaline-2-Carboxalidene-2-aminophenol [Co(QAP)<sub>2</sub>] and Manganese Quinoxaline-2-Carboxalidene-2-aminophenol [Mn(QAP)<sub>2</sub>] shows two absorption bands. But in the case of Copper Quinoxaline-2-Carboxalidene-2-aminophenol [Cu(QAP)<sub>2</sub>] the low energy absorption band is missing. In all these samples the high energy absorption bands extend from 300 to 450 nm region and they are known as the Soret band or S-band. The low energy bands called (Q-bands) are having slightly different ranges. The red shift in the absorption bands (Q-band) in these metal QAP's is found to be proportional to the atomic number of the central metal atom present. But in chloroform, only Ni(QAP)<sub>2</sub> shows two absorption bands. All the other samples show only high energy band. This clearly shows that the solvent induces chemical changes in the samples under investigation and this is reflected in the measured values of NLO parameters

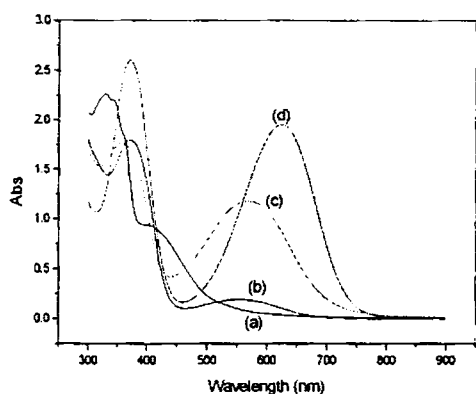


Fig. 4.5 Absorption spectrum of (a) Cu (QAP)<sub>2</sub>, (b) Mn (QAP)<sub>2</sub>, (c) Co (QAP)<sub>2</sub>, (d) Ni (QAP)<sub>2</sub>,

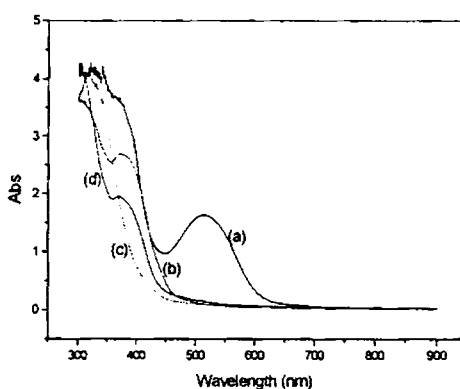


Fig. 4.6 Absorption spectrum of 0.25 mM solutions of (a) Ni (QAP)<sub>2</sub>, (b) Mn (QAP)<sub>2</sub>, (c) Cu (QAP)<sub>2</sub>, (d) Co (QAP)<sub>2</sub>,

### 4.3.1 Degenerate Four Wave Mixing

The experiments were carried out with freshly prepared samples in spectroscopic grade solvents DMF and Chloroform. The Degenerate Four Wave Mixing (DFWM) experiments carried out in these samples shows a cubical dependence of the phase conjugate signal over the pump signal.

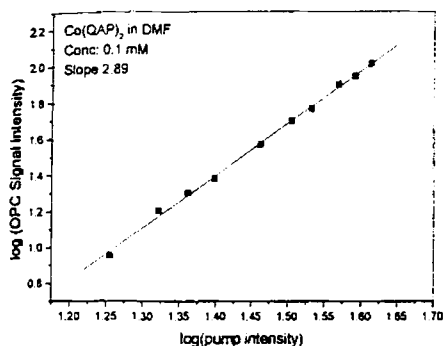


Fig. 4.7 log-log plot of Co (QAP)<sub>2</sub>

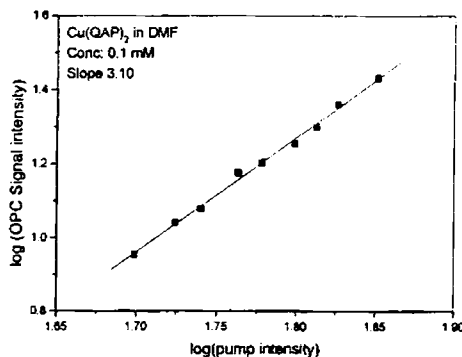


Fig. 4.8 log-log plot of Cu (QAP)<sub>2</sub>

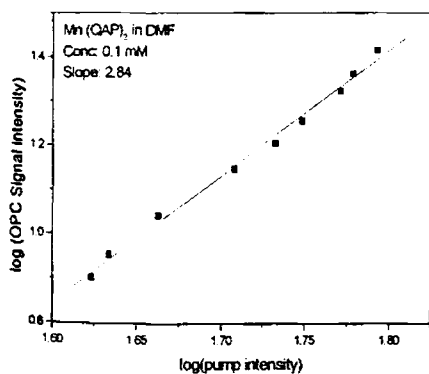


Fig. 4.9 log-log plot of Mn (QAP)<sub>2</sub>

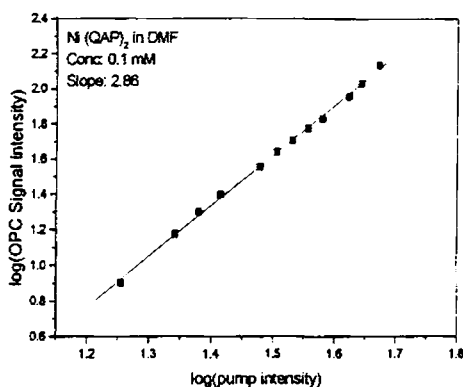
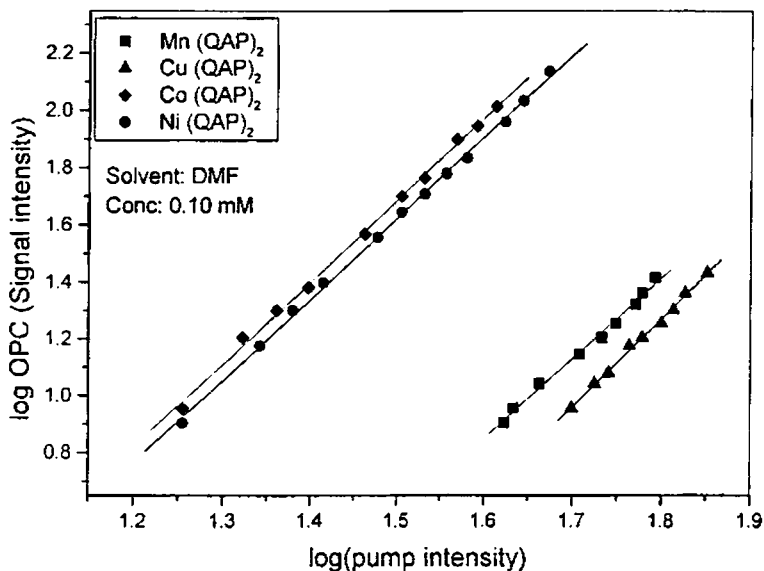


Fig. 4.10 log-log plot of Ni (QAP)<sub>2</sub>

Investigations of nonlinear .....



**Fig. 4.11** log-log plot of different QAP's in DMF

Figure 4.7 to 4.11 shows the phase conjugate signal versus input intensity of these samples in DMF. The concentration of the samples was kept at 0.1 mM. Similarly Fig. 4.12 to 4.16 shows the log-log plots obtained with DFWM experiments in these samples in chloroform. In this case the concentration of the samples used are 0.25 mM.

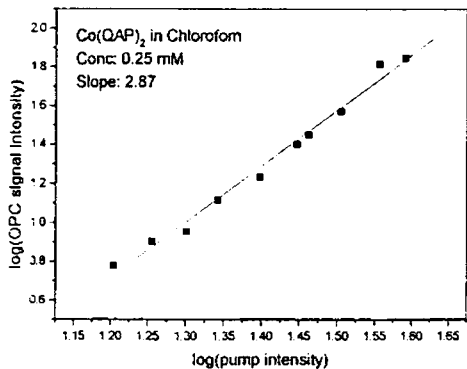


**Fig. 4.12** log-log plot of  $\text{Co}(\text{QAP})_2$  in  $\text{CHCl}_3$

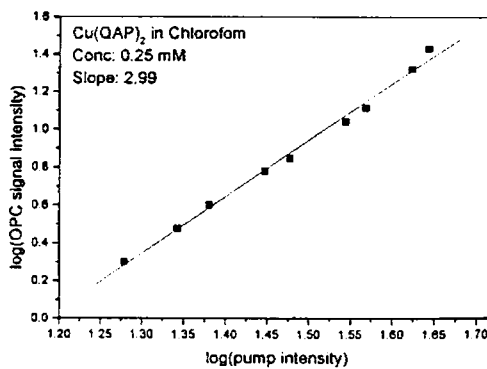


**Fig. 4.13** log-log plot of  $\text{Cu}(\text{QAP})_2$  in  $\text{CHCl}_3$

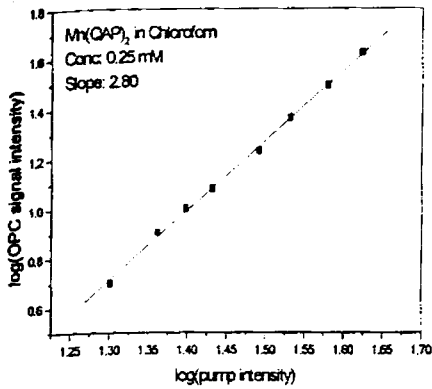


Fig. 4.14 log-log plot of  $\text{Mn}(\text{QAP})_2$  in  $\text{CHCl}_3$

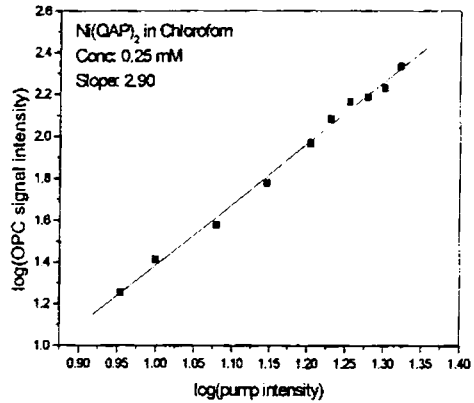


Fig. 4.15 log-log plot of  $\text{Ni}(\text{QAP})_2$  in  $\text{CHCl}_3$

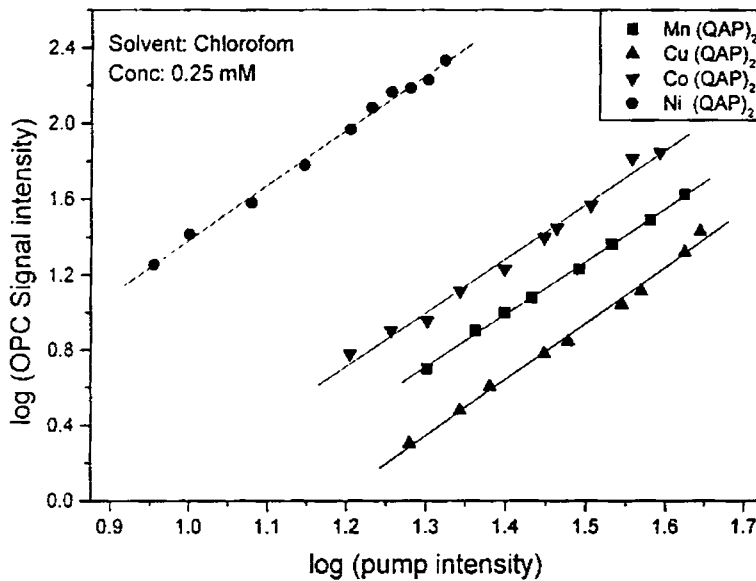


Fig. 4.12 log-log plot of QAP's in  $\text{CHCl}_3$

A slope of 3 in the log-log plots between the pump and phase conjugate signal indicates the third order nature of the process involved as well as the absence of saturation or nonlinearity in the measurements. The straight line graphs

## Investigations of nonlinear .....

obtained in all these experiments are fitted by using a cubical function defined by Eq. 2.40 in chapter 2.

There are several processes, which can influence the degenerate four wave mixing experiments. Two photon absorption (TPA) is one among them. If TPA is present in the samples the slope of the straight line obtained in the log-log plot between the pump intensity and the optical phase conjugate signal (OPC) should be 5 instead of 3 [31-32]. All the samples studied here gives plots with slope 3 and hence the presence of TPA contribution to the measurements can be ruled out. Since the experiments were done with samples dissolved in spectroscopic grade solvents, it is possible to evaluate the microscopic molecular property viz. second hyper polarizability  $\langle\gamma\rangle$ . Measured values of third order susceptibility ( $\chi^{(3)}$ ), Figure of merit (F), Extinction coefficient ( $\varepsilon$ ) and Second hyper polarizability  $\langle\gamma\rangle$  are given in the table 4.1 and 4.2 given below. For the calculation of the Figure of merit (F) of a nonlinear optical material we have used the relation

$$F = \frac{\chi^{(3)}}{\alpha} \quad (4.5)$$

where  $\alpha$  is the linear absorption coefficient of the sample. The extinction coefficient will be given by [33]

$$\varepsilon = \frac{\sigma N_A}{\ln(10)} \times 10^{-3} \quad (4.6)$$

where  $\sigma$  is the absorption cross section and  $N_A$  is the Avogadro number. From the extinction coefficient  $\varepsilon$  we can calculate the oscillator strength of the molecule. It is a very important parameter, which can heavily influence the second hyper polarizability  $\langle\gamma\rangle$ [34-36] and is related to the extinction coefficient by the following relation.

$$f = \left(\frac{1}{n}\right) \times 4.319 \times 10^{-9} \int \varepsilon dv \quad (4.7)$$

Sample in DMF (0.1 mM)	Linear Absorption Coefficient $\alpha$ (cm <sup>-1</sup> )	Extinction coefficient $\epsilon \times 10^3$ ltr cm <sup>-1</sup> mol <sup>-1</sup>	Third order Susceptibility $\chi^{(3)}$ (x 10 <sup>-13</sup> esu)	Figure of Merit F (x 10 <sup>-13</sup> esu-cm)	Second Hyper polarizability $\langle \gamma \rangle$ (x 10 <sup>-30</sup> esu)
Co (QAP) <sub>2</sub>	1.054	4.579	12.65	12.00	6.42
Cu (QAP) <sub>2</sub>	0.136	0.591	2.54	18.65	1.29
Mn (QAP) <sub>2</sub>	0.183	0.795	3.08	16.85	1.56
Ni (QAP) <sub>2</sub>	0.708	3.074	11.40	16.10	5.78

**Table 4.1** Extinction coefficient, Third order susceptibility, Figure of merit and Second hyper polarizability of different QAP's measured in Dimethyl formamide

Sample (in chloroform)	Linear Absorption Coefficient $\alpha$ (cm <sup>-1</sup> )	Extinction coefficient $\epsilon \times 10^3$ ltr cm <sup>-1</sup> mol <sup>-1</sup>	Third order Susceptibility $\chi^{(3)}$ (x 10 <sup>-13</sup> esu)	Figure of Merit F (x 10 <sup>-13</sup> esu-cm)	Second Hyper polarizability $\langle \gamma \rangle$ (x 10 <sup>-30</sup> esu)
Co (QAP) <sub>2</sub>	0.113	0.195	10.55	93.74	2.04
Cu (QAP) <sub>2</sub>	0.082	0.142	04.98	60.85	0.96
Mn (QAP) <sub>2</sub>	0.073	0.126	07.32	100.49	1.41
Ni (QAP) <sub>2</sub>	1.5379	2.672	53.12	34.54	10.25

**Table 4.2** Extinction coefficient, Third order susceptibility, Figure of merit and Second hyper polarizability of different QAP's measured in Chloroform



## Investigations of nonlinear .....

Table 4.1 and 4.2 shows the NLO parameters calculated in various QAP's in DMF (0.1 mM) and Chloroform (0.25 mM) respectively by using the DFWM technique. From the table 4.1 we can see that in DMF the Figure of merit of all these samples are more or less same. Out of the four QAP's studied here Co (QAP)<sub>2</sub> gives the lowest value of Figure of merit and highest value for second hyper polarizability. The largest value of Figure of Merit calculated is in Cu (QAP)<sub>2</sub>. In chloroform the maximum and minimum values of figure of merit is obtained in Mn (QAP)<sub>2</sub> and Ni (QAP)<sub>2</sub> respectively. But the maximum and minimum values of second hyper polarizability is in Ni (QAP)<sub>2</sub> and Cu (QAP)<sub>2</sub>.

### 4.3.2 Z-Scan

Fig. 4.13 to 4.16 shows the open aperture z-scan curves obtained with 0.25 mM solutions of these samples in chloroform. All these samples show similar behaviour. The nonlinear absorption coefficient ( $\beta_{eff}$ ) in these samples can be calculated using the model suggested by Sheik Bhahe et.al. [37] explained in chapter 3. The imaginary part of the nonlinear susceptibility ( $Im(\chi_{eff}^3)$ ) can be calculated from  $\beta_{eff}$  using the expression

$$Im(\chi_{eff}^3) = \frac{\lambda \epsilon_0 n^2 c \beta_{eff}}{4\pi} \quad (4.8)$$

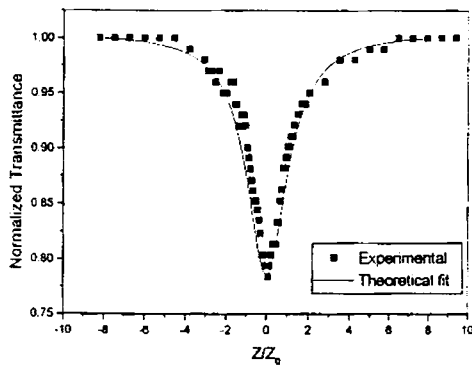


Fig. 4.13 Open aperture z-scan curve of 0.25 mM Ni (QAP)<sub>2</sub> in chloroform

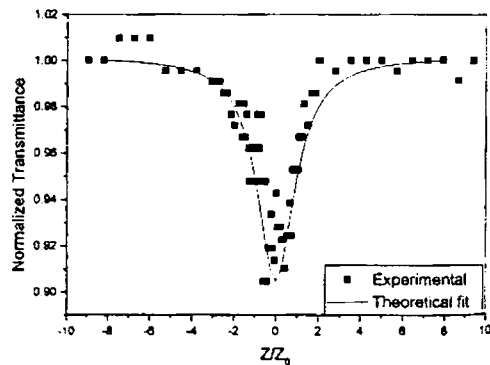


Fig. 4.14 Open aperture z-scan curve of 0.25 mM Mn (QAP)<sub>2</sub> in chloroform

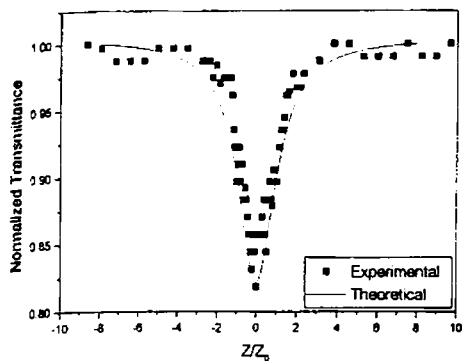


Fig. 4.15 Open aperture z-scan curve of 0.25 mM Cu (QAP)<sub>2</sub> in chloroform

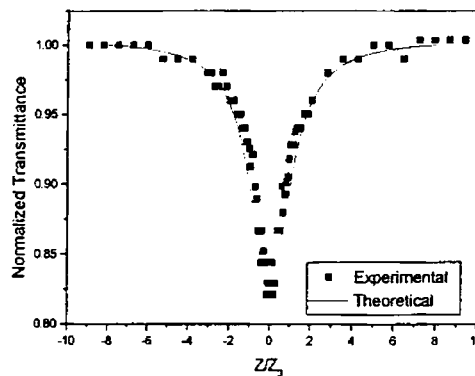


Fig. 4.16 Open aperture z-scan curve of 0.25 mM Co (QAP)<sub>2</sub> in chloroform

Table 4.3 gives the NLO parameters, nonlinear absorption coefficient ( $\beta_{\text{eff}}$ ) and the imaginary part of the nonlinear susceptibility ( $\text{Im}\chi_{\text{eff}}^3$ ) calculated using the open aperture z-scan measurements carried out in these samples.

Table 4.3

Sample	Absorption Coefficient $\alpha$ (cm <sup>-1</sup> )	$\beta_{\text{eff}}$ (m/GW)	$\text{Im}(\chi_{\text{eff}}^3)$ $\times 10^{-17}$ m <sup>2</sup> V <sup>-2</sup>
Ni (QAP) <sub>2</sub>	1.538	4.578	10.73
Co (QAP) <sub>2</sub>	0.113	3.415	8.00
Cu (QAP) <sub>2</sub>	0.0818	3.315	7.77
Mn (QAP) <sub>2</sub>	0.0730	1.515	3.55

#### 4.4 Discussion

We have studied the nonlinear optical behaviour of four different metal QAP's by using the DFWM and Z-Scan techniques. The usefulness of these samples to protect the light sensitive instruments from intense light radiations has been studied using the optical limiting technique. The second hyper polarizability  $\langle\gamma\rangle$  of a material depends on many factors.  $\pi$ -electron conjugation length [38,39], Oscillator Strength [36, 40-41], Metal substituents in the molecule [40, 42-45], Dimensionality of the molecule [46-49], Axial and peripheral substituents [50-56] etc. are the important parameters determining the Second hyper polarizability  $\langle\gamma\rangle$  values of a material. The  $\langle\gamma\rangle$  values measured can have a cumulative contribution from these parameters.

The metal atoms present in various QAP's plays a very important role in the nonlinear as well as spectroscopic properties of the samples studied here. For example, from the absorption spectra in DMF we can see that the redshifts of peak wavelength of Q-bands in these samples are proportional to the atomic number of the metal present in the complex. Here we consider only the influence of metal ions on the third order NLO properties of these samples. The effect of metal ions in the NLO properties of compounds like Phthalocyanines, Porphyrins etc. are well known and the mechanism of interaction which leads to the modification of the nonlinear behaviour is really interesting since it will give greater insights into the NLO properties of this class of compounds [38, 40, 43, 57, 58]. Metal substitution, on many occasions, improves the magnitude of nonlinear optical response through the polarisable valance electrons. Among a number of metal ions transition metal with incompletely filled d-shells have been found to be very effective in enhancing the third order nonlinear properties. [38,40]. From the tables 4.1 to 4.3 we can observe that in QAP's also the NLO properties are modified by the nature of the metal ion present. As mentioned earlier, several mechanisms can have cumulative effects in the measured second hyperpolarizability  $\langle\gamma\rangle$  values of a NLO material. One of the major

Reason for the observed large value of second hyperpolarizability  $\langle\gamma\rangle$  of Ni and Co QAP's in DMF can be attributed to the larger oscillator strength of these compounds. The second hyperpolarizability  $\langle\gamma\rangle$  values of the same set of samples, given in table 4.2, measured in Chloroform confirms our observation in DMF. In this case, Ni (QAP)<sub>2</sub> which is having the largest value of extinction coefficient  $\epsilon$  has got the maximum value for oscillator strength defined by the equation 4.7 and hence the largest value for the second hyperpolarizability  $\langle\gamma\rangle$ .

The  $\pi$ -electrons present in the system get perturbed by the metal ions and this in turn affect the spectral features of the material by the introduction of low lying charge transfer (CT) states in the HOMO-LUMO gap through charge transfer mechanisms. The charge transfer mechanism means the interaction of the valance electrons of the metal ions with  $\pi$ -electrons of the complex molecular system and the CT mechanism include metal-ligand, ligand-metal and metal-metal CT processes. The location of the CT states depends on the overlap between the orbitals and separation between filled and unfilled states [59]. This can also contribute to the measured values of second hyperpolarizability.

Dimensionality of the molecule is another important factor contributing to the nonlinear properties of the materials [50]. Out of the samples studied here Co (QAP)<sub>2</sub> is having tetrahedral structure. Ni (QAP)<sub>2</sub> and Cu (QAP)<sub>2</sub> are having square planar geometry [60]. When the dimensions of the molecules are increased the effective conjugation length available for an electron to respond to applied optical field decreases and consequently the magnitude of  $\langle\gamma\rangle$  values decreases [61]. For example, Kumar et al. [62] have measured  $\chi^{(3)}$  values of basket handle porphyrins and observed a decrease in third order nonlinearity due to the deviation from planarity of molecules.

## Investigations of nonlinear .....

Resonance is another important process, which influence the nonlinear properties of materials. A salient feature of resonant nonlinearity is the considerable enhancement in the magnitude of nonlinear coefficients with respect to nonresonant quantity [50]. In most of the experimental situations a combination of a weak resonant and a background nonresonant nonlinearity is observed instead of a completely resonant or completely nonresonant nonlinearity. A fundamental drawback of resonant nonlinearity is its slow response [63]. But its advantage is its enormously large magnitude. A large number of resonant transitions, such as electronic, vibrational and rotational transitions are possible in macromolecules with large number of  $\pi$ -electrons. Each of these transitions may produce resonance effects. The relative strength of different transitions varies over several orders of magnitude [50]. From the absorption spectra (Fig. 4.5 and 4.6) we can see that at the wavelength of excitation there are some resonance effects. This resonance effect is more prominent in Ni (QAP)<sub>2</sub> in chloroform. Compared to the second hyperpolarizability  $\langle\gamma\rangle$  values of the samples other than Ni (QAP)<sub>2</sub> large value for  $\langle\gamma\rangle$  in this sample when taken in chloroform may be due to the resonance enhancement. The low figure of merit of this sample in this case is an indication of this effect. Therefore the observed large value of Ni and Cu QAP's has a combined effect of several processes, out of which the combined effect of nonlinear absorption, large oscillator strength and resonance effects are the major contributors to the second hyperpolarizability of these molecules. This observation is well supported by the nonlinear absorption coefficient  $\beta_{\text{eff}}$  and imaginary part of nonlinear susceptibility [ $\text{Im}(\chi^{(3)})$ ] values obtained with the z-scan technique given in table 4.3.

To explain nonlinear absorption under nanosecond excitation, we suggest a five level model involving the states  $S_0$ ,  $S_1$ ,  $S_2$ ,  $T_1$  and  $T_2$  as shown in Fig. 4.17 Here  $S_n$  and  $T_n$  are the singlet and triplet states respectively where  $n=0, 1$  or  $2$  and every electronic energy level involves many vibronic sublevels. When interacting with a laser pulse at 532 nm, atoms get excited from the  $S_0$  ( $v=0$ ) to the upper vibrational

level of  $S_1$ . Here  $\nu$  corresponds to the vibrational quantum number. Through the nonradiative decay within picosecond time scales, they can relax to the lowest vibrational level of  $S_1$  ( $\nu=0$ ). Since QAP's have very low fluorescence the transition from  $S_1$  ( $\nu=0$ ) to  $S_0$  can be neglected. The occurrence of the  $S_2 \leftarrow S_1$  transition does not appreciably deplete the  $S_1$  state, as the  $S_1 \leftarrow S_2$  decay also takes place within picoseconds. However the cross section of the  $T_1(\nu=0) \leftarrow S_1(\nu=0)$  intersystem crossing is large, leading to a strong triplet – triplet absorption  $T_2 \leftarrow T_1$ . Here we assume that the intersystem crossing [64] is fast compared with the laser pulse width (9 ns) and virtually all the atoms excited from  $S_0$  reach the first excited triplet state  $T_1$ . Therefore under nanosecond pulse excitation, the nonlinear absorption observed here is a consequence of  $T_2 \leftarrow T_1$  absorption [ $T_2 \leftarrow T_1(\nu=0)$ ]

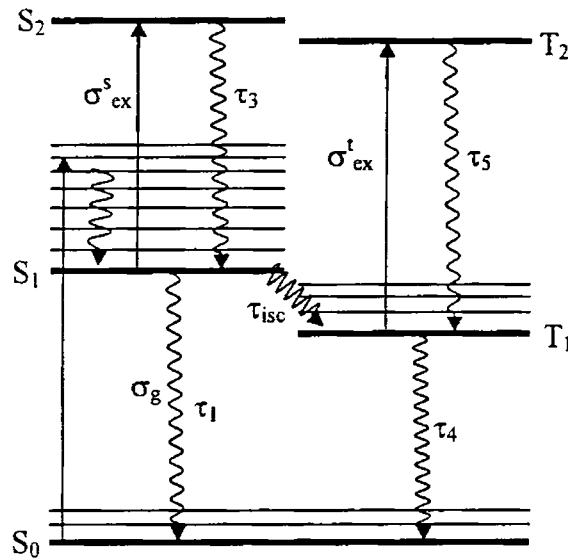


Fig. 4.17 Five level energy diagram for metal QAP's.  $S_n$  ( $n = 0,1,2$ ): Singlet levels;  $T_n$ ( $n = 1, 2$ ): Triplet levels

The nonlinear absorption coefficient ( $\beta_{\text{eff}}$ ) and the imaginary part of the nonlinear susceptibility ( $\text{Im}\chi_{\text{eff}}^3$ ) calculated in these samples shows that Ni (QAP)<sub>2</sub> is having the best nonlinear optical parameters.

### 4.5 Optical Limiting

The nonlinear absorption seen in these samples reveals that they can be used as potential optical limiters. Therefore, the optical limiting behaviour of these samples was investigated and Fig. 4.17 to 4.21 represents the optical limiting graphs generated from the z-scan curves given earlier. For being used as a good optical limiter, a number of important requirements should be met by the nonlinear material. Fast response, high damage threshold and an excited state absorption cross-section larger than the ground state absorption cross-section are the most important among them [65]. It is well known that materials which are having excited state absorption cross section larger than the ground state absorption cross section are better optical limiters and they can respond to both fast and slow laser pulses via the ( $S_2 \leftarrow S_1$ ) and ( $T_2 \leftarrow T_1$ ) transitions respectively

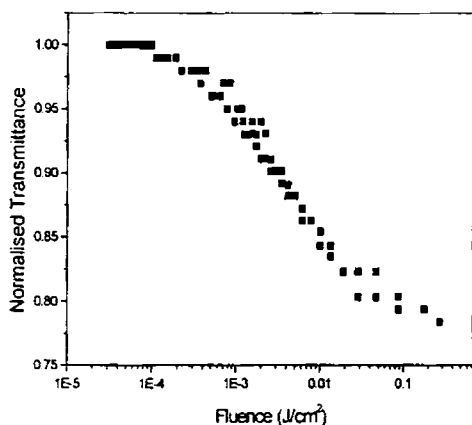


Fig. 4.17 Optical limiting in 0.25 mM Ni (QAP)<sub>2</sub> in chloroform

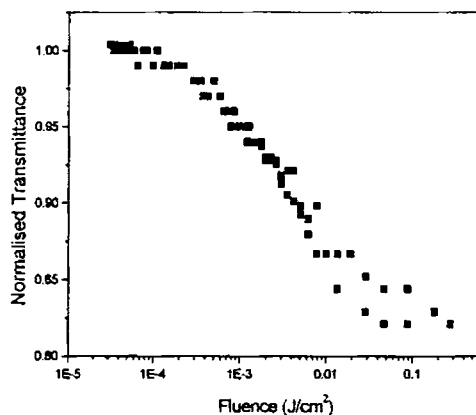


Fig. 4.18 Optical limiting in 0.25 mM Co (QAP)<sub>2</sub> in chloroform

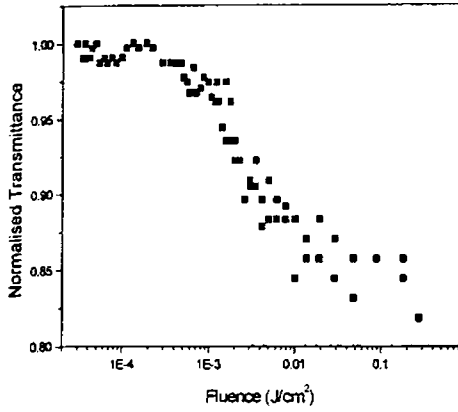


Fig. 4.19 Optical limiting in 0.25 mM Cu (QAP)<sub>2</sub> in chloroform

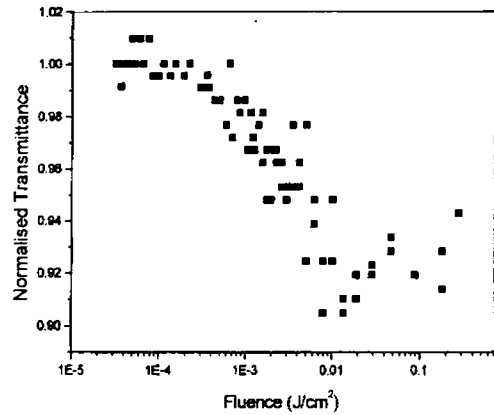


Fig. 4.20 Optical limiting in 0.25 mM Mn (QAP)<sub>2</sub> in chloroform

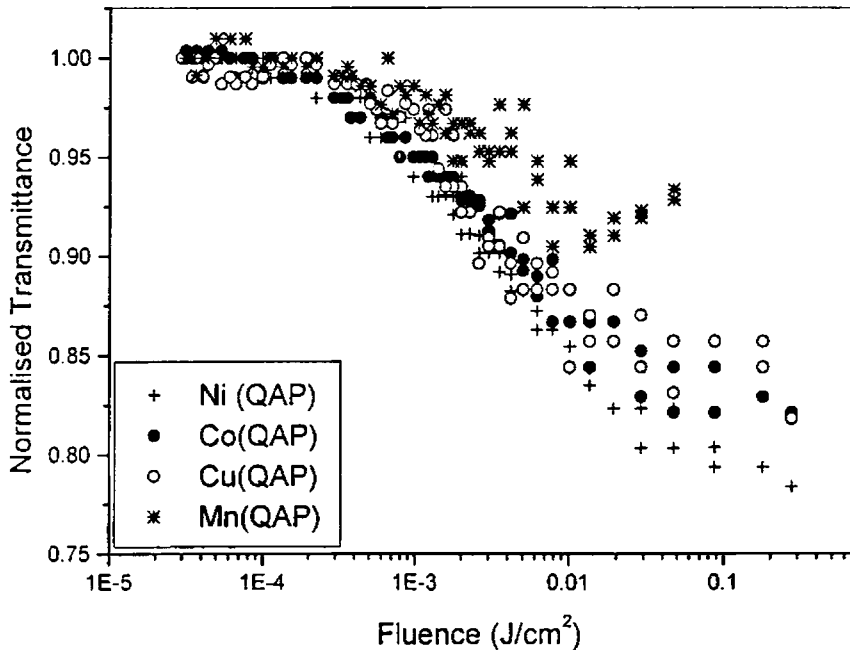


Fig. 4.21 Optical limiting in 0.25 mM Ni, Co, Cu and Mn (QAP)<sub>2</sub> in chloroform



## Investigations of nonlinear .....

From these graphs it is clear that all the QAP samples studied here show better optical limiting at the excitation wavelength of 532 nm. Out of the four samples the optical limiting in Ni (QAP)<sub>2</sub> is really commendable because it shows the highest degree of limiting. It is a potential candidate for device applications at the wavelength of excitation considered in the present studies.

### 4.6 Conclusions

Degenerate Four Wave Mixing (DFWM), Z-Scan and optical limiting studies have been carried out in certain selected metal complexes of QAP's at 532 nm under nanosecond excitation. For the DFWM measurements the polarization of the interacting beams were so chosen that electronic response is obtained. Third order susceptibility, figure of merit of third order nonlinearity and nonlinear absorption coefficient of these samples are calculated. The measured nonlinear parameters of these samples are explained as due to the combined effect of nonlinear absorption, oscillator strength and resonance effects at the wavelength of excitation. It is observed that Ni (QAP)<sub>2</sub> and Co (QAP)<sub>2</sub> are promising NLO materials and their importance in the context of device applications is confirmed by the optical limiting studies carried out in these samples.

**4.7 References:**

1. A F Garito, R F Shi and M H Wu, *Physics Today*, 47 (1994) p.51
2. J L Bredas, C Adant, P Tackx, A Petersons and B M Pierce *Chem. Rev.* **94** (1994) p.243
3. H. Haug (ed.): *Optical nonlinearities and instabilities in semiconductors*, Academic, New York (1998)
4. A Grund, A Kaltbeitzel, A Mathy, R Schwarz, C Bubeck, P Vermeheren and M Hanak *J. Phys. Chem.* **96** (1992) p.7450
5. M A Kramer, W R Tompkin and R W Boyd: *Phys. Rev. A* **34**, 2026 (1986)
6. S Guha, K Kang, P Porter, J F Roach, D E Remy, F J Aranda and D V G L N Rao *Opt. Lett.* **17**, (1992) p.264
7. C. Taliani, G Ruani and R. Zamboni (eds): *Fullerenes: Status and Perspectives*, World Scientific, Singapore (1992)
8. M A Diaz-Garcia, I Ledoux, J A Duro, T Torres, F Agullo-Lopez and J Zyss *J. Phys. Chem.* **98** (1994) p.8761
9. H S Nalwa: *Nonlinear optics of organic molecules and polymers*, C R C Press, Boca Raton, FL, (1997) p. 611
10. G L Wood, M J Miller and A G Mott *Opt. Lett.* **20** (1995) p.973
11. P Palffy-Muhoray: *Liquid crystals: Applications and uses*, Vol.1 World Scientific, Singapore, (1991) p. 493
12. C Y S Fu, H S Lackritz, D B Priddy and J E McGrath *Chem. Mater.* **8** (1996) p.514
13. Stephanie K. Hurst, Nigel T. Lucas, Mark G. Humphrey, Takashi Isoshima, Kurt Wostyn, Inge Asselberghs, Koen Clays, André Persoons, Marek Samoc and Barry Luther-Davies, *Inorganica Chimica Acta*, **350**, (2003) p.62
14. F Hacke, D Richard and C Flytzanis *J. Opt. Soc. Am. B* **3** (1986) p.1647
15. H S Nalwa: *Appl. Organomet. Chem.* **5**, 349 (1991)
16. K Kandasamy, S Shetty, P N Puntambekar T S Srivastava, T Kundu and B P Singh *J. Porphy. Phthalo.* **3** (1999) p. 81
17. Danilo Dini, Markus Barthel, Thorsten Schneider, Martin Ottmar, Sanjiv Verma and Michael Hanack, *Solid State Ionics* **165**, (2003) p.289
18. B P Singh, R Vijaya, S J Shetty, K Kandasamy, P N Puntambekar and T S Srivastava *J. Porphy. Phthalo.* **4** (2000) p. 659
19. B Aneeshkumar, Pramod Gopinath, C P G Vallabhan, V P N Nampoori and P Radhakrishna, *J. Opt. Soc. Am. B* **20**(7), 1486 (2003)
20. K P Unnikrishnan, Jayan Thomas, V P N Nampoori and C P G Vallabhan *Chem. Phys.* **279** (2002) p.209
21. S A Jenekhe, C J Yang, H Vanherzeele and J S Meth *Chem. Mater.* **3** (1991) p.985
22. K S Lee and M Samoc *Polymer.* **32** (1991) p.361
23. M H Ohle, *BER*, **74B**, (1941) p.13
24. C L Leese and H N Rydon, *J. Chem. Soc.* (1955) p.303
25. S Mayadevi, *Ph.D. thesis*, Dept. of Applied Chemistry, CUSAT, Cochin-22, (1997)
26. J R G Thorne, S M Kuebler, R G Denning, I M Blake, P N Taylor, H L Anderson. *Chem. Phys. Lett.* **248** (1999) p. 181
27. Jun Ichi Sakai. *Phase Conjugate Optics*. Mc. Graw Hill, New York
28. M. -T. Zhao, B.P. Singh, and P.N. Prasad, *J. Chem. Phys.* **89**, 5535, 1988.
29. R A Fisher (Ed.) *Optical Phase Conjugation*, Academic Press, New York, 1983.

## Investigations of nonlinear .....

30. M S Bahae, A A Said, T H Wei, D J Hagan, E W V Stryland. *IEEE J. Quantum Electronics*, **26** (1990) p. 760
31. S Wu, X C Chang and R L Fork. *Appl. Phys. Lett.* **61** (1992) p. 919
32. M Zhao, Y Cui, M Samoc and P N Prasad. *J. Chem. Phys.* **95** (1991) p. 3991
33. T H Wei, D J Hagan, M L Sence, E W V Stryland, J W Perry and D R Coutler. *Appl. Phys. B.* **54** (1992) p. 46
34. K Kandasamy, S J Shetty, P N Puntambekar, T S Srivastava, T Kundu and B P Sing. *J. Porphyrins and Phthalocyanines* **3** (1999) p. 81
35. M G Kuzyk and C W Dirk. *Phys. Rev. A* **41**(1990) p. 5098
36. I Renge, H Wolleb, H Spahn and U P Wild. *J. Phys. Chem. A* **101** (1997) p. 6202
37. Mansoor Sheik Bahae, Ali A Said, Tai -Huei Wei, David J Hagan and E W Van Stryland *IEEE J. Quant. Electron.* **26** (4), 760 (1990)
38. K P Unnikrishnan, Jayan Thomas, V P N Nampoori and C P G Vallabhan *Chem. Phys.* **279** (2002) p.209
39. M K Casetevens, M Samoc, J Pflieger and P N Prasad *J. Chem. Phys.* **92** (1990) p.2019
40. K Kandasamy, S J Shetty, P N Puntambekar, T S Srivastava, T Kundu and B P Sing. *J. Porphyrins and Phthalocyanines* **3** (1999) p. 81
41. M G Kuzyk and C W Dirk. *Phys. Rev. A* **41**(1990) p. 5098
42. A Yamashita, S Matsumoto, S Sakata and T Hayashi., H Kanbara, *J. Phys. Chem. B* **102** (1998) p. 5165
43. J S Shirk, J R Lindle, F J Bartoli and M E Boyle. *J. Phys. Chem.* **96** (1992) p. 5847
44. K Kamada, M Ueda, T Sakaguchi, K Ohta and T Fukumi. *J. Opt. Soc. Am. B* **15** (1998) p. 838
45. M Koshino, H Kurata, S Isoda and T Kobayashi. *ICR Annual Report.* **7** (2000) p.6
46. H S Nalwa, S Kobayashi. *J. Porphyrins and Phthalocyanines.* **2** (1998) p. 21
47. Ifor. D W Samuel, I Ledoux, C Delporte, D L Pearson and James M Tour. *Chem. Mater.* **8** (1996) p. 819
48. G R Kumar, M Ravikanth, S Banerjee, Armen Sevian. *Optic. Commun.* **144** (1997) p. 245
49. D S Chemla, J Zyss. *Nonlinear Optical Properties of Organic Molecules and Crystals.* Quantum Electronics. Principles and Applications. Academic Press (1987) Florida
50. A Sastre, M A Diaz-Garcia, D del Rey, C Dhenaut, J Zyss, I Ledoux, F Agullo Lopez and T Torres. *J. Phys. Chem. A* **101** (1997) p. 9773
51. K S Suslick, C T Chen, G R Meredith, and L T Cheng. *J. Am. Chem. Soc.* **114** (1992) p. 6928
52. B K Mandal, B Bihari, A K Sinha and M Kamath. *Appl. Phys. Lett.* **66** (1995) p. 932
53. A K Sinha, B Bihari and B K Mandal. *Macromolecules.* **28** (1995) p.5681
54. H S Nalwa, A Kakuta. *Thin Solid Films.* **254** (1995) p.218
55. K Kandasamy, S J Shetty, P N Puntambekar, T S Srivastava, T Kundu and B P Singh. *Chem. Commun.* (1997) p. 1159
56. H Kanbara, T Maruno, A Yamashita, S Matsumoto, T Hayashi, H Konami, N Tanaka. *J. Appl. Phys.* **80** (1996) p. 3674
57. K P Unnikrishnan, Jayan Thomas, V P N Nampoori and C P G Vallabhan, *Opti. Commun.* **204** (2002) p.385
58. S V Rao, N K M Naga Srinivas, D N Rao, L Giribabu, B G Maiya, Reji Philip and G R Kumar, *Opt. Commun.* **182** (2000) p.255

## Chapter 4: Degenerate four .....

59. T Kimura, M Sumimoto, Ssakaki, H Fujimoto, Y Hashimoto, S Matsuzaki, *Chem. Phys.* **253** (2000) p.125
60. Ph. D. Thesis, S Mayadevi, Dept. of Applied Chemistry, CUSAT, Cochin-22
61. M Hosoda, T Wada, A Yamada, A F Garito and H Sasbe, *Jpn. J. Appl.Phys.* **30** (1991) p.1715
62. G R Kumar, M Ravikanth, S Banergee, A Sevian, *Opt. Commun.* **144** (1997) p.245
63. R Philip, G R Kumar, M Ravikanth, G Ravindrakumar, *Opti. Commun.* **165** (1999) p.91
64. Tiejun Xia, D J Hagan, A Dogariu, A A Said and E W Van Stryland, *Appl. Opt.* **36**, (1997) p.4110
65. H steil, A Volkmer, I Ruckmann, A Zeug, B Ehrengerg and B Roder, *Opt. Commun.* **155**, (1998) p.135

## Chapter 5

### Z-Scan and Degenerate Four Wave Mixing Studies on Certain Selected Tetra Phenyl Phorphyrins

#### Abstract

Z-scan and Degenerate four wave mixing studies were carried out in tetra phenyl porphyrins having different peripheral substituents with varying electron affinities. Figure of merit of third order nonlinearity ( $F$ ), Third order susceptibility ( $\chi^3$ ) and Second hyper polarizability  $\langle\gamma\rangle$  of these samples were measured using DFWM technique. The effect of wavelength, concentration and solvents on the NLO behaviour of these samples were also studied using z-scan technique and the nonlinear absorption coefficient ( $\beta_{eff}$ ) and imaginary part of susceptibility tensor [ $\text{Im}(\chi_{eff}^3)$ ] were measured. The measured nonlinear parameters of these samples are explained on the basis of the combined effect of nonlinear absorption, oscillator strength and internal charge transfer mechanism. The optical limiting studies carried out in these samples shows that the unsubstituted porphyrins posses comparably better limiting nature over the other samples.

## 5.1 Introduction

During the last two decades the search for better nonlinear optical materials has gained much importance among the scientific community due to their potential applications in different fields of science and technology. As nonlinear materials find direct applications in optical communications, data storage, electro-optical signal processing etc. molecules with nonlinear optical properties have been extensively investigated. A collective effort from physicists, chemists and material scientists is in progress to understand the basic process responsible for the nonlinear behaviour of various compounds found in nature as well as of those synthesized in the laboratory [1-5].

Among the various types of nonlinear optical materials investigated, organic compounds have received much attention because of their large nonlinearity as well as the opportunity they offer in design and formulation of more efficient nonlinear materials for specific applications [6]. Porphyrins, Phthalocyanines, Naphthalocyanines, Fullerenes etc. belong to this class of materials and considerable data on the nonlinear optical properties of these materials is now available in the literature [7-14]. Harmonic generation, wave mixing, optical limiting, optical switching etc. have been demonstrated in various NLO materials [15-18]. Out of the large number of NLO materials available, porphyrins form a distinct class of compounds having important biological representatives. The nonlinear optical properties as well as photochemical reactions of different types of porphyrin compounds have been studied for a long time from various viewpoints. They are the key compounds to investigate mechanisms and dynamics of the energy and electron transfer in photosynthetic model systems. They are also of crucial importance for synthesizing various compounds aiming to construct ultra fast photo responsive devices in general. Rich electronic and vibronic characters combined with molecular configuration dominate the linear and nonlinear optical properties in

Investigations of nonlinear .....

porphyrins and metallo-porphyrins systems [19]. The basic structure of the porphyrin macrocycle is as shown in Fig. 4.1 [20]

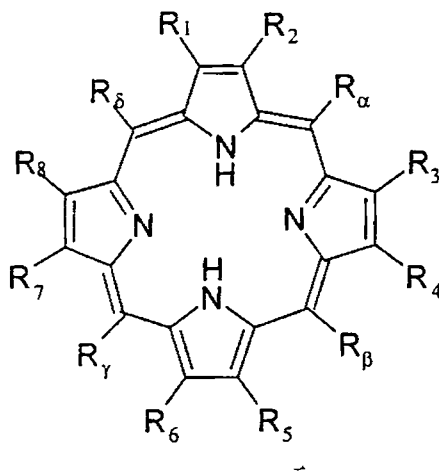


**Fig. 4.1** Basic structure of porphyrin

Porphyrins differ in the nature of the bridging groups occupying meso position in the porphyrin molecule. The bridging groups may only be  $-\text{CH}=\text{}$ ,  $-(\text{X})\text{C}=\text{}$ ,  $-\text{N}=\text{}$  or their combinations. The structural diversity of porphyrins is further enhanced by the presence of various pyrrole substituents ( $\text{R}_1\text{-R}_8$ ) which may be  $\text{H}$ ,  $\text{CH}_3$ ,  $\text{C}_2\text{H}_5$ ,  $\text{CH}=\text{CH}_2$ ,  $\text{CH}(\text{OH})\text{CH}_3$ ,  $\text{C}(\text{O})\text{H}$ ,  $\text{COOH}$ ,  $\text{CH}_2\text{COOH}$ , and  $\text{CH}_2\text{CH}_2\text{COOH}$ . If it is also taken into consideration that one or more pyrrole double bonds may be hydrogenated and that adjacent substituents  $\text{R}_1\text{-R}_8$  and  $\text{R}_\alpha\text{-R}_\beta$  may form closed cycles, then the diversity of molecular structures of porphyrins, chlorines, azaporphyrins, Phthalocyanines, phorbins and so on becomes evident.[ 20]

These specific features and the great diversity of porphyrins are the factors responsible for their importance and wide distribution in nature as well as the

large number of applications. The structural diversity of porphyrins and metalloporphyrins opens up enormous possibilities for studying the effect of functional substituents and central atoms on the properties of porphyrins. Although the porphyrin ring is a macromolecule, it is highly flexible and a number of structural changes involving different central metal ions and peripheral substituents can be introduced without compromising its excellent chemical and thermal stability [21-30]. This architectural aspect is relevant to nonlinear optics in developing materials with optimum nonlinearity and response time. Porphyrins and porphyrin derivatives which are two dimensional molecules characterized by highly developed  $\pi$ -conjugation, present nonlinear optical properties such as the intensity dependent refractive index and/or nonlinear absorption whose magnitude and time response depend upon the dominant physical process as well as the environment [31-38]

Metal substitution in the central position forms a group of metalloporphyrins and introduces low lying energy states derived from metal-to-ligand and ligand-to-metal charge and energy transfer. The optical processes of the excited state are highly related to the characteristics of central metal ions and the coupling between the  $\pi$ -electron and the metal ion. Dimensionality, axial and peripheral substitutions are the other two important parameters which determine the nonlinear behaviour of various types of porphyrin molecules [39]. Thus the NLO properties of this group of compounds are very relevant to photonics and there exist a large number of reports in the literature in this topic [40-46].

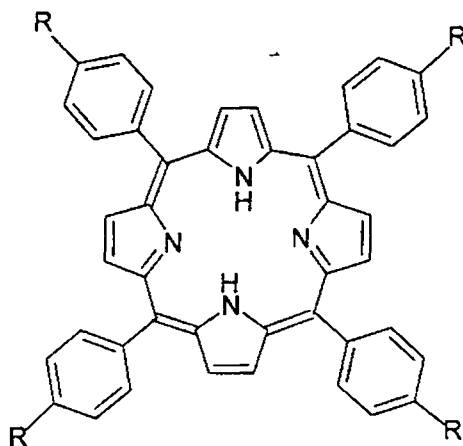
Second hyper-polarizability  $\langle \gamma \rangle$  is a measure of the nonlinear behavior of a material and this can be measured using different techniques like Optical Kerr effect,



## Investigations of nonlinear .....

Degenerate Four Wave Mixing (DFWM), Z-Scan etc. In the case of linear  $\pi$ -conjugated molecular systems the major contribution to the second hyper-polarizability  $\langle \gamma \rangle$  comes from  $\gamma_{xxxx}$  component. But, in porphyrins and related molecules  $\gamma_{yyyy}$ ,  $\gamma_{xxyy}$ ,  $\gamma_{xyxy}$ ,  $\gamma_{yyxx}$ ,  $\gamma_{yxyx}$  and  $\gamma_{yxxy}$  also contribute to the total  $\langle \gamma \rangle$ . The properties with special reference to  $\langle \gamma \rangle$  for a number of Porphyrins and their derivatives have been studied in various media like different solvents, thin films, polymers, sol-gels, glass etc. [46-54].

The structure of the porphyrin molecules which have been investigated in this thesis is presented in Fig. 4.2



R = H	Tetra Phenyl Porphyrin
R = OCH <sub>3</sub>	Tetra 4 Methoxy Phenyl Porphyrin
R = OH	Tetra 4 Hydroxy Phenyl Porphyrin
R = ON	Tetra 4 Nitro Phenyl Porphyrin

**Fig. 4.2** Structure of Porphyrins used for the present study

In this chapter we present our results on the measurements of the third order optical nonlinearity and nonlinear absorption studies in Tetra Phenyl Phorphyrins with peripheral substituents having different electro-negativities. These compounds have been synthesized in a different department in the author's institution. The techniques of Degenerate Four Wave Mixing (DFWM) in the backward configuration and z-scan have been employed for the studies on the NLO properties of the above molecule.

## **5.2 Experimental**

The samples are synthesized and purified according to the reported procedures in literature [55]. Each sample is subjected to a column chromatographic purification process just prior to the measurements. The samples are dissolved in highly purified, spectroscopic grade toluene and the absorption spectra are recorded using a UV/VIS/NIR spectrophotometer (Jasco V-570). In all experiments, sample solutions are taken in 1-mm quartz cuvettes. Fresh solutions are prepared for each measurement to avoid any complications arising from photodegradation.

### **5.2.1 Degenerate Four Wave Mixing**

Detailed theory and experimental setup for degenerate four wave mixing were discussed in chapter 2. We employ here, the standard back scattering geometry for making the measurements. 532 nm radiation from a Q-switched Nd:YAG laser is used as the source of excitation. One of the advantages of DFWM experiment is that by suitably choosing the polarizations of interacting beams we can select different components of third order susceptibility tensor [56-57].

This property is exploited to avoid thermal contribution occurring in experiments with nanosecond pulses. In the present experiment, polarizations of the interacting beams

## Investigations of nonlinear .....

were so chosen that measurements gave only electronic response. The two pump beams were vertically polarized and the probe beam was horizontally polarized. The polarization of the phase conjugate beam is same as that of pump beam. The angle between the pump and probe beams is  $\sim 8^\circ$  and the phase conjugate signal which is counter propagating to the probe beam is separated by using a beam splitter. The energy of the phase conjugate signal as well as the pump beams were measured by using a dual channel energy ratio meter Rj-7620 and Rjp-735 pyroelectric probes (Laser Probe International, USA).

The values of the susceptibility ( $\chi^3$ ) and second hyperpolarizability  $\langle \gamma \rangle$  were calculated using the following equations

$$\chi_s^{(3)} = \chi_{ref}^{(3)} \left[ \frac{(I/I_0^3)}{(I/I_0^3)_{ref}} \right]^{\frac{1}{2}} \left( \frac{n_0}{n_{ref}} \right)^2 \left( \frac{l_{ref}}{l} \right) \left( \frac{\alpha l \exp(\alpha l/2)}{1 - \exp(-\alpha l)} \right) \quad (4.1)$$

and

$$\langle \gamma \rangle = \frac{\chi^{(3)}}{L^4 N} \quad ; \quad L = \frac{n^2 + 2}{3} \quad (4.2)$$

where 'n' is the refractive index 'l' is the length of the sample, ' $\alpha$ ' is the linear absorption coefficient and 'I' is the intensity. For a solution of non-interacting particles, the effective  $\chi^{(3)}$  assuming a pairwise additive model [58] is given by

$$\chi_{solution}^{(3)} = L^4 [N_{solvent} \gamma_{solvent} + N_{solute} \gamma_{solute}] \quad (4.3)$$

where  $N_{solute}$ ,  $N_{solvent}$  are the number densities of molecules of the solute and the solvent respectively. For dilute solutions with  $N_{solute} = (A \times C)/M$ , we may write

$$\chi_{solution}^{(3)} = \chi_{solvent}^{(3)} + \frac{L^4 \gamma_{solute} A x C}{M} \quad (4.4)$$

where 'A' being the Avagadro's number, 'M' being the molecular weight and 'C' the concentration of the solute in g/ml. For lower concentrations, the  $\chi^{(3)}$  of the solution follows a linear relationship with respect to the concentration of the solute.  $\chi^{(3)}$  may have both real and imaginary components originating from the solute as well as solvent. The real part is responsible for the nonlinear refraction whereas the imaginary part is responsible for nonlinear absorption (SA, TPA or ESA etc.). The real part can be positive or negative. The figure of merit, independent of concentration, F is defined as  $\chi^{(3)}/\alpha$ . We have taken the value of  $\chi^{(3)}$ , for the reference sample CS<sub>2</sub> as  $2.73 \times 10^{-13}$  esu [59]. L is the local field correction factor and N is the number density of the solute molecules in solution. The  $\chi^{(3)}$  contribution from solvent is taken to be zero, as it is negligibly small in comparison to the solute.

### 5.2.1.1 Calibration

For the measurements of the nonlinear parameters using degenerate four wave mixing technique the experimental setup has to be standardized using a nonlinear optical material. Carbon disulphide (CS<sub>2</sub>) is used as the standard material because of its completely non-resonant Kerr nonlinearity due to orientational response. Fig. 4.3 shows the log-log plot of optical phase conjugate signal intensity against pump beam intensity for CS<sub>2</sub> when the probe beam was orthogonal to the pump beam. The graph obtained is a straight line with slope 2.98 which is very close to the theoretical value 3 showing the cubic dependence of phase conjugate signal against the pump beam intensity.

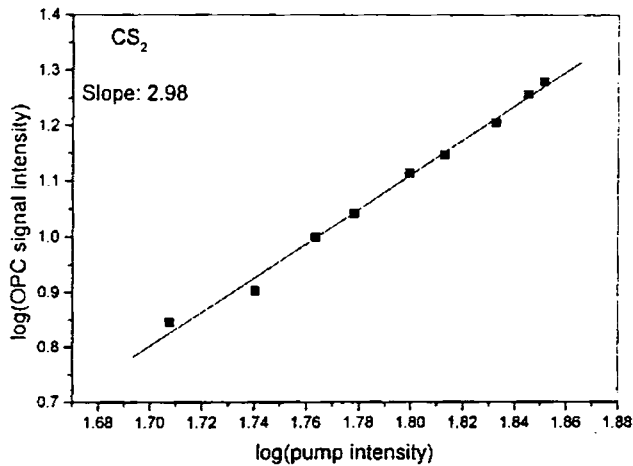


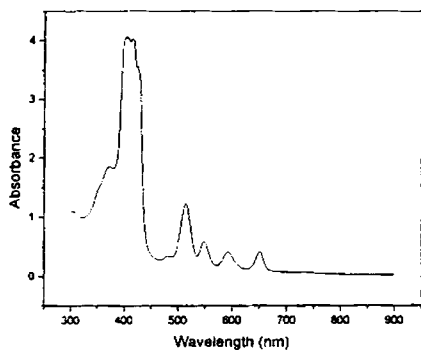
Fig. 4.3 log-log plot of OPC signal against pump intensity

### 5.2.2 Z-Scan

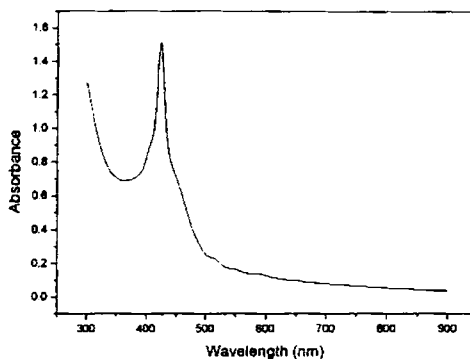
The detailed theory of the z-scan measurements was explained earlier in this thesis. Here also we have used the standard open aperture z-scan technique developed by Sheik Bahae *et. al.* [60]. for evaluating the nonlinear optical parameters of the samples. A 532 nm radiation from a Q-switched Nd:YAG laser was used for the excitation. The samples were taken in 1 mm quartz cuvette and scanned across the focus a lens of 20 cm focal length by using a micrometer translation stage. This configuration gives a Raleigh range of 1.36 mm so that the thin sample approximation condition is satisfied for the measurements carried out here. The input and output energies were measured by using a dual channel energy ratio meter (Rj-7620, Laser Probe International, USA) with pyroelectric detector heads (Rjp-735)

### 5.3 Results

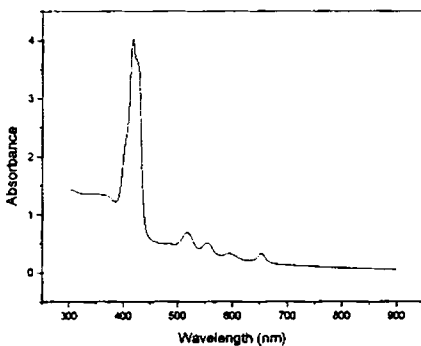
All samples used in this study show the linear absorption features typical of Porphyrins, namely the high energy B (Soret) band and the low energy Q band(s) except for Nitro-TPP. Fig. 4.4 (a – d) illustrates the UV-Visible spectra recorded at room temperature. In the case of Nitro-TPP the low energy band is almost absent. The experiments were carried out with samples having a concentration in the range of  $10^{-4}$  to  $10^{-5}$  M corresponding to an absorbance of less than 0.5.



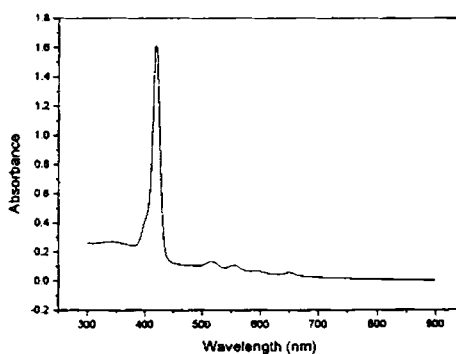
(a) TPP in Toluene



(b) Nitro-TPP in Toluene



(c) Methoxy-TPP in Toluene



(d) Hydroxy-TPP in Toluene

**Fig. 4.4 (a-d)** Absorption spectra of 0.1 mM solutions of various TPP's

## Investigations of nonlinear .....

Fig.4.5 to 4.9 shows the plots of phase conjugate signal verses input intensity. The cubic dependence of the phase conjugate signal with the input intensity has been verified for all the samples. All the graphs obtained are straight lines and are fitted to a cubic function defined by the Eq. 2.40 in chapter 2. A slope of 3 in the log-log plot between the pump and phase conjugate signal indicates the third order nature of the process involved as well as the absence of saturation of nonlinearity in the measurements.

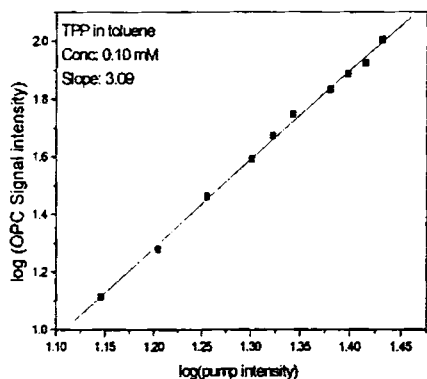


Fig. 4.5 log-log plot of TPP in Toluene

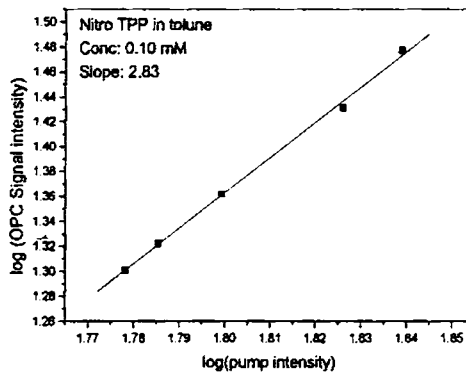


Fig. 4.6 log-log plot of Nitro-TPP in Toluene

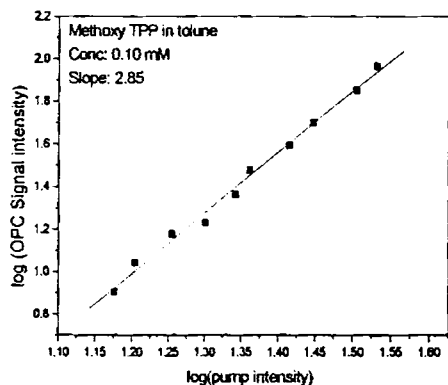


Fig. 4.7 log-log plot of Methoxy-TPP in Toluene

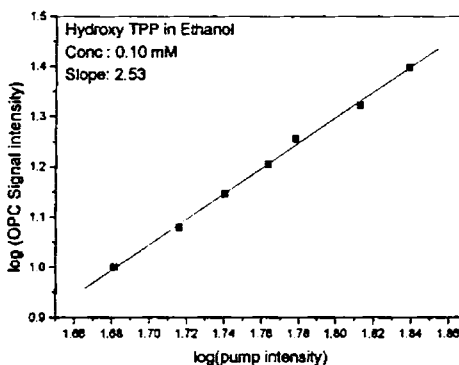
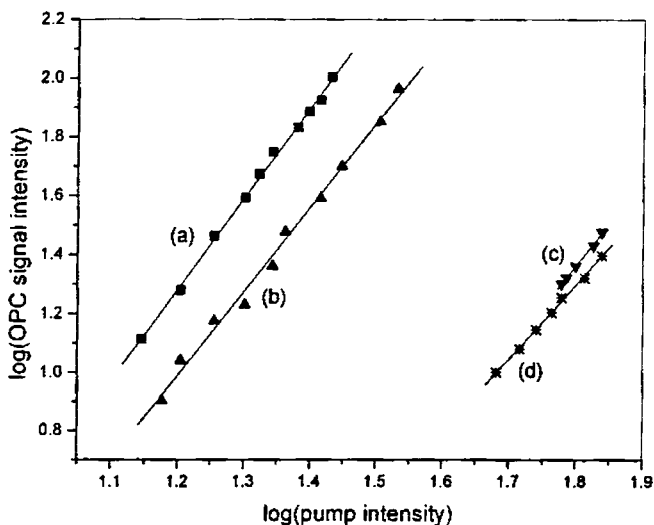


Fig. 4.8 log-log plot of Hydroxy-TPP in Toluene



**Fig. 4.9** Log-log plot of OPC signal intensity versus pump intensity of 0.1 mM (a) TPP, (b) Methoxy TPP, and (c) Nitro TPP in Toluene and (d) Hydroxy TPP in Ethanol

One of the important processes that can influence the degenerate four wave mixing measurements is the two photon absorption (TPA). If TPA is present in the samples the measured slope of the straight line obtained in the log-log plot between the pump intensity and the optical phase conjugate signal (OPC) should be 5 instead of 3 [ 61-62]. All the samples studied gives a slope of 3 and this rules out the presence of TPA contribution to the measurements. Since the experiments were done with samples dissolved in spectroscopic grade solvents (Toluene in the case of TPP, Methoxy-TPP and Hydroxy-TPP and Ethanol in the case of Nitro-TPP), it is possible to evaluate the microscopic molecular property viz. second hyper polarizability  $\langle\gamma\rangle$ . Measured values of third order susceptibility ( $\chi^{(3)}$ ), Figure of merit (F), Extinction coefficient ( $\epsilon$ ) and Second



Investigations of nonlinear .....

hyper polarizability  $\langle \gamma \rangle$  are given in the table 4.1. The Figure of merit (F) of a nonlinear optical material is defined by the relation

$$F = \frac{\chi^{(3)}}{\alpha} \quad (4.5)$$

where  $\alpha$  is the linear absorption coefficient of the sample. The extinction coefficient will be given by the relation [63]

$$\varepsilon = \frac{\sigma N_A}{\ln(10)} \times 10^{-3} \quad (4.6)$$

where  $\sigma$  is the absorption cross section and  $N_A$  is the Avogadro number.

Sample (in Toluene) 0.1 mM	Linear Absorption Coefficient $\alpha$ (cm <sup>-1</sup> )	Extinction coefficient $\varepsilon \times 10^3$ ltr cm <sup>-1</sup> mol <sup>-1</sup>	Third order Susceptibility $\chi^{(3)}$ ( $\times 10^{-13}$ esu)	Figure of Merit F ( $\times 10^{-13}$ esu-cm)	Second Hyper polarizability $\langle \gamma \rangle$ ( $\times 10^{-30}$ esu)
TPP	0.377	1.638	23.27	61.72	10.81
Methoxy TPP	0.473	2.054	16.11	34.06	08.18
Hydroxy TPP (Ethanol)	0.097	0.422	2.40	24.74	01.48
Nitro TPP	0.180	0.725	3.12	17.32	01.59

**Table 4.1** Extinction coefficient, Third order susceptibility, Figure of merit and Second hyperpolarizability of different TPP's measured using DFWM technique

From the table 4.1 it is clear that the highest value for Figure of merit as well as second hyper polarizability were obtained in unsubstituted tetraphenyl porphyrin. The lowest value of Figure of merit and second hyper polarizability is obtained in the case of Nitro-TPP. This clearly shows the effect of peripheral substituents on the nonlinear properties porphyrin samples.

Fig 4.10 shows the open aperture z-scan graphs obtained with these samples. Out of the samples studied here unsubstituted porphyrin which is having the highest  $\langle \gamma \rangle$  value as measured using DFWM technique shows the deeper valley in the z-scan graph. All the samples show similar behaviour. Because of the near-resonant excitation, the nonlinearity in the ns time scales could be due to the thermal excitation of the medium. Depending on the pulse duration, pump intensity and wavelength, nonlinear absorption can be from (a) the ground state  $S_0$  to higher excited singlet states  $S_n$ , (b) the first excited singlet state  $S_1$  to higher excited states  $S_n$ , or from (c) the  $T_1$  to  $T_n$  states in the triplet manifold. The last two processes are known as excited state absorption (ESA), but if their cross sections are larger than that of linear absorption, then these are referred to as reverse saturable absorption (RSA).

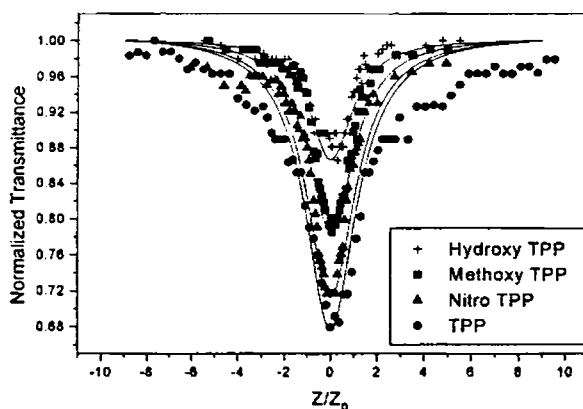


Fig. 4.10 Open aperture z-scan curve obtained with different TPP's (0.25 mM)

Sample	Concentration (mM)	Absorption Coefficient $\alpha$ (cm <sup>-1</sup> )	$\beta_{\text{eff}}$ (m/GW)	$\text{Im}(\chi_{\text{eff}}^3)$ $\times 10^{-17} \text{ m}^2 \text{ V}^{-2}$
Hydroxy TPP (in Ethanol)	0.25	0.42	2.31	4.82
Methoxy TPP (in MMA)	0.25	1.69	4.62	10.38
Nitro TPP (in MMA)	0.25	0.79	6.87	15.45
TPP (in MMA)	0.25	1.47	8.62	19.39

**Table 4.2** Nonlinear absorption coefficient and imaginary part of susceptibility of different TPP's measured using z-scan technique

Table 4.2 summarises the results obtained from the z-scan studies carried out in 0.25 mM solutions of these samples in methyl methacrylate monomer. From the table it is clear that unsubstituted porphyrin gives the highest nonlinear absorption coefficient  $\beta_{\text{eff}}$  and imaginary part of the nonlinear susceptibility ( $\text{Im}\chi_{\text{eff}}^3$ ) and the smallest value is observed in Hydroxy TPP.

#### 5.4 Wavelength Dependence

Fig. 4.11 shows the z-scan curves obtained at different wavelengths of excitation in 0.25 milli molar solutions of tetra phenyl porphyrin (TPP) in toluene. In the range of wavelengths selected for excitation, maximum nonlinear behaviour of the sample is observed at 540 nm. As the wavelength increases from this value the depth of the z-scan curve decreases and this shows the wavelength dependent variation of the NLO

behaviour of the sample considered. The effect of wavelength on the nonlinear properties of znmp TBP and bis-phtanlocyanines were already reported [64-65]. As in the previous reports we do not observe any saturation absorption in the wavelength considered in our experiments.

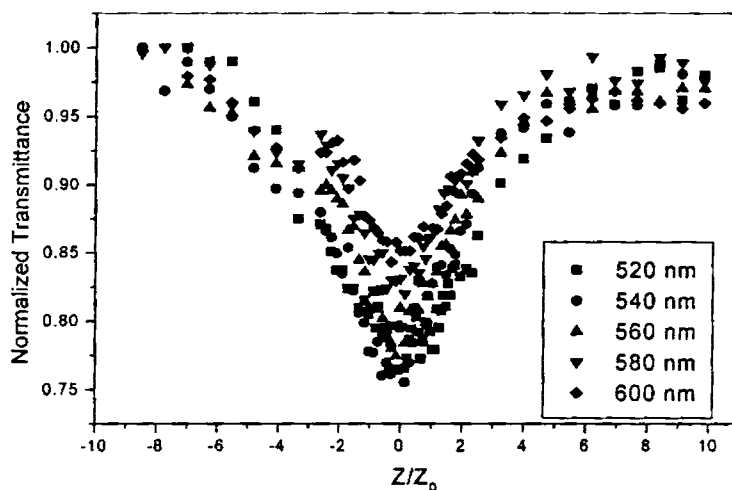
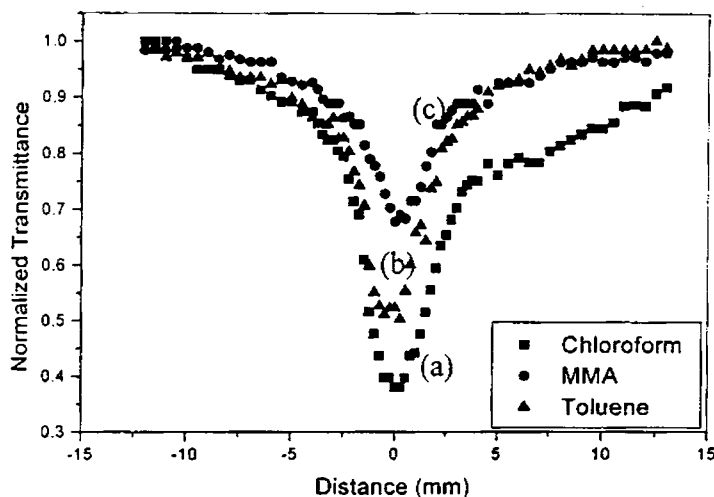


Fig. 4.11 Z-Scan curve obtained at 520, 540, 560, 580, and 600 nm in 0.25 mM TPP in Toluene

### 5.5 Solvent Effect

As the wavelength of excitation, the solvent can also influence the NLO behaviour of the sample. Fig. 4.12 the z-scan graphs obtained with TPP in Toluene, chloroform and Methyl methacrylate monomer (MMA).



**Fig. 4.12** Open aperture z-scan curves of 0.25 mM solutions of TPP in (a) Chloroform (b) Toluene and (c) MMA

The nonlinear absorption coefficient  $\beta_{\text{eff}}$  of tetra phenyl porphyrin in these solvents at different concentrations were calculated. Fig. 4.13 to 4.15 and tables 4.3 to 4.5 shows the z-scan graphs thus obtained and the corresponding nonlinear absorption coefficient  $\beta_{\text{eff}}$  and imaginary part of the nonlinear susceptibility ( $\text{Im}\chi_{\text{eff}}^3$ ) values calculated. From the open aperture z-scan experimental data, nonlinear absorption coefficient  $\beta_{\text{eff}}$  is calculated using the model suggested by Sheik Bhahe et.al. [60] and the details of this is explained in chapter 2 and 3. The imaginary part of the nonlinear susceptibility ( $\text{Im}\chi_{\text{eff}}^3$ ) can be calculated from  $\beta_{\text{eff}}$  using the Eq. 3.13

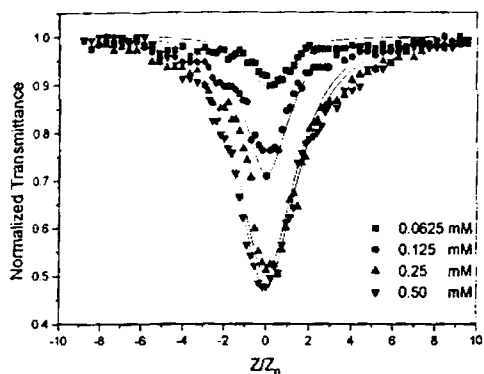


Fig. 4.13 Open aperture z-scan graph of various concentrations of TPP in toluene

Conc. (mM)	Absorption Coefficient $\alpha$ (cm <sup>-1</sup> )	$\beta_{\text{eff}}$ (m/GW)	$\text{Im}(\chi_{\text{eff}}^3) \times 10^{-17}$ m <sup>2</sup> V <sup>-2</sup>
0.06	0.24	1.67	4.21
0.12	0.47	6.76	17.04
0.25	0.94	21.00	52.92
0.50	1.89	24.85	62.61

Table 4.3

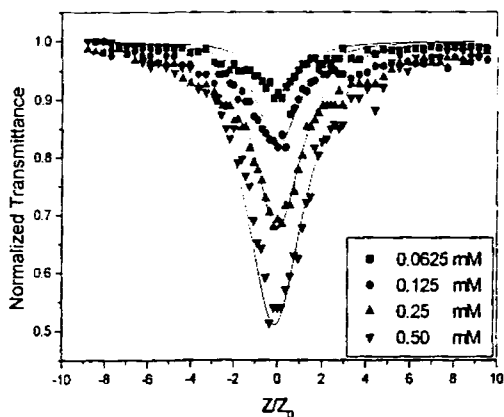


Fig. 4.14 Open aperture z-scan graph of various concentrations of TPP in MMA

Conc (mM)	Absorption Coefficient $\alpha$ (cm <sup>-1</sup> )	$\beta_{\text{eff}}$ (m/GW)	$\text{Im}(\chi_{\text{eff}}^3) \times 10^{-17}$ m <sup>2</sup> V <sup>-2</sup>
0.06	0.37	1.59	3.56
0.12	0.74	3.43	7.70
0.25	1.47	8.62	19.39
0.50	2.94	21.78	48.96

Table 4.4

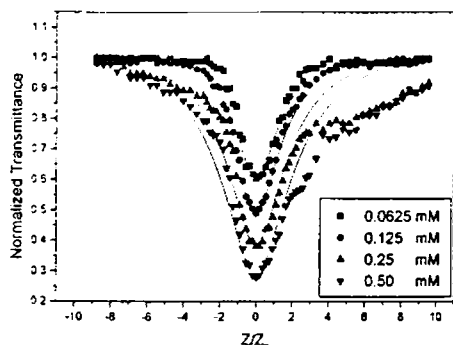


Fig. 4.15 Open aperture z-scan graph of various concentrations of TPP in  $\text{CHCl}_3$

Conc. (mM)	Absorption Coefficient $\alpha$ ( $\text{cm}^{-1}$ )	$\beta_{\text{eff}}$ (m/GW)	$\text{Im}(\chi_{\text{eff}}^3) \times 10^{-17} \text{ m}^2 \text{V}^{-2}$
0.06	0.38	12.02	28.18
0.12	0.75	21.06	49.37
0.25	1.47	39.56	92.77
0.50	3.01	76.43	179.22

Table. 4.5

From the calculated values of  $\beta_{\text{eff}}$  and  $\text{Im}\chi_{\text{eff}}^3$  given in tables 4.3 to 4.5 it is clear that out of the three different solvents used, sample dissolved in chloroform gives better NLO properties. The better nonlinear behaviour of the sample in chloroform is assumed to be due to the polar nature of the solvent.

Results of the studies on nonlinear optical properties of various types of porphyrins carried out by several people were reported in the literature [66-70]. S V Rao et. al. [71] has reported the NLO properties of several Tetra Toly Porphyrin (TTP) using nano second and pico second optical pulses. The effect of peripheral ligands on the NLO properties of several dendritic porphyrins has been reported by B. P Sing et. al [72] and they have observed very high values for the second hyper polarizability  $\langle \gamma \rangle$ . W. Huang et. al. [73] reported the nonlinear behaviour of porphyrin Phthalocyanine metal triple decker complexes. Nonlinear optical studies have been carried out in porphyrin samples different host matrices. For example, Kandasamy et. al [74] have investigated optical nonlinearity in a porphyrin (T 3, 4, BCEMPP) doped in boric acid glass, using Z-scan techniques, at selected  $\text{Ar}^+$  ion laser wavelengths

### 5.6 Optical Limiting

The reverse saturation absorption property of porphyrin molecules can be well used for the design of optical limiters to protect light sensitive devices from intense laser radiations. N. Ono et. al. [75] studied the optical limiting property of meso-substituted tetra benzyl porphyrins and tetra phenyl porphyrins and they have observed that the compounds with electron donating ligands to the base porphyrin ring show very good optical limiting. The optical limiting property of our samples is also studied using the standard experimental techniques explained earlier. Fig 4.16 shows the nonlinear transmission of the porphyrins investigated here. These plots were generated from respective z-scan graphs recorded. All these samples have nearly identical concentrations (0.25 mM) and methyl methacrylate monomer was used as the solvent.

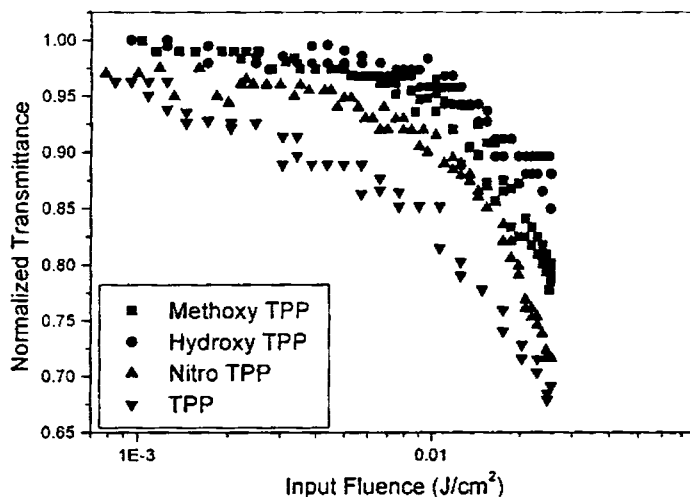


**Fig. 4.16** Optical limiting in 0.25 mM solutions of TPP, Methoxy-TPP, and Nitro-TPP in MMA and Hydroxy-TPP in ethanol



## Investigations of nonlinear .....

It can be seen that the unsubstituted porphyrin as well as the nitro-TPP show very good optical limiting compared with the other two samples. This observation is in agreement with the DFWM measurements carried out in these samples. Here the better limiting nature of nitro-TPP which shows only very small second hyper polarizability value in comparison with other samples studied is really interesting and it may be due to the higher ESA of this compound in the wavelength of excitation.

### 5.7 Discussion

The second hyper polarizability  $\langle\gamma\rangle$  of nonlinear optical materials depend on many factors. In the case of organic molecules it is known that the  $\langle\gamma\rangle$  values depend heavily on the extend of  $\pi$  electron conjugation. Therefore if the  $\pi$  electron conjugation is high the corresponding  $\langle\gamma\rangle$  values is also large. But there are reports on the saturation of  $\langle\gamma\rangle$  values after a finite degree of conjugation [76] and hence it cannot increase indefinitely. Apart from the  $\pi$  electron conjugation there are many other factors that can influence the  $\langle\gamma\rangle$  values. Oscillation strength [77-79], Nature of the metal substituents [77, 80-83], Dimensionality of the molecule [84-87], axial and peripheral substituents [88-94] etc are the important factors influencing the  $\langle\gamma\rangle$  values. Out of these various contributing factors we are concentrating on the effect of peripheral substitution to the porphyrin ring on the second hyper polarizability. The samples selected do not have any central metal ion in the porphyrin ring but all them have different peripheral substituents like Nitro, Hydroxy, Methoxy groups attached to the outer benzene ring.

As mentioned earlier, due to the high flexibility of porphyrin molecules for structural modifications, it is possible to incorporate various chemical groups having different electronegativities to the porphyrin macrostructure with out compromising its excellent chemical and thermal stability. Chemical groups like  $-\text{OH}$ ,  $\text{NH}_2$  etc. have

strong electron donating character while  $-\text{NO}_2$ ,  $-\text{COOH}$  etc. are having high electron accepting nature. Chemical groups like  $-\text{C}_6\text{H}_5\text{O}$ ,  $-\text{CH}_3$  etc. have intermediate electronegativities. Therefore the incorporation of chemical groups having different electronegativities to various positions can probe the effect of peripheral substitution to the NLO properties of the base molecules. These types of compounds are called push pull compounds and they have donor-conjugate electron-acceptor structure [95]. As in the case of metal ion substitution at the center of the ring, axial or peripheral substitution can also affect the  $\langle\gamma\rangle$  value of the molecule by introducing intramolecular charge transfer mechanisms (ICT). The ICT processes are associated with change in dipole moment between the ground state and the first excited state of the molecules. Hammett free energy relationships are used to describe how substituents alter the electronic structure of the molecules. Hammett free energy is usually expressed using the equation [88]

$$\log k = \log k_0 + \rho\sigma \quad (3.7)$$

where  $k$  and  $k_0$  denote equilibrium constants for substituted and unsubstituted compounds respectively.  $\sigma$  is characteristic of the substituents indicating its behaviour as an electron donor or electron acceptor and  $\rho$  is a measure of the sensitivity of the processes to alteration in the substituents.

The difference in the  $\langle\gamma\rangle$  values of the samples can be explained in terms of the influence of intermolecular charge transfer mechanism and other parameters like oscillator strength as follows. Among the various TPP's studied, the unsubstituted TTP has the highest and Nitro-TTP has the lowest  $\langle\gamma\rangle$  value. The chemical groups attached to the porphyrin molecules have different electronegativities. Among the axial ligands,  $-\text{OH}$  group is having high electron donating property while the  $-\text{NO}_2$  is of high electron accepting nature. The electronegativity of the 'methyl' group is in between that of

## Investigations of nonlinear .....

'hydroxy' and 'nitro' groups. Due to this nature of the axial ligand the electron density in the porphyrin core is heavily perturbed and this leads to the change in the observed  $\langle\gamma\rangle$  values. The measured  $\langle\gamma\rangle$  values of Hydroxy-TPP as well as Nitro-TPP is considerably smaller than the  $\langle\gamma\rangle$  of the unsubstituted TPP. This indicates that the very high electron donating as well as electron accepting nature of the axial ligand from the porphyrin ring decreases the second hyper polarizability  $\langle\gamma\rangle$  of the base material. Apart from the electron accepting as well as electron donation to the porphyrin ring the oscillator strength of the molecule can also affect  $\langle\gamma\rangle$  value of the samples [96]. Among the TPP's studied the Methoxy TPP is having the highest value of oscillation strength because of its large value of extinction coefficient  $\epsilon$ . Therefore the considerably large value of  $\langle\gamma\rangle$  in the case of Methoxy-TPP is attributed to the effect of oscillator strength of the molecule. The effect of oscillator strength on the  $\langle\gamma\rangle$  values in the case of Nitro TPP and Hydroxy TPP is also evident. The oscillator strength of these samples is considerably small in comparison to that of unsubstituted TPP and Methoxy TPP. Therefore the charge transfer due to the peripheral ligands combined with the oscillator strength of the molecules explain the calculated  $\langle\gamma\rangle$  values.

The z-scan studies carried out on these samples also support the DFWM measurements. The largest value of nonlinear absorption coefficient  $\beta_{\text{eff}}$  and imaginary part of the nonlinear susceptibility ( $\text{Im}\chi_{\text{eff}}^3$ ) are obtained in the case of unsubstituted porphyrin sample. The nonlinear absorption observed in these samples can be explained using a five level model involving the states  $S_0$ ,  $S_1$ ,  $S_2$ ,  $T_1$  and  $T_2$  as explained in chapter 4 [71]. Here  $S_n$  and  $T_n$  are the singlet and triplet states respectively (where  $n=0, 1$  or  $2$ ) and every electronic energy level involves several vibronic levels. On interaction with laser pulses at 532 nm, atoms get excited from the  $S_0$  to upper vibrational levels of  $S_1$ . Through nonradiative decay within picosecond time scale the excited molecules can relax to the

lowest vibrational level of  $S_1$ . There is a definite probability for the atoms to get de-excited back to the appropriate vibrational level in the ground state through fluorescence emission. But the fluorescence spectra observed in the samples under consideration are so weak that we can rule out the  $S_1 \rightarrow S_0$  transitions. Moreover, the  $S_1$  to  $S_2$  transition does not deplete the  $S_1$  state because the  $S_1$  to  $S_2$  transition takes place within the picosecond time scale. However, the intersystem crossing in these samples is very large and this result in strong triplet – triplet absorption [65]. Here we assume that the intersystem crossing is fast compared with the laser pulse width and virtually all the atoms excited from  $S_0$  reach the first excited triplet state  $T_1$ . Therefore, under nanosecond pulse excitation, the nonlinear absorption observed in these samples is a consequence of triplet-triplet ( $T_1 \rightarrow T_2$ ) absorption. The Nitro-TPP which is having very low  $\langle \gamma \rangle$  value is having fairly good nonlinear absorption coefficient ( $\beta_{\text{eff}}$ ) and this is attributed to the high excited state absorption of this sample.

### 5.8 Conclusions

Degenerate four-wave mixing, z-scan and optical limiting studies were carried out in solutions of porphyrin samples with different peripheral substituted ligands. Third order susceptibility  $\chi^{(3)}$ , Figure of merit of third order nonlinearity (F), Second hyper polarizability  $\langle \gamma \rangle$  were measured. TPP with out any peripheral ligands exhibited the highest value of figure of merit as well as second hyper polarizability indicating that it possess maximum third order nonlinearity for a given absorption loss. The  $\langle \gamma \rangle$  values measured were explained on the basis of internal charge transfer mechanism and oscillator strength of the molecules. The effects of wavelength, concentration and solvents on the NLO behaviour of the samples were studied using the z-scan technique. The optical limiting nature of these samples was studied and it is observed that unsubstituted porphyrin and nitro-TPP show the maximum optical limiting property.

## Investigations of nonlinear .....

### 5.9 Reference:

1. H S Nalwa and Seizo Miyata, Eds, *Nonlinear optics of organic molecules and polymers*, C RC Press, New York, (1997)
2. D.S. Chemla, J. Zyss, Eds., *Nonlinear Optical Properties of Organic Molecules and Crystals*, Vols., 1 and 2, Academic Press, Orlanda, FL, USA, (1987)
3. S.R. Marder, J.E. Sohn, G.D. Stucky, Eds., *Materials for Nonlinear Optics: Chemical Perspectives*, ACS Symposium Series, American Chemical Society, Washington , DC (1991)
4. J.L. Bredas, C. Adant, P. Tackx, and A. Persoons, *Chem. Rev.* **94**, (1994) p.243
5. *Molecular Nonlinear Optics*, Ed. J. Zyss, Academic, New York, USA, 1994
6. G. de la Torre, P Vazquez, F Agullo-Lopez and T Torres, *J. Mater. Chem.* **8(8)** (1998) p.1671
7. D N Rao, *Optical Materials*, **21**, (2002) p.45
8. W Huang, S Wang, H Yang, Q Gong, x Zhan, Y Liu and D Zhu, *Chem. Phys. Lett* **350** (2001) p. 99
9. Danilo Dini, Markus Barthel, Thorsten Schneider, Martin Ottmar, Sanjiv Verma and Michael Hanack, *Solid State Ionics*, **165** (2003) p.289
10. L W Tutt and T F Boggess, *Prog. Quant. Electr.* **17** (1993) p.299
11. K P Unnikrishnan, Jayan Thomas, V P N Nampoori and C P G Vallabhan, *Opti. Commun.* **204** (2002) p.385
12. K P Unnikrishnan, Jayan Thomas, V P N Nampoori and C P G Vallabhan *chemical Physics.* **279** (2002) p.209
13. T. Zhang, J Li, P Gao, Q Gong, K Tang, X Jin, S Zheng and l Li, *Opti. Commun.* **150** (1998) p.201
14. D Vincent and J Cruickshank, *Appl. Opt.* **36(30)**, (1997) p. 7794
15. L Marrucci, D Paparo, G Cerrone, C De Lisio, E Santamato, S Solimeno, s Ardizzone and P Quagliotto, *Optics and Lasers in Engg.* **37(5)**, (2002) p. 601
16. G S He, *Prog. Quant. Electr.* , **26(3)**, (2002) p.131
17. M Hanack, T Schneider, M Barthel, J s Shirk, S R Flom and R G s Pong, *Coord. Chem. Reviews.* **219** (2001) p.235
18. S A Podoshvedov and Y V Miklyaev *Opti. Commun.* **171 (4)**, (1999) p.301
19. P.N. Prasad and D.J. Williams, *Introduction to Nonlinear Optical Effects in Molecules and Polymers*, Wiley, New York, (1991)
20. B D Berezin, *Coordination compounds of Porphyrins and Phthalocyanines*, John Wiley and Sons, New York.
21. P Chen, I V Tomov, A S Dvornikov, M Nakashima, J F Roach, D M Alabran and P M Rentzepis, *J. Phys. Chem.* **100**, (1996) p.17507
22. M Brunel, F Chaput, S A Vinogradov, B Campagne, M Canva, J P Boilot and A Brun, *Chem. Phys.* **218** (1997) p. 301
23. K Kandasamy, S J Shetty, P N Puntambekar, T S Srivastava, T Kundu and B P Singh, *Chem. Commun.* (1997) p. 1159
24. D N Rao and S V Rao, *Asian Journal of Physics*, **9(2)**, (2000) p.145

25. R Kumble, S Palese, V S Y Lin, M J Therien and R M Hochstrasser, *J. Am. Chem. Soc.* **120**, (1998) p. 11489
26. B P Singh, R Vijaya, T Kundu, K Kandasamy, P N Puntambekar, S J Shetty and T S Srivastava, *J. Porph. Phthalo* **5**, (2001) p. 439
27. S Gentemann, C J Medforth, T Ema, N Y Nelson, K M Smith, J Fajer and Dewey Holten, *Chem. Phys. Lett* **245** (1995) p. 441
28. J R G Thorne, S M Kuebler, R G Denning, I M Blake, P N Taylor and H L Anderson, *Chem. Phys. Lett* **248** (1999) p. 181
29. M Tarazima, H Shimizu and A Osuka, *J. Appl. Phys.* **81(7)**, (1997) p. 2946
30. F Z Henari, W J Balu, L R Milgrom, G Yahioğlu, D Phillips and J A Lacey, *Chem. Phys. Lett* **267** (1997) p. 229
31. S Guha, K Kang, Porter, J F Roach, D E Remy, F J Aranda, D V G L N Rao, *Opt. Lett.* **17** (1992) 264
32. K Dou, X Sun, W Wang, R Parkhill, Y Guo, E T Knobbe, *Solid state commun.* **107** (1998) 101
33. S R Mishra, H S Rawat, M Laghat, *Opt. Commun.* **147** (1998) 328
34. K Kandasamy, P N Puntambekar, B P Singh, S J Shetty, T S Srivastava, *J. Nonlinear Opt. Phys. Mater.* **6** (1997) 361
35. R Bonnett, *Chem. Soc. Rev.* **24** (1995) 19
36. W Sun, C C yeon, C M Lawson, G M Gray, D Wang, *Appl. Phys. Lett.* **74** (1999) 3254
37. R A Norwood, J R Sounik, *Appl. Phys. Lett.* **60** (1992) 295
38. D V G L N Rao, F J Aranda, J F Roach, D E Remy, *Appl. Phys. Lett.* **58** (1991) 1241
39. K Dou, X Sun, X Wang, R Parkhill, Y Guo, E T Knobbe, *IEEE J. of Quantum elec.* **35(7)**, (1999) 1004
40. C. Meloney, H. Byrne, W.M. Dennis, W. Blau, and J.M. Kelly, *Chem. Phys.* **121**, 21, 1988
41. S. Guha, K. Kang, P. Porter, J.F. Roach, D.E. Remy, F.J. Aranda, and D.V.G.L.N. Rao, *Opt. Lett.* **17**, 264, 1992
42. T. Sakaguchi, Y. Shimizu, M. Miya, T. Fukumi, K. Ohta, and A. Nagata, *Chem. Lett.* **281**, 1992
43. J. Qin, T. Wada, and H. Sasabe, *Mol. Cryst. Liq. Cryst.* **217**, (1992) p.47
44. M. Hosoda, T. Wada, A.F. Garito, and H. Sasabe, *Jpn. J. Appl. Phys.* **31**, L249, 1992
45. K.S. Suslick, C. -T. Chen, G.R. Meredith, and L -T. Cheng, *J. Am. Chem. Soc.* **114**, 6928, 1992
46. F.Z. Henari, W.J. Blau, L.R. Milgrom, G. Yahioğlu, D. Phillips and J.A. Lacey, *Chem. Phys. Lett.* **267**, 229, 1997
47. G.R. Kumar, M. Ravikanth, S. Banrjee, A. Sevian, *Opt. Commun.* **144**, 245, 1997
48. M. Terazima, H. Shimizu, and A. Osuka, *J. Appl. Phys.*, **81**, 2946, 1997
49. K. Kandasamy, S.J. Shetty, P.N. Puntabekar, T.S. Srivastava, T. Kundu, and B.P. Singh, *J. Chem. Soc., Chem. Commun:* (1997) p.1159
50. D. Beljonne, G.E. O'Keefe, P.J. Hamer, R.H. Friend, H.L. Anderson, and J.L. Bredas, *J. Chem. Phys.*, **106**, 9439, 1997.

## Investigations of nonlinear .....

51. H.L. Anderson, S.J. Martin, and D.D.C. Bradley, *Angew. Chem. Int. Ed. Eng.* **33**, (1994) p.655
52. R.V. Honeychuck, *Polym. Preprints* **32**, (1992) p.138
53. M. Brunel, F. Chaput, S.A. Vinogradov, B. Campagne, M. Canva, J.P. Boilot, and A. Brun, *Chem. Phys.* **218**, 301, 1997
54. K. Kandasamy, K.D. Rao, R. Deshpande, P.N. Puntabekar, B.P. Singh, S.J. Shetty, and T.S. Srivastava, *Appl. Phys. B*, **64**, 479, 1997.
55. A Sreekanth, Ph. D. Thesis, Department of Chemistry, CUSAT, Cochin-22
56. J R G Thorne, S M Kuebler, R G Denning, I M Blake, P N Taylor, H L Anderson, *Chem. Phys. Lett.* **248** (1999) p. 181
57. Jun Ichi Sakai, *Phase Conjugate Optics*. McGraw Hill, New York
58. M. -T. Zhao, B.P. Singh, and P.N. Prasad, *J. Chem. Phys.* **89**, 5535, 1988.
59. R A Fisher (Ed.) *Optical Phase Conjugation*, Academic Press, New York, 1983.
60. M S Bahae, A A Said, T H Wei, D J Hagan, E W V Stryland. *IEEE J. Quantum Electronics* **26** (1990) p. 760
61. S Wu, X C Chang and R L Fork, *Appl. Phys. Lett.* **61** (1992) p. 919
62. M Zhao, Y Cui, M Samoc and P N Prasad, *J. Chem. Phys.* **95** (1991) p. 3991
63. T H Wei, D J Hagan, M L Sence, E W V Stryland, J W Perry and D R Coutler, *Appl. Phys. B*. **54** (1992) p. 46
64. K P Unnikrishnan, Jayan Thomas, V P N Nampoori and C P G Vallabhan, *Opt. Commun.* **204**, (2002) p.385
65. N K M N Srinivas, S V Rao, D V G L N Rao, B K Kimball, M Nakashima, B S Decristofano and D Narayana Rao *J. Porphyrins and Phthalocyanines*, **5** (2001), p.549
66. M. Gouterman, *The Porphyrins*, Vols. I-VII, D. Dolphin Ed., Academic Press, New York, (1978)
67. K. Smith, *Porphyrins and Metalloporphyrins*, Amsterdam, The Netherlands: Elsevier/North-Holland Biomedical Press, (1976)
68. S V Rao, N K M M Srinivas, D N Rao, L Giribabu, B G Maiya, Reji Philip and G Ravindra Kumar, *Opt. Commun.* **192** (2001) p. 123
69. M. Ravikanth and G.R. Kumar, *Current Science*, **68**, (1995) p.1010
70. M. Gouterman, P. Rentzepis, Ed.'s, *Porphyrins: Excited State and Dynamics*, *Am. Chem. Soc. Symp. Ser.* (1987) p.321
71. S V Rao, N K M M Srinivas, D N Rao, L Giribabu, B G Maiya, Reji Philip and G Ravindra Kumar, *Opt. Commun.* **182** (2000) p. 255
72. B P Singh, R Vijaya, S J Shetty, K Kandaswamy, P N Puntambeka and T S Srivastava, *J. Porph. Phthalo* **4**, (2000) p. 659
73. W Huang, H Xiang, Q. Gong, Y Huang, C Huang and J Jiang, *Chem. Phys. Lett* **374** (2003) p. 639
74. K Kandasamy, K D Rao, R Deshpande, P N Puntambekar, B P Sing, S J Shetty, T S Srivastava, *Appl Opt. B* **64** (1997) p. 479
75. N Ono, S Ito, C H Wu, C H Chen and T C Wen, *Chem. Phys.* **262** (2000) p. 467
76. M K Cassetevens, M Samoc, J Pflieger and P N Prasad, *J. Chem. Phys.* **92** (1990) p. 2019

77. K Kandasamy, S J Shetty, P N Puntambekar, T S Srivastava, T Kundu and B P Sing, *J. Porphyrins and Phthalocyanines* **3** (1999) p. 81
78. M G Kuzyk and C W Dirk, *Phys. Rev. A* **41**(1990) p. 5098
79. I Renge, H Wolleb, H Spahni and U P Wild, *J. Phys. Chem. A*, **101** (1997) p. 6202
80. A Yamashita, S Matsumoto, S Sakata and T Hayashi., H Kanbara, *J. Phys. Chem. B* **102** (1998) p. 5165
81. J S Shirk, J R Lindle, F J Bartoli and M E Boyle, *J. Phys. Chem.* **96** (1992) p. 5847
82. K Kamada, M Ueda, T Sakaguchi, K Ohta and T Fukumi, *J. Opt. Soc. Am. B* **15** (1998) p. 838
83. M Koshino, H Kurata, S Isoda and T Kobayashi, *ICR Annual Report.* **7** (2000) p.6
84. H S Nalwa and S Kobayashi, *J. Porphyrins and Phthalocyanines.* **2** (1998) p. 21
85. Ifor. D W Samuel, I Ledoux, C Delporte, D L Pearson and James M Tour, *Chem. Mater.* **8** (1996) p. 819
86. G R Kumar, M Ravikanth, S Banerjee, Armen Sevian, *Optic. Commun.* **144** (1997) p. 245
87. D S Chemla, J Zyss. *Nonlinear Optical Properties of Organic Molecules and Crystals.* Quantum Electronics. Principles and Applications. Academic Press (1987) Florida
88. A Sastre, M A Diaz-Garcia, D del Rey, C Dhenaut, J Zyss, I Ledoux, F Agullo Lopez and T Torres, *J. Phys. Chem. A* **101** (1997) p. 9773
89. K S Suslick, C T Chen, G R Meredith, and L T Cheng, *J. Am. Chem. Soc.* **114** (1992) p. 6928
90. B K Mandal, B Bihari, A K Sinha and M Kamath, *Appl. Phys. Lett.* **66** (1995) p. 932
91. A K Sinha, B Bihari and B K Mandal. *Macromolecules.* **28** (1995) p.5681
92. H S Nalwa, A Kakuta, *Thin Solid Films.* **254** (1995) p.218
93. K Kandasamy, S J Shetty, P N Puntambekar, T S Srivastava, T Kundu anf B P Singh, *Chem. Commun.* (1997) p. 1159
94. H Kanbara, T Maruno, A Yamashita, S Matsumoto, T Hayashi, H Konami, N Tanaka, *J. Appl. Phys.* **80** (1996) p. 3674
95. J Oberle, L Bramerie, G Jonusauskas and C Rulliere, *Opt. Commun.* **169** (1999) p.325
96. I Renge, H Wolleb, H Spahni and U P Wild, *J. Phys. Chem. A* **101** (1997) p. 6202



## Chapter 6

### **DFWM Studies on Cobalt Ternary Complexes of 2-Hydroxy Acetophenone N(4) Phenyl Semicarbazone Containing Heterocyclic Coligands**

#### **Abstract**

Degenerate four wave mixing studies were carried out in Cobalt Ternary Complexes of 2-Hydroxy Acetophenone N(4) Phenyl Semicarbazone Containing Heterocyclic Coligands. The experimental details are same as explained in earlier chapters. As in the case of QAP's and TPP's, the Figure of merit of third order nonlinearity ( $F$ ), Third order susceptibility ( $\chi^3$ ) and Second hyper polarizability  $\langle \gamma \rangle$  of these samples were measured. The nonlinear parameters thus obtained have been interpreted by considering the influence of oscillator strength and atomic substituents.

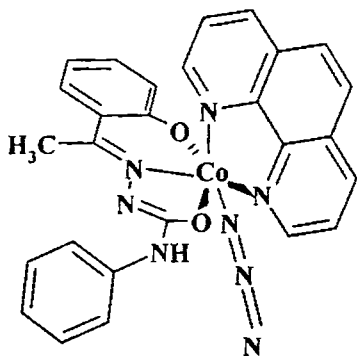
## 6.1 Introduction

As was noted in earlier chapters the nonlinear optical (NLO) properties of inorganic complexes and organometallics have created significant interest in the scientific field because of their importance in this area [1-8]. The nonlinear parameters of a vast number of compounds studied so far depend on various aspects related to their structure and composition. The  $\pi$ - conjugate electrons, presence of donor-acceptor ligands, dimensionality etc. of the compounds play crucial role in determining the NLO behaviour of various materials [9-13]. The achievement of controlled modulation of optical properties of materials constitutes the first step towards the development of photonic devices and the effort in this direction is really worth mentioning. Measurement of NLO parameters becomes a crucial step in this direction in verifying whether the desired properties are truly available in the newly synthesized organic materials. This is the motivation of the measurements presented in this chapter.

New materials are the key elements to future photonic technologies in which their functions can be integrated with other electrical, optical and magnetic components of these compounds. Semicarbazones are compounds with versatile structural features and are reported to possess antifungal and antibacterial properties [14-16]. The nonlinear properties of these compounds are not yet reported to the best of our knowledge. In this chapter we present our results on the measurements of the third order nonlinear optical studies in Cobalt Ternary Complexes of 2-Hydroxy Acetophenone N(4) Phenyl Semicarbazone containing Heterocyclic Coligands synthesized in our institute. Second hyper-polarizability is a measure of the nonlinear behavior of a material and this can be measured using different techniques like Optical Kerr effect, Degenerate Four Wave Mixing (DFWM), Z-Scan etc. For the present study Degenerate Four Wave Mixing (DFWM) in the backward configuration has been used.

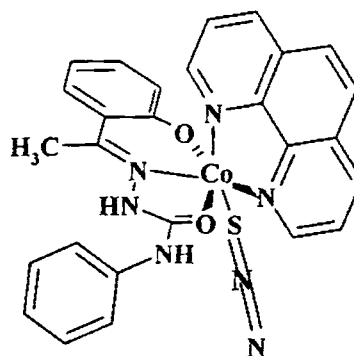
Investigations of nonlinear .....

The structure of various compounds used for the present study is as given in Fig. 6.1



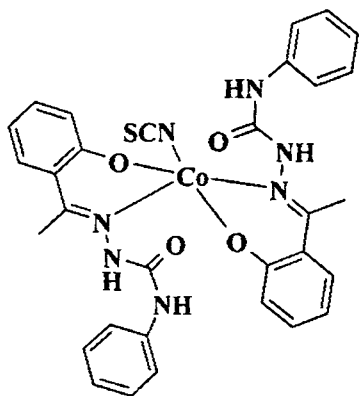
COMP I: Cobalt (III) complex

(a)



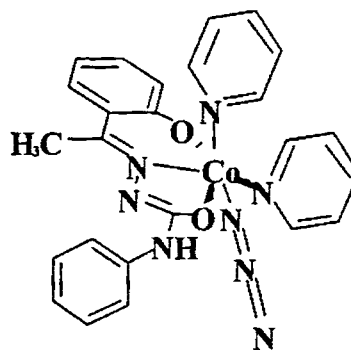
COMP II: Cobalt (II) complex

(b)



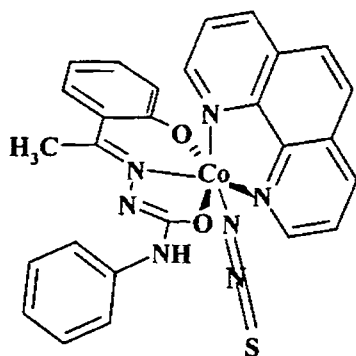
COMP III: Cobalt (II) Complex

(c)



COMP IV: Cobalt (III) Complex

(d)



**COMP V: Cobalt (III) Complex**

(e)

**Fig. 6.1 (a-e)** Structure of various Cobalt Ternary Complexes of 2-Hydroxy Acetophenone N(4) Phenyl Semicarbazone containing Heterocyclic Coligands

## 6.2 Experimental

The experimental part of the present study is divided into two sections viz. Sample Preparation and Degenerate Four Wave Mixing

### 6.2.1 Sample Preparation

The samples used for the present study were prepared by the method explained below.

#### 6.2.1.1 Preparations of $H_2L$

4-Phenyl semicarbazide, 2-hydroxyacetophenone and 1, 10 phenanthroline required for the present syntheses are used as received from reputed firms and all solvents were distilled before use. A methanolic solution of 4-phenyl semicarbazide was added to a solution of 2-hydroxyacetophenone in methanol. To the resulting solution

## Investigations of nonlinear .....

two drops of conc. acetic acid was added and the reaction mixture was refluxed for 3 hours on water bath. On cooling off white colored crystals of H<sub>2</sub>L are separated and this is filtered out from the mixture.

### 6.2.1.2 Synthesis of complexes

All complexes were prepared by adding a methanolic solution of cobaltous acetate to a mixture of methanolic solutions of the H<sub>2</sub>L and heterocyclic base. The green coloured solution was stirred for 10 minutes and a methanolic solution of NaN<sub>3</sub>/ KCNS was added and the reaction mixture was refluxed for 20 minutes. The complexes, which separated as microcrystalline powders in decent yields, were filtered and washed with diethyl ether and dried over P<sub>4</sub>O<sub>10</sub> *in vacuo*. Each sample is subjected to a column chromatographic purification process just prior to the measurements. The samples are dissolved in highly purified, spectroscopic grade Dimethyl Formamide (DMF) and the absorption spectra are recorded using a UV/VIS/NIR spectrophotometer (Jasco V-570). In all experiments, sample solutions are taken in 1-mm quartz cuvettes. Fresh solutions are prepared for each measurement to avoid any complications arising from photodegradation.

### 6.2.2 Degenerate Four Wave Mixing

Detailed theory and experimental setup of degenerate four wave mixing was discussed in chapter 2. The experimental conditions and finer details are same as in the previous chapters of the present thesis. We employ the standard back scattering geometry for making the measurements. 532 nm radiation from a Q-switched Nd:YAG laser is used as the source of excitation. The values of the second hyperpolarizability  $\langle\gamma\rangle$  were calculated using the following equations

$$\chi_s^{(3)} = \chi_{ref}^{(3)} \left[ \frac{(I/I_0^3)}{(I/I_0^3)_{ref}} \right]^{\frac{1}{2}} \left( \frac{n_0}{n_{ref}} \right)^2 \left( \frac{l_{ref}}{l} \right) \left( \frac{al \exp(al/2)}{1 - \exp(-al)} \right) \quad (6.1)$$

and

$$\langle \gamma \rangle = \frac{\chi^{(3)}}{L^4 N} \quad L = \frac{n^2 + 2}{3} \quad (6.2)$$

where 'n' is the refractive index 'l' is the length of the sample, 'α' is the linear absorption coefficient and 'P' is the intensity.

The effective  $\chi^{(3)}$  values of the samples were calculated by assuming a pairwise additive model and is given by

$$\chi_{solution}^{(3)} = \chi_{solvent}^{(3)} + \frac{L^4 \gamma_{solute} Ax C}{M} \quad (6.3)$$

where 'A' being the Avagadro's number, 'M' being the molecular weight and 'C' the concentration of the solute in g/ml. We have taken the value of  $\chi^{(3)}$ , for the reference sample CS<sub>2</sub> as 2.73 x 10<sup>-13</sup> esu and the  $\chi^{(3)}$  contribution from solvent is taken to be zero, as it is negligibly small in comparison to the solute. The energy of the phase conjugate signal as well as the pump beams were measured by using a dual channel energy ratio meter Rj-7620 and Rjp-735 pyroelectric probes (Laser Probe International, USA).

### 6.2.2.1 Calibration

For the measurements of the nonlinear parameters using degenerate four wave mixing technique the experimental setup has to be standardized using a nonlinear optical material. Carbon disulphide (CS<sub>2</sub>) is used as the standard material because of its completely non-resonant Kerr nonlinearity due to orientational response.

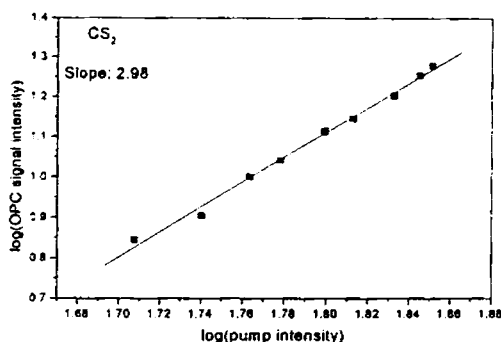


**Fig. 6.2** log-log plot of OPC signal against pump beam intensity

Fig. 6.2 shows the log-log plot of optical phase conjugate signal intensity against pump beam intensity for CS<sub>2</sub> when polarization of the probe beam was orthogonal to the pump beam. The graph obtained is a straight line with slope 2.98 which is very close to the theoretical value 3 showing the cubical dependence of phase conjugate signal against the pump beam intensity.

### 6.3 Results

All samples used in this study show similar type of linear absorption and figure 6.2 shows the UV-Visible spectra obtained. The experiments were carried out with samples having a concentration in the range of  $10^{-4}$  to  $10^{-5}$  M corresponding to an absorbance of less than 0.2

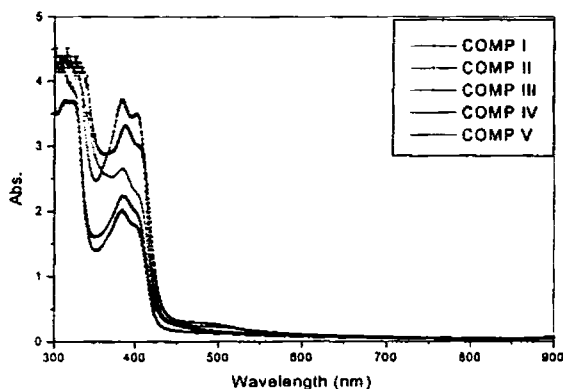


**Fig. 6.3** Absorption spectra of the compounds used for the present study

From the absorption spectra it is clear that there is no linear absorption corresponding to the wavelength of excitation (532 nm). Hence the nonlinearity observed in these samples is due to the excited state absorption present in these samples and therefore electronic in origin. The cubic dependence of the phase conjugate signal with the input intensity has been verified for all the samples and Fig. 6.4 to 6.8 shows the plots of phase

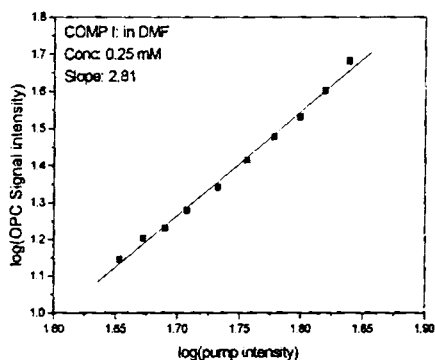


Fig. 6.4 log-log plot of COMP I

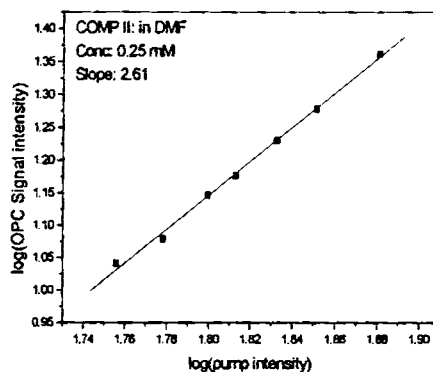


Fig. 6.5 log-log plot of COMP II

conjugate signal verses input intensity. The concentration of the samples was kept at 0.25 mM and Chloroform was used as the solvent. All the graphs obtained are straight lines and are fitted to a cubic function defined by the Eq. 2.40 in chapter 2. A slope of 3 in the log-log plots between the pump and phase conjugate signal indicates the third order nature of the process involved as well as the absence of saturation of nonlinearity in the measurements.

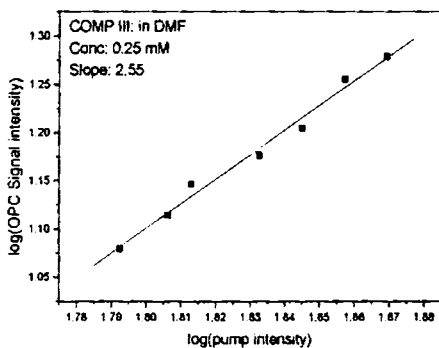


Fig. 6.6 log-log plot of COMP III

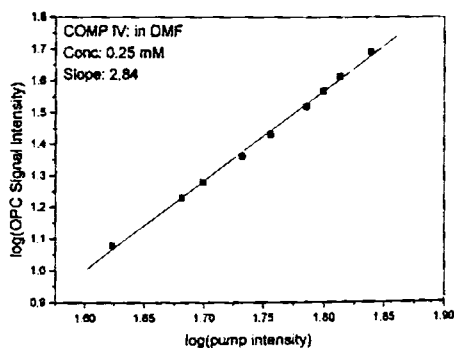


Fig. 6.7 log-log plot of COMP IV



## Investigations of nonlinear .....

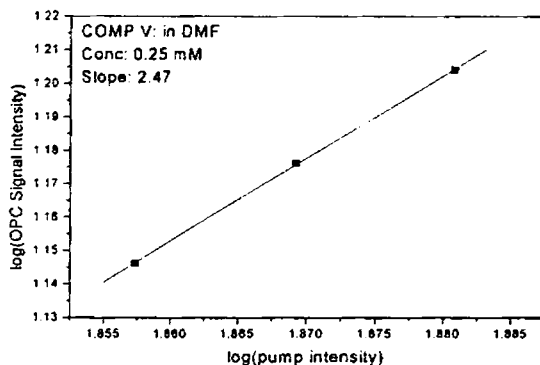


Fig. 6.8 log-log plot of COMP V

As in the case of studies carried out in compounds presented earlier in this thesis, contribution of two photon absorption (TPA) is absent in the value of nonlinear parameters calculated using DFWM technique. If TPA were present the slope of the log-log plot between the pump intensity and phase conjugate signal in these samples would have been 5 instead of the observed value of 3 [17-18]. Therefore the contributions of TPA in the measured values are ruled out.

Since the experiments were done with samples dissolved in spectroscopic grade solvents, it is possible to evaluate the microscopic molecular property viz. second hyper polarizability  $\langle\gamma\rangle$ . Measured values of third order susceptibility ( $\chi^{(3)}$ ), Figure of merit (F), Extinction coefficient ( $\epsilon$ ) and Second hyper polarizability  $\langle\gamma\rangle$  are given in the table 6.1. Figure of merit (F) and extinction coefficient  $\epsilon$  of these material are calculated using the equations 4.5 and 4.6 given in the fourth chapter of this thesis.

From the extinction coefficient  $\epsilon$  we can calculate the oscillator strength of the molecule. It is a very important parameter, which can heavily influence the

second hyper polarizability  $\langle\gamma\rangle$ [19-21] and is related to the extinction coefficient as shown in Eqn. 4.7

**Table 6.1** Nonlinear parameters measured in metal complexes of semicarbazone

Sample (in CHCl <sub>3</sub> ) 0.25 mM	Linear Absorption Coefficient $\alpha$ (cm <sup>-1</sup> )	Extinction coefficient $\epsilon \times 10^3$ ltr cm <sup>-1</sup> mol <sup>-1</sup>	Third order Susceptibility $\chi^{(3)}$ ( $\times 10^{-13}$ esu)	Figure of Merit F ( $\times 10^{-13}$ esu-cm)	Second Hyper polarizability $\langle\gamma\rangle$ ( $\times 10^{-31}$ esu)
COMP: I	0.183	0.317	3.553	19.45	7.21
COMP: II	0.122	0.212	2.186	17.87	4.44
COMP: III	0.106	0.184	2.053	19.30	4.12
COMP: IV	0.188	0.327	3.616	19.17	7.34
COMP: V	0.104	0.181	1.789	17.18	0.36

From the nonlinear parameters, measured using DFWM technique, given in table 6.1 we can see that compound I and compound IV are having almost same second hyperpolarizability and their values are considerably better than that of other compounds studied here. Similarly compound II and III have almost same second hyperpolarisabilities but the value calculate in the case of compound V is very small as compared to that of other samples.

#### 6.4 Discussion

We have studied the nonlinear optical behaviour of five different Cobalt Ternary Complexes of 2-Hydroxy Acetophenone N(4) Phenyl Semicarbazone containing

## Investigations of nonlinear .....

Heterocyclic Coligands by using the DFWM techniques. The parameters thus obtained are presented in table 6.1. These samples have more or less similar structures and the  $\pi$ -electron density is also almost same in these samples. Apart from the  $\pi$ -conjugated electrons there are many other factors that can influence the measured second hyperpolarizability values of the samples. For example, oscillator strength plays an important role in determining the measured  $\langle\gamma\rangle$  values [19-21].

Oscillator strength is related to the extinction coefficients by the relation as given in chapter 4 (Eqn.4.7). From the relation between oscillator strength and extinction coefficient it is clear that oscillator strength is larger if extinction coefficient is large. Similarly the presence of metal substituents, dimensionality of the molecule, axial and peripheral substituents etc. also play important role in determining the nonlinear parameters of the materials[22-36]. The effect of these various aspects can have a cumulative nature on determining the NLO parameters but the strength of influence varies from materials to materials. In the present case the observed values of second hyperpolarizability  $\langle\gamma\rangle$  can be explained in terms of the influence of the presence of substituents as well as the oscillator strength of the molecules.

Among the five metal complexes of semicarbazones considered here the oscillator strength of compounds I and IV are considerably larger than that of other compounds and accordingly the measured second hyperpolarizability values of these compounds are larger. This observation proves the dominant effect of oscillator strength of the molecules on the nonlinear parameters of this class of compounds.

From the structure of the compounds (Fig.6.1) given we can see that compounds II, III and V consist of sulphur atoms. Moreover even though the oscillator strengths of these compounds are almost same the  $\langle\gamma\rangle$  value of compound V is considerably smaller than that of other two compounds. The only difference between the structures of compounds II and V is in the position of the sulphur atom in

these compounds. Somehow the presence of Co-S bond in compound II enhances nonlinearity. This clearly shows the influence of substituents atoms in the  $\langle\gamma\rangle$  values of this class of compounds. In general, it can be inferred that the presence of sulphur atom decreases the  $\langle\gamma\rangle$  values of this class of compounds. In addition to the presence of the sulphur atom, the position of the same in the complex considered too is important. Therefore the observed nonlinear parameters of metal complexes considered here can be explained in terms of the influence of oscillator strength and substituents atoms.

It may be appropriate to compare the measured nonlinear parameters of these compounds with that of the results obtained in other compounds. The second hyperpolarizability values obtained in QAP's and TPP's are presented in tables 4.1, 4.2 and 5.1. By comparing  $\langle\gamma\rangle$  values presented in these tables with the same given in table 6.1 we can see that the  $\langle\gamma\rangle$  values obtained in the case of metal complexes of semicarbazones studied here are lower at least by an order of magnitude. Hence even though these compounds are not very good NLO materials, detailed studies in these compounds can give better insight into the nonlinear behaviour of various materials.

## 6.5 Conclusion

The nonlinear behaviour of five Cobalt Ternary Complexes of 2-Hydroxy Acetophenone N(4) Phenyl Semicarbazone containing Heterocyclic Coligands has been investigated using DFWM technique at 532 nm excitation. Third order susceptibility, figure of merit of third order nonlinearity and second hyperpolarizability of these samples are measured and the observed nonlinear behaviour of this class of compounds have been interpreted by considering the influence of oscillator strength and atomic substituents. The  $\langle\gamma\rangle$  values of metal complexes of semicarbazones studied here is at least one order of magnitude smaller than the same in QAP's and TPP's presented in earlier chapters.

## 6.6 Reference:

1. S K Hurst, M G Humphrey, T. Isoshima, K Wostyn, I Asselberghs, K Clays, A Persoons and B Luther-Davies, *Organometallics*, **21** (2002) p.2024
2. Dalino Dini, M Bartherl, T Schneider, M Ottmar, S Verma and M Hanak, *Solid State Ionics*, **165** (2003) p.289
3. S K Hurst, N T Lucas, M G Humphrey, T Isoshima, K Wostyn, I Asselberghs, K Clays, a Persoons, M Samoc and B Luther-Davies, *Inorg. Chimica Acta*, **350** (2003) p. 62
4. I R Whittall, A M McDonagh, M G Humphrey and M Samoc, *Adv. Organomet. Chem.* **42** (1998) p.291
5. K P Unnikrishnan, Jayan Thomas, V P N Nampoori and C P G Vallabhan, *Chem. Phys.* **279** (2002) p.209
6. I R Whittall, A M McDonagh, M G Humphrey and M Samoc, *Adv. Organomet. Chem.* **43** (1999) p.349
7. S R Marder, *Inorganic Materials*, Wiley, Chichester (1992) p.116
8. S V Rao, N K M N Srinivas, D Narayana Rao, L Giribabu, B G Maiya, Reji Philip and G Ravindra Kumar, *Opt. Commun.* **192** (2001) p.123
9. G Padmanabhan and S Ramakrishnan, *J. Am. Chem. Soc.* **122** (2000) p.2244
10. E J Williams, *Appl. Phys. B* **63** (1996) p.47
11. J Y Lee, S B Suh and K S Kim, *J. Chem. Phys.* **112**(1), (2000) p. 344
12. K Kandasamy, S J Shetty, P N Puntambekar, T S Srivastava, T Kundu and B P Singh, *J. Porphy. and Phthalo.* **3** (1999) p.81.
13. P Mathur, S Ghose, R. Trivedi, M Gelinsky, M Rombach, H Vahrenkamp, S Banerjee, Reji Philip and G Ravindra Kumar, *J. Organomet. Chem.* **595** (2000) p. 140
14. M. Akkurt, S. Ozfuric, S. Ide, *Anal. Sci.* **16** (2000) p.667.
15. J.R. Dimmock, R.N. Puthucode, J.M. Smith, M. Hetherington, J.W. Quail, U. Pugazhenthii, *J. Med. Chem.* **39** (1996) p.3984.
16. J.R Dimmock, K.K. Sidhu, S.D. Tumber, S.K. Basran, M. Chen, J.W. Quail, *Eur. J. Med. Chem.* **30** (1995) p.287.
17. S Wu, X C Chang and R L Fork. *Appl. Phys. Lett.* **61** (1992) p. 919
18. M Zhao, Y Cui, M Samoc and P N Prasad. *J. Chem. Phys.* **95** (1991) p. 3991
19. K Kandasamy, S J Shetty, P N Puntambekar, T S Srivastava, T Kundu and B P Sing. *J. Porphyrins and Phthalocyanines* **3** (1999) p. 81
20. M G Kuzyk and C W Dirk. *Phys. Rev. A* **41**(1990) p. 5098
21. I Renge, H Wolleb, H Spahni and U P Wild. *J. Phys. Chem. A* **101** (1997) p. 6202
22. A Yamashita, S Matsumoto, S Sakata and T Hayashi., H Kanbara *J. Phys. Chem. B* **102** (1998) p. 5165
23. J S Shirk, J R Lindle, F J Bartoli and M E Boyle. *J. Phys. Chem.* **96** (1992) p. 5847
24. K Kamada, M Ueda, T Sakaguchi, K Ohta and T Fukumi, *J. Opt. Soc. Am. B* **15** (1998) p.838
25. M Koshino, H Kurata, S Isoda and T Kobayashi, *ICR Annual Report.* **7** (2000) p.6
26. H S Nalwa and S Kobayashi., *J. Porphyrins and Phthalocyanines.* **2** (1998) p. 21
27. Ifor. D W Samuel, I Ledoux, C Delporte, D L Pearson and James M Tour, *Chem. Mater.* **8** (1996) p. 819
28. G R Kumar, M Ravikanth, S Banerjee, Armen Sevian, *Optic. Commun.* **144** (1997) p. 245

29. D S Chemla, J Zyss. *Nonlinear Optical Properties of Organic Molecules and Crystals*. Quantum Electronics. Principles and Applications. Academic Press (1987) Florida
30. A Sastre, M A Diaz-Garcia, D del Rey, C Dhenaut, J Zyss, I Ledoux, F Agullo Lopez and T Torres, *J. Phys. Chem. A* **101** (1997) p. 9773
31. K S Suslick, C T Chen, G R Meredith, and L T Cheng. *J. Am. Chem. Soc.* **114** (1992) p. 6928
32. B K Mandal, B Bihari, A K Sinha and M Kamath, *Appl. Phys. Lett.* **66** (1995) p. 932
33. A K Sinha, B Bihari and B K Mandal, *Macromolecules*. **28** (1995) p.5681
34. H S Nalwa, A Kakuta, *Thin Solid Films*. **254** (1995) p.218
35. K Kandasamy, S J Shetty, P N Puntambekar, T S Srivastava, T Kundu and B P Singh, *Chem. Commun.* (1997) p. 1159
36. H Kanbara, T Maruno, A Yamashita, S Matsumoto, T Hayashi, H Konami, N Tanaka, *J. Appl. Phys.* **80** (1996) p. 3674

# Chapter 7

## General Conclusion and Future Prospects

### 7.1 General Conclusion

Last part of the 20<sup>th</sup> century witnessed the emergence of Photonics as a new branch of Science and Technology and it is a field of promise to the years to come. Up to this time Electronics was playing the lead role in the field of science and technology. But now it is giving way to photonics. By this time, Photonics has already established its relevance in communication, instrumentation, measurements and control, optical computing, information processing, displays etc. Photonics encompasses diverse areas such as nonlinear optics, optical fibers, integrated optics, harmonic generation of laser radiation, optical switches and display devices. The discovery of new intense monochromatic light sources and materials with special properties intensified the growth in various fields of photonics. Materials that are very useful for light based applications are collectively called photonic materials and most of the technological applications exploit the nonlinear optical (NLO) properties of these materials in one way or the other. Therefore the investigations of NLO properties of different photonic materials become very important and this led to the discovery as well as characterization of large number of NLO materials. All over the world active research in this field is in progress. In this context, study of NLO properties of certain photonic materials, which include a number of organo-metallic compounds were chosen as the topic of the present research work.

Some of the essential requirements of good photonic materials are large and fast nonlinearity, synthetic flexibility and ease of processing. Wave Mixing, Z-Scan, Optical Limiting, Third Harmonic Generation (THG) etc. are the most commonly used

Investigations of nonlinear .....

techniques for the evaluation of the nonlinear behaviour of most of the NLO materials. Metal substituted phthalocyanines belong to the class of efficient photonic materials and the nonlinearity of these compounds is well studied in various solvents. But there are not many reports on the properties of these materials in solid matrices. When device applications are considered, the incorporation of these materials into solid matrices and the study of their behaviour in different host materials become important. Hence, we studied the NLO properties of Samarium Phthalocyanine in solid (PMMA) as well as liquid (MMA) matrices.

Using the open aperture z-scan technique, the effective nonlinear absorption coefficient  $\beta_{\text{eff}}$  and imaginary part of the nonlinear susceptibility ( $\text{Im}\chi_{\text{eff}}^3$ ) of Samarium Phthalocyanine in Methyl Methacrylate at 532 nm has been measured, in both liquid and solid media. The optical limiting nature of the samples is also studied. The samples exhibit obvious nonlinear behaviour and the nonlinearity originates from the large excited state absorption cross section, the characteristic property of Phthalocyanines. Enhancement in optical limiting property of samples in liquid phase over the solid phase is attributed to the bimolecular processes taking place in liquid media. The measured  $\beta_{\text{eff}}$  values as well as the optical limiting curves show that samples in liquid phase are moderately better in their optical limiting efficiency. However, the solid matrix gives rigidity to the nonlinear medium and the handling is more convenient. Therefore for a device application the polymeric solid matrix may be preferred over the monomeric solution phase. The concentration dependence on the optical limiting nature is also studied both in liquid as well as in solid medium and the role of RSA in the limiting behaviour is verified.



Degenerate Four Wave Mixing (DFWM), Z-Scan and optical limiting studies has been carried out in certain selected metal complexes of QAP's at 532 nm under nanosecond excitation. For the DFWM measurements the polarization of the interacting beams were so chosen that electronic response is obtained. Third order susceptibility, figure of merit of third order nonlinearity and nonlinear absorption coefficient of these samples are calculated. The measured nonlinear parameters of these samples are explained as due to the combined effect of nonlinear absorption, oscillator strength and resonance effects at the wavelength of excitation. It is observed that Ni (QAP)<sub>2</sub> and Co (QAP)<sub>2</sub> are promising NLO materials and their importance in device applications is confirmed by the optical limiting studies carried out in these samples.

Another NLO material studied is certain selected porphyrins with different peripheral constituents. The effect of peripheral substitution is studied using Degenerate four-wave mixing technique. The nonlinear absorption in these samples was studied using z-scan and optical limiting nature is verified using the graphs generated from z-scan data. Third order susceptibility  $\chi^{(3)}$ , Figure of merit of third order nonlinearity (F) and Second hyper polarizability  $\langle\gamma\rangle$  were measured. TPP with out any peripheral ligands exhibited the highest value of figure of merit as well as second hyper polarizability indicating that it possesses maximum third order nonlinearity for a given absorption loss. The  $\langle\gamma\rangle$  values measured were explained on the basis of internal charge transfer mechanism and oscillator strength of the molecules. The effects of wavelength, concentration and solvents on the NLO behaviour of the samples were also studied using the z-scan technique. The optical limiting nature of these samples was studied and it is observed that unsubstituted porphyrin and nitro-TPP shows the best optical limiting.

## Investigations of nonlinear .....

The nonlinear behaviour of five Cobalt Ternary Complexes of 2-Hydroxy Acetophenone N(4) Phenyl Semicarbazone containing Heterocyclic Coligands has been investigated using DFWM technique. Third order susceptibility, figure of merit of third order nonlinearity and second hyperpolarizability of these samples are measured and the observed nonlinear behaviour of this class of compounds has been interpreted by considering the influence of oscillator strength and atomic substituents. The  $\langle\gamma\rangle$  values of metal complexes of semicarbazones studied here is at least one order of magnitude smaller than the same in QAP's and TPP's presented. Even though these compounds are not very good NLO materials, detailed studies in these compounds can give better insight into the origin of nonlinear behaviour of various materials.

### 7.2 Future Prospects

Large and fast nonlinearity, synthetic flexibility, ease of processing and good chemical and thermal stability are being the essential properties of a good photonic material. Search for such a material is highly active all over the world. Material, which satisfies all these qualities are not yet identified. Nonlinearity observed at resonant fields shows very large magnitude but has slow response. On the contrary, non-resonant nonlinearity is very fast in response but low in magnitude. Many organometallic compounds and organic-inorganic systems satisfy many of the essential requirements of good nonlinear material. Organometallic compounds similar to those studied in the present investigations can be tested for various device applications like optical limiters, optical logic gates etc. A good deal of work is required in this field for the realization of an ideal NLO material for various technological applications.

G18642